One Pathway to Rule Them All: Wnt Signaling Guides Specification and Axon Growth in VD13

By

Meagan Kurland

B.S., Ursinus College, 2015

Submitted to the graduate degree program in Molecular, Cellular, and Developmental Biology and the Graduate Faculty of the University of Kansas in partial fulfillment of the requirements for the degree of Doctor of Philosophy.

Title Page

_____

Chair: Brian D Ackley

_____

Erik Lundquist

_____

Stuart Macdonald

_____

Robert Unckless

_____

John Kelly

_____

Date Defended: 10 December 2020

The dissertation committee for Meagan Kurland certifies that this is the approved version of the following dissertation:

One Pathway to Rule Them All: Wnt Signaling Guides Specification and Axon Growth in VD13

_____

Chair: Brian D Ackley

Date Approved: 10 December 2020

Abstract

The nervous system is highly complex, and its formation is regulated and guided from the moment a neuron is born to throughout its life. Neurons must undergo a series of steps throughout development, typically including a combination of the following: specification, migration, axon outgrowth, target recognition, synapse formation, and synapse maintenance and change. These developmental steps are largely driven by both extrinsic signaling cues and intrinsic programs, which work together to create the myriad of diversity that we see throughout the nervous system. Here, we will look at two such developmental regulators. The canonical Wnt signaling pathway is a signaling system with an extrinsic ligand, and the Hox genes are intrinsic molecules that work to pattern the anterior/posterior axis. We will specifically look at the role Wnt signaling and the Hox genes play in specification and axon growth, two critical parts of neuronal development.

Specification is a hierarchical process in which neurons undergo a series of developmental changes, in which each step defines a more precise neuronal identity. Thus, identifying the genes required for proper specification is vital to understanding the development of the nervous system. The genes and receptors which a neuron express during the stages of specification will influence subsequent steps in its development, such as migration, axon growth, and synapse formation. Here, we will also examine axon growth, and the cues that function to provide both attractive and repulsive signals to guide the growing axon to its target location. We find that similar signals function in both specification and axon growth in the D-type GABAergic motor neuron, VD13.

In Chapter III, we describe a novel transgenic marker, *lhIs97*, which utilizes a fragment of the *plx-2* promoter to drive mCherry expression in the most posterior of the D-type GABAergic motor neurons, VD13, as well as in the bilaterally symmetrical LUA neurons, LUAL and LUAR. Using this marker, we provide evidence that the Wnt signaling pathway and the Hox gene *egl-5* may function as terminal

selectors for VD13, assigning its final, terminal identity as the most posterior D-type neuron. Additionally, we show the underlying morphology to the previously published under- and over-growth phenotype reported when Wnt pathway signaling members or *egl-5* are mutated.

In Chapter IV, we look further into specification, first by looking at known factors involved in the specification of all of the VD neurons. Here, we find that *unc-55*, which is involved in the differentiation of the VD neurons from the DD neurons, is not required for expression of mCherry via *lhIs97*, our VD13 specific marker. *plx-2* and *mab-20*, which are, respectively, a transmembrane receptor and a semaphoring signaling molecular, are also not required for expression of RFP in VD13. We also show that when the heparan sulfate proteoglycan *sdn-1* is lost, there is increased expression of *lhIs97* in DD6, but no significant difference in expression in VD13. Thus, while *sdn-1* may somehow be involved in differentiating DD6 from VD13, *unc-55*, *plx-2*, and *mab-20* are not necessary for *lhIs97* expression in VD13.

Additionally, in Chapter IV, using *lhIs97*, we perform a genetic screen for temperature sensitive alleles involved in VD13 specification and, potentially, axon growth. We report eight candidate lines which all have varying loss of expression of *lhIs97* mCherry in VD13. Five of the eight new alleles appear to be temperature sensitive. The *lh40* line has a premature stop codon in *sma-9*. *sma-9* is a known transcription factor that has been implicated in many different processes in the worm, including in dorsal-ventral patterning. Based on available evidence, we think it is a candidate to be involved in specification and axon growth in VD13. None of our lines completely lost expression of the RFP marker in VD13, which suggests that our screen has not reached saturation for potential candidates that are involved in specification and axon growth in VD13. Thus, further screens may well provide additional candidates that are involved in this system.

Finally, in Chapter V, we look further into the role that the Wnt signaling pathway has in directional axon growth and repulsion. Here, we show that *bar-1*/β-catenin*,* frequently an effector of Wnt signaling, is instead epistatic to the Wnt ligands *egl-20* and *lin-44* in axon growth. Additionally, we show that, of the three *C. elegans* Dishevelеds, *dsh-1* and *mig-5*, but not *dsh-2*, are necessary for axon growth. Finally, we find that the Hox gene *egl-5* acts cell autonomously to regulate axon outgrowth.

Overall, in this report we show that the Wnt signaling pathway and the Hox gene *egl-5* regulate specification and axon growth in the most posterior D-type GABAergic motor neuron, VD13.

Acknowledgements

There are so many people who I need to thank.

Firstly, to my parents, for always supporting me, even when it meant driving 18 hours to Kansas to move me to grad school. To my mom, who always urged me to reach for what I wanted, and always being there to offer advice or to be a shoulder to cry on. To my dad, for making the best egg sandwiches, always picking the best movies on Sunday mornings, and for being the one to makes those drives to Kansas (and being willing to bring home a cat this time… and a fish). To both of them for always making my ears ring by talking about my works, my paper, with literally everyone they knew. Thank you.

And, of course, I'd be remiss to forget the rest of my family. To my little brother, for being a huge nerd and always wanting to talk about it. To my whole extended family, my aunts and uncles and cousins and grandparents, for all of the love and support that I've had my whole life that allowed me to get to this point.

To all of my friends, I love you all so much, and it's my dissertation so I'm going to shout out some of you in particular. To Aaron and Laura, for sharing in all of the frustration and the rare triumphs. To Tori, for all of the love and bunny pics. To Ashley, for commiserating with me about the job search, and always being there to catch up for hours after both of our lives get busy. To Silver, for somehow being an unending optimist, celebrating every small victory with me, and always being there to watch a baking show (or two) when I was taking a break from writing. To my D&D group, for making Thursday night the best night of the week. And, to my guild, for always welcoming me back with open arms, even when I disappear for months at a time to work on school.

To my supervisor, Winter, for never letting me work for too long without taking a break. And for being the best decision I ever made, so I didn't have to weather the pandemic totally alone.

To the Molecular Biosciences Department, thank you for this opportunity. A huge thank you to the professors who I've been able to teach with over the years, I have truly enjoyed the experience. Thank you to my great classes of students over the past 6 years. Thank you to my committee members. To the Lundquist lab, for providing support and ideas during lab meetings. And to KU CAPS.

To my lab. To EVL. To Wendy and Natasha and Patrick and Vaishnavi. To Dana and Vi and Mike. To Bryn. You have been the best undergrad and 'second author on a paper' that anyone could ask for. Finally, to Molly. It has been an insane 6 years, but I am so glad we decided to go to that first Pentatonix concert together and join the same lab (even if you took the scope). It was all made so much better by having someone to always talk to and having such a fun and supportive lab.

To my Boss. For always knowing when to poke fun at my crazy, and always being there to listen. For helping me through all the mistakes made in lab, talking me through the failures, and celebrating in the triumphs. For never forgetting to tell me to stop using the passive voice. And, maybe most importantly, for always being there to tell me that everything would be okay, and that I needed to just breath. (Please don't forget to water the plants when I'm gone).

Finally, to my Pap, for just wanting me to do what makes me happy. The weather was beautiful today. I promise I'll be good.

Table of Contents

Chapter I: Introduction

1.1 Specification and Neuronal Identity

Neurons are not born as their final, specific type of neuron. Pyramidal or Purkinje neurons do not emerge, fully formed, as those specialized neuron types. Instead, neurons undergo multiple steps during development to ensure they will be located in the correct place and assigned the correct neuronal identity. The steps that neurons undergo can include specification, migration, neurite outgrowth, target recognition, synapse formation, and changes to (or maintenance of) synaptic strength. These are general steps, and not all neurons will undergo all steps. As an example, some neurons will undergo long range migrations, such as the AQR and PQR neurons in *C. elegans*, where AQR travels from the posterior tail to the anterior head. Other neurons, such as the DD and VD neurons, undergo little migration, obtaining their final position with the terminal cell division. All of these steps are guided by signaling molecules and intrinsic programs, which will direct the neuron during migration and outgrowth, as well as by activating transcription factors, which will influence the specification of the neuron.

There are multiple signaling molecules that play a role during development. These signaling molecules are often secreted, and thus act as extrinsic signals which guide the development of the neuron. One highly conserved set of secreted signaling molecules are the Wnt ligands. Wnt ligands are involved in human development, but also have conserved roles in model organisms such as mice, *D. melanogaster*, and *C. elegans*, making these ideal systems in which to study the role of Wnts and their downstream pathway components. Wnts are involved in everything from asymmetric cell division to cell polarity, cell migration, axon growth, *etc.* (for review see [1, 2]). In addition to secreted signaling molecules, cell intrinsic and transmembrane molecules also play a role in development. As an example, the Hox genes are a subset of homeobox genes, specifically known for patterning tissues along the anterior/posterior

axis, as well as being involved in neuronal development. Both the Wnts and the Hox genes are also known to be involved in the specification of neurons.

Specification is the process by which a neuron is assigned its identity. Neuronal identity can consist of a generic 'type' of neuron, *i.e.* motor or sensory, as well as the necessary shape of neuronal processes, *i.e*. axons and dendrites, and what neurotransmitters those processes will respond to and release. All of these aspects must be properly assigned within the neuron to give the neuron its correct identity, and insure its proper growth and function (for review see [3]). Neuronal identity is assigned via hierarchical rounds of specification, wherein within each round, the identity of the neuron will become slightly more detailed (Figure 1.1). Here, we will delve more deeply into the process of specification.

To begin with a generic example, a cell will first be assigned as a neuron. Then, the neuron will further be specified into types and then subtypes. These rounds of specification are directed by transcription factors, which will alter the gene expression of the neuron to influence its subtype. As there are numerous different types of neurons, but only a discreet number of transcription factors, transcription factors will work together to create distinct gene expression outcomes to influence specification. Finally, in order to secure a neurons final fate, there are specific transcription factors which will act together, to specify and reinforce this terminally differentiated state. Transcription factors which aid in specifying and reinforcing a terminally differentiated state are often expressed throughout the life of the neuron. These transcription factors can be referred to as terminal selectors [4].

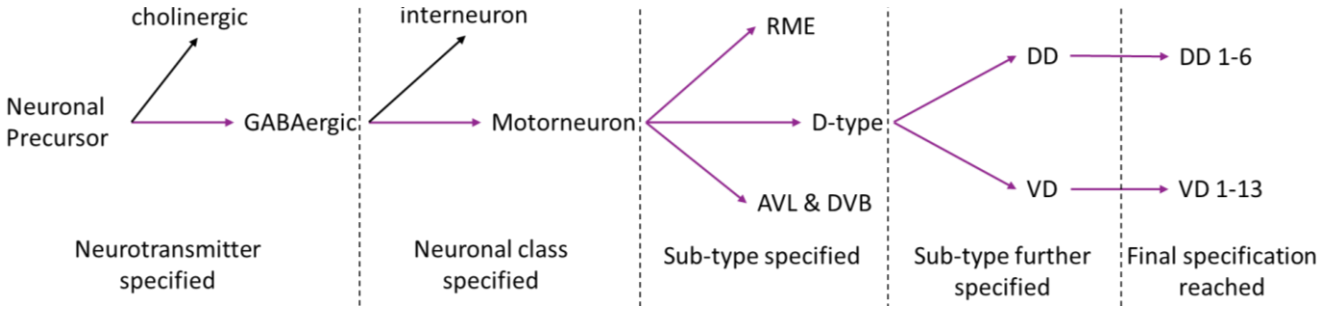

Figure 1.1. Neural Specification begins with a precursor cell, which then goes through iterative rounds of specification, until it reaches its terminal specification. As an example, here, a neuronal precursor goes through five rounds of specification, in which the neurotransmitter that the neuron will utilize is specified, then the neuron class, and three rounds of subtype refining to reach a final specification point, that of one of the 19 DD or VD neurons.

Terminal selectors are transcription factors which function by binding to certain sites within promoters to activate select sets of gene expression in a discrete number of cells. By doing this, terminal selectors are able to contribute to assigning a unique identity to cells. As an example, sensory neurons can further differentiate into a number of subtypes, including chemosensory, mechanosensory, thermosensory, olfactory, *etc*. These are all broadly classified as sensory neurons, but they have been further specified to function in more specific roles. This can be seen in *C. elegans*, where the homeodomain factor *lin-11* is involved in the differentiation of both chemosensory and olfactory-like neurons, the ASG and the AWA neurons, respectively [5]. The differentiation of these two sets of neurons occurs, in part, through both differential expression of *lin-11*, and through the regulation of different downstream genes, to confer the separate identities of the ASG and the AWA neurons [5]. Thus, terminal selectors, in general, could be classified as those genes that function to specify and maintain the final distinctions between the different classes of sensory neurons.

Terminal selectors can be identified by a number of characteristics. In addition to their function in conferring a unique identity to a cell via changes in gene expression, loss of a terminal selector also often confers certain characteristics. Phenotypically, the neurons still develop, but they can have defects

in their function, and these neurons often do not express the markers that are known to be specific to that neuron. As, if the neuronal identity is lost, then certain proteins which are specific to that subtype may not be expressed, and thus neither will the markers that rely on the expression of those proteins [4]. Thus, loss of a terminal selector may affect neuronal morphology, identity, and the expression of cell-specific proteins, amongst other characteristics.

In *C. elegans*, multiple genes have been described to act as terminal selectors. During the development of the ALM and BDU neurons, UNC-86, a homeodomain protein, can bind to either MEC-3, leading to the induction of the ALM identity, or PAG-3, leading to the BDU neuronal identity [6]. To specifically look at the BDU neurons, Gordon and Hobert found that the BDU neurons will form and express *unc-86* in the absence of *pag-3*, but they will not be terminally differentiated into BDU neurons. Thus, depending on which protein UNC-86 binds to, MEC-3 or PAG-3, will influence the fate of the precursor for the ALM and BDU neurons.

The binding of UNC-86 to MEC-3 or PAG-3 is only one step in the specification of the ALM and BDU neurons. *ser-2* and *ceh-14* are also known terminal identity regulatory genes for the BDU neurons. Both *ser-2* and c*eh-14* also contain UNC-86 and PAG-3 binding sites, and deletion of these UNC-86 and PAG-3 binding sites leads to a loss of expression of *ser-2* and *ceh-14* reporters. Additionally, in loss of function mutants, *ceh-14* animals lose expression of some, but not all, of the BDU identity marker genes examined. Thus, *ser-2* and *ceh-14* function downstream of *unc-86* and *pag-3* in establishing BDU neuronal identity, and require *unc-86* and *pag-3* to be properly expressed in the BDU neurons [6]. To summarize, one factor, *unc-86*, can function as a terminal selector for two different sets of neurons, the ALM and the BDU, depending on which co-factor interacts with UNC-86, and the downstream genes that the UNC-86/cofactor pair transcriptionally affect (Figure 1.2).

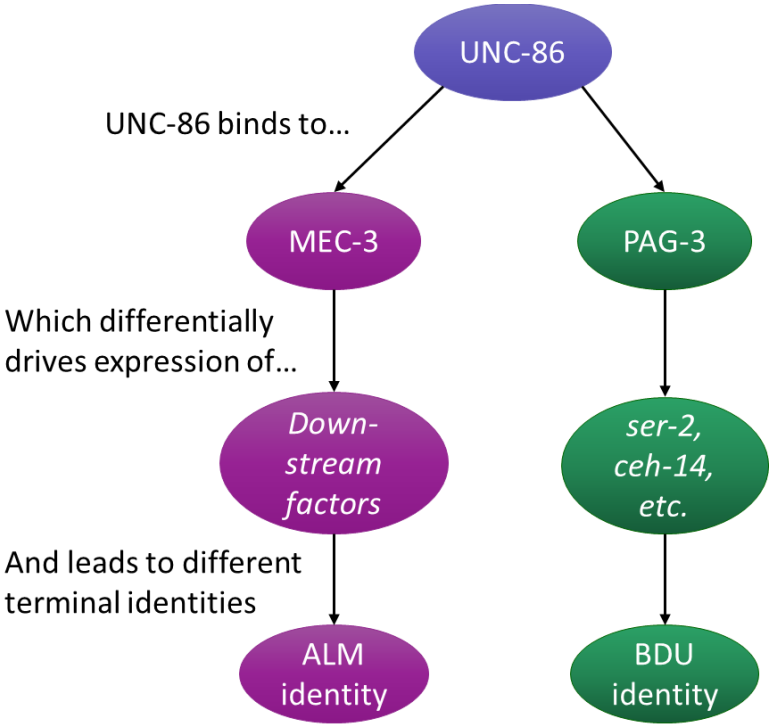

Figure 1.2. *unc-86* acts as a terminal selector for both the ALM and BDU neurons in *C. elegans*. This occurs due to UNC-86 being able to bind to both MEC-3 and PAG-3, and, depending on which is bound to UNC-86, will influence the expression of downstream factors, and thus confer differential identities on the neurons. Based on figures from [6].

Terminal selectors are not specific to *C. elegans*. As an example, in *Drosophila*, the dAp neurons and the Tv1 neurons are separated spatially and develop at different times, yet have highly similar morphology. These neurons also use the same neuropeptide, Nplp1. It was found that these neurons activate the same terminal selector, and thus the same subsequent changes in gene expression, to ultimately be able to utilize Nplp1. However, given their differences in developmental location and timeline, these neurons use different factors to induce that same terminal selector [7]. Thus, these neurons can exist in different spaces, but still achieve a similar result during development and have a highly similar specification assigned.

In vertebrates, research is still ongoing to identify terminal selector genes within the nervous system, though there are some promising candidates from mice. One such candidate is the LIM-type

homeodomain protein LHX1. When LHX1 was knocked out in 8-week-old mice, there was a loss of expression of glutamatergic specific markers in some neurons which, typically, were also shown to express LHX1. Specifically, markers were lost in those glutamatergic neurons which express BRN3a, a member of the POU family of transcription factors, and vesicular glutamate transporter 2 (VGLUT2). Notably, other, non-glutamatergic, LHX1 expressing neurons were unaffected. This suggests that LHX1 may specifically play a role in the terminal identity of these glutamatergic neurons [8]. This ongoing research suggests that the method of specifying and maintaining the terminal identity of neurons via terminal selector genes is, most likely, conserved from invertebrates to vertebrates.

1.2 Axon Guidance

During development, neurons extend neurites, which are directed by extracellular factors to target areas. Typically, these neurites will either be axons, which are polarized to send signals, or dendrites, which function to receive signals. However, as in much of biology, not all neurites will fall exactly into one of these two categories. Neurons can firstly range from unipolar to multipolar, depending on the number of neurites they extend (Figure 1.3). As an example, a unipolar neuron will only extend one neurite versus a pseudounipolar neuron, which will also only extend one neurite, but that one neurite will then bifurcate into multiple branches. Thus, in the case of the pseudounipolar neuron, one initially projected neurite will eventually function to both send and receive signals. Additionally, once a neurite has initially extended, it sometimes must continue to grow with the growing organism, thus requiring axon elongation and stretching, versus general outgrowth (for review see [9]). However, here we will focus on the generalities of the initial neurite outgrowth.

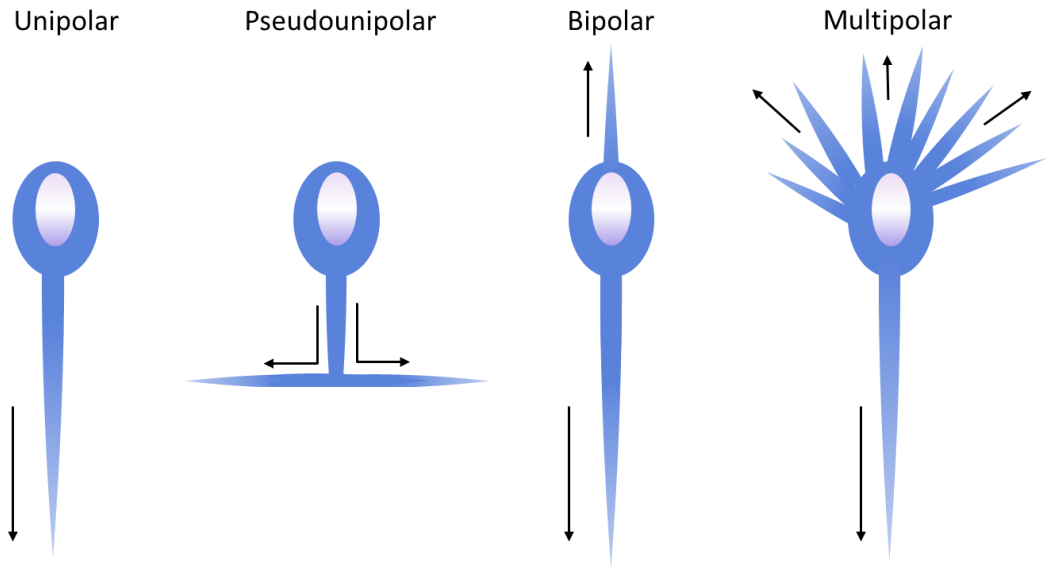

Figure 1.3. Neuron types. The four general types of neurons are: unipolar, pseudounipolar, bipolar, and multipolar, depending on the number of neurites extended, as well as the function and characteristics of those neurites, *i.e.* axon or dendrite. Arrows point to the direction of growth.

Neurite growth is dependent on microtubules and actin. Some neurites form an obvious structure called a growth cone. Growth cones function to interpret environmental cues and lead the outgrowth at the end the growing neurite (for review see [10, 11]). Growth cones have a core base of microtubules, as well as long extensions, which consist of lamellipodia and filopodia. Lamellipodia and filopodia contain networks of a mesh-like or filamentous actin, respectively. In response to signals, these structures can rapidly polymerize actin to push the membrane forward, thus driving the forward movement of the neurite via extension of the growth cone or depolymerize actin to result in retraction [12]. While both lamellipodia and filopodia are found at the peripheries of the growth cone, they have distinct roles. Specifically, as previously mentioned, lamellipodia consist of networks of mesh-like actin, and form in crisscrossing patterns to help to support the protruding growth cone. Filopodia consist of actin bundles, and, as such, are able to further push out the membrane in a specific area, thus extending the membrane further out in a long protrusion. As this is happening, the cell is adding both cytoplasm and

plasma membrane, as well as organelles and vesicles via transport down the microtubules at the base of the growth cone, to allow for physical growth of the neurite (for review see [13]).

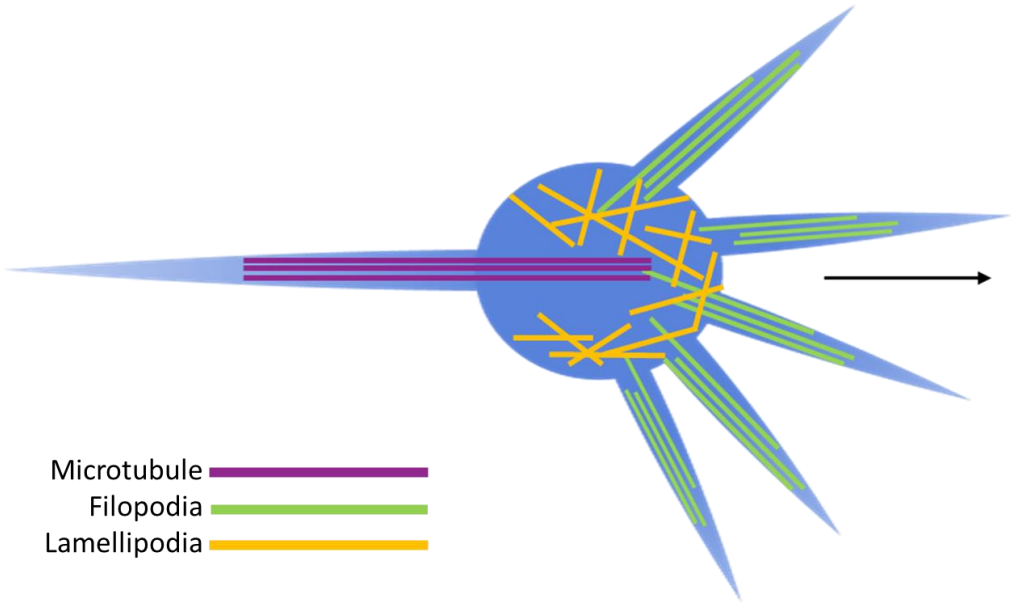

Figure 1.4. Structure of the Growth Cone. The growth cone consists of a core of microtubules (purple) and a periphery supported by filamentous actin. Here, the lamellipodia (orange) form around the edges of the growth cone, to provide support, while the filopodia (green) extend outwards and support the long protrusions. Both are highly dynamic and will rapidly polymerize to push out the membrane at the periphery of the growth cone, allowing for movement and growth of the extending neurite. Based on figures from [10].

To direct the growth of the extending neurite, there are receptors on the extending processes that are able to receive signals from the environment, these signals trigger signaling pathways, which will result in either an attractant or repulsive signal, thus directing the growing neurite to its target location. As an example, Netrin (*unc-6* in *C. elegans* [14]) is a highly conserved signaling molecule, which is involved in polarity and protrusion at the growth cone [15-18]. Additional guidance cues and their receptors include: semaphorins, slits, ephrins, Wnts, *etc.* (for review see [19]). It is also important to note that not all extending neurites have an obvious growth gone.

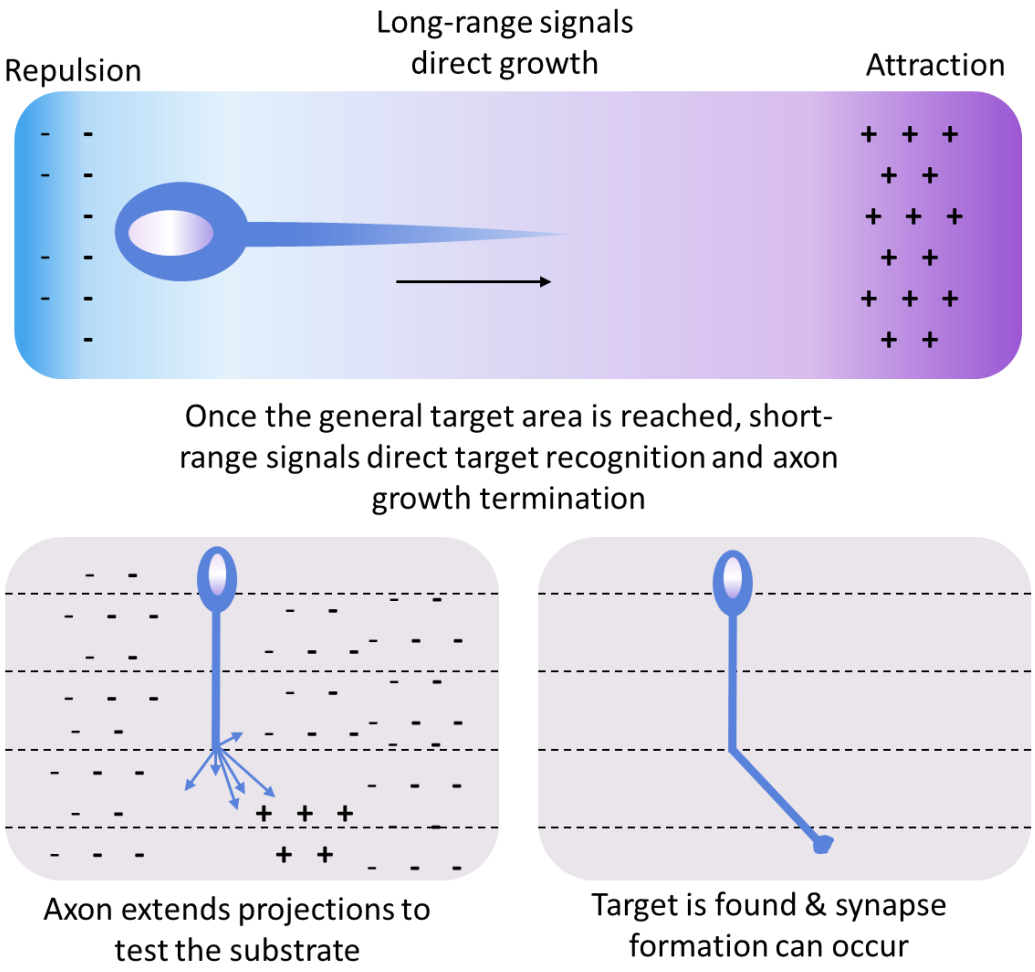

Figure 1.5. Neurite Growth and Extension. Initially, long range signals direct the growth of the protruding neurite. As a neurite nears its destination, it will begin to extend multiple projects to test the substrate, and further refine its growth. Once a target is reached, synapse formation can occur. Some axons and dendrites will only form one synapse, while other will continue growing, and form multiple synapses.

Once that location is reached, target selection must take place. In this target location, a neurite will begin to extend branches in multiple directions, 'testing' the area for a signal directing its growth. Eventually, a signal will direct the neurite to a more general location, then a specific layer, and, finally, direct the neurite to connect, establish synapses, and innervate its target cells (Figure 1.5). This final target pathfinding and synapse formation is led by guidance molecules and receptors on the presynaptic (growth cone) and postsynaptic surfaces, such as dendritic spines, for those neurons that form synapses

with dendrites, or, for motor neurons, synapses are formed with the membrane of the muscle fiber (for review see [20-22]).

Synapse target recognition is more complex when one considers that not all neurons function as 'one axon, one target'. There are many neuronal types that instead form multiple synapses along one axon, each innervating their own target, and yet the axon must still eventually receive the terminal signal to stop growing. An example of this comes from *C. elegans*. The DA motor neurons consist of a ventral cell body, with an anteriorly directed dendrite and a posterior axon, which forms multiple synapses with both the dorsal body wall muscles and the VD motor neurons [23]. Here, the Wnt signaling pathway functions as an inhibitory signal to properly position the formation of not only the presynaptic domains, but the formation of fully functional synapses in the DA9 motor neuron (Figure 1.6) [24]. The full range of guidance cues and their receptors, and how they function to direct axon growth and termination, is still not completely described.

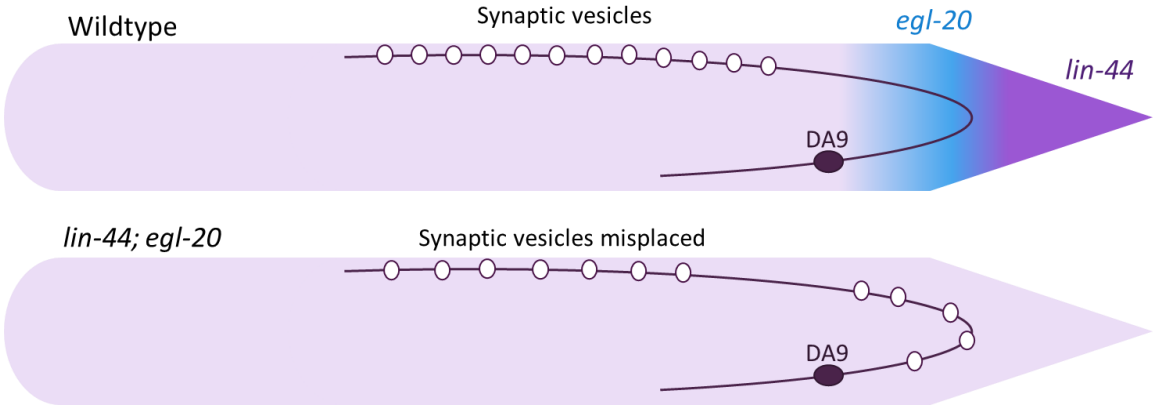

Figure 1.6. Wnt signaling is involved in patterning the presynaptic domains of the DA9 motor neuron in *C. elegans*. In the DA9 motor neuron, Wnt signaling functions as an inhibitory signal, ensuring that the synaptic vesicles are properly aligned along the dorsal side of the animals. In Wnt mutants, the synapses are misplaced, expressed along the entirety of the neuron, including in the posterior of the animal. Based on figures from [24].

1.3 The D-type GABAergic Motor Neurons

C. elegans in particular presents an excellent system to study axon growth (for review see [25]). The *C. elegans* nervous system consists of 302 neurons in the adult, hermaphroditic worm [26]. One subset of these neurons is the D-type γ-amino butyric acid (GABA)-ergic motor neurons. These motor neurons utilize the neurotransmitter GABA to send inhibitory signals to the dorsal and ventral muscles, and are required for proper locomotion of the animal [27]. These motor neurons consist of two distinct types, the dorsal D (DD) neurons, and the ventral D (VD) neurons. These neurons innervate the dorsal and ventral wall muscles, respectively. There are six DD neurons and 13 VD neurons, which are laid out like tiles along the anterior/posterior axis of the animal (Figure 1.7). The DD neurons form first, during the 2-fold stage of embryogenesis, and are fully formed by the time the animal hatches as a L1 larvae. The VD neurons begin to develop later, after hatching, near the end of the L1 stage. Additionally, the VDs develop in order, with VD1 forming first in the head, and VD13 forming last in the tail. The VD neurons are not finished growing until the L2 stage [28, 29].

We utilize the D-type GABAergic motor neurons to study the role of Wnt signaling in neuronal development. Specifically, we utilize the three most posterior D-type motor neurons, VD12, DD6, and VD13 (Figure 1.7). Recently, with the addition of a new, VD13 specific marker, we have also further refined our research to individually studying VD13, the most posterior GABAergic D-type motorneuron.

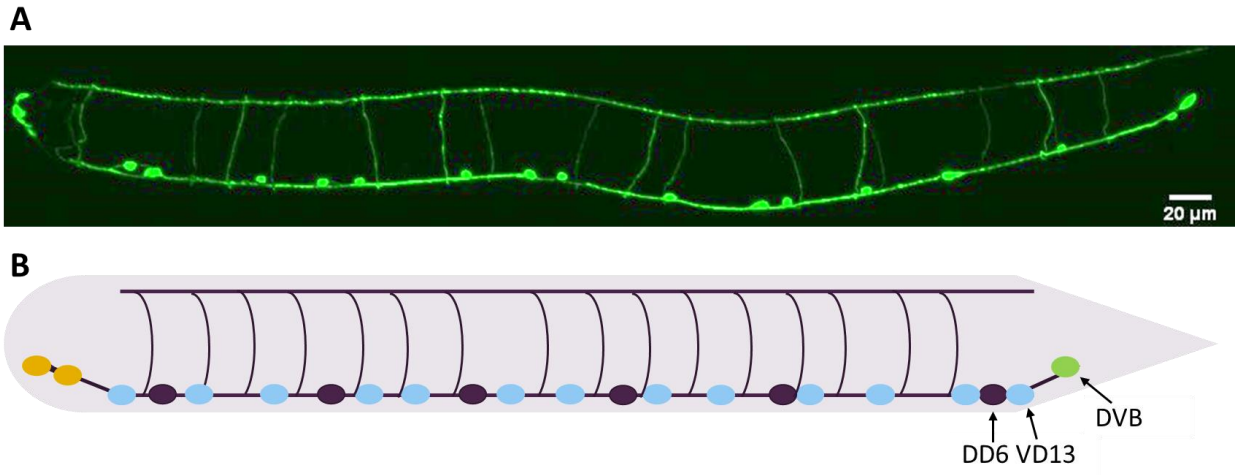

Figure 1.7. The D-type GABAergic motorneurons. In *C. elegans*, there are 19 D-type motorneurons, six dorsal D (DD) neurons and 13 ventral D (VD) neurons. These neurons are laid out like tiles along the anterior-posterior axis of the worm, with their cell bodies along the ventral cord, and their axons extending up to and along the dorsal cord. In particular, we study the poster posterior D-type neurons, DD6 and VD13. A) A confocal image utilizing the *unc-25* GABAergic specific promoter to drive GFP. B) A schematic, roughly showing the positions of the 19 GABAergic motor neurons. DDs are the purple cell bodies, and VDs are the blue cell bodies. The DVB neuron is shown in green in the posterior tail. DVB uses GABA, but obtains if from the environment, and does not synthesize it, so it is not labeled by the *unc-25* promoter used to label the cells in (A)

1.4 Wnt Signaling

Wnts are a family of secreted glycoproteins that function as short-range signaling molecules. As short-range signaling molecules, Wnts will bind to receptors present on the cell surface. Once bound, these ligand/receptor complexes will, potentially via recruitment of other effector proteins, activate pathways which lead to changes in target gene transcription, among other outcomes [30]. The Wnt pathway can be broadly separated into two categories: the canonical and the non-canonical pathways. At their core, the main difference between these two categories is that the canonical pathway leads to the activation of the transcription factor β-catenin, whereas the non-canonical pathway will act through other factors, such as calcium, CAMKII, Rho, Rac, *etc.*, to enact changes (for review see [31, 32]).

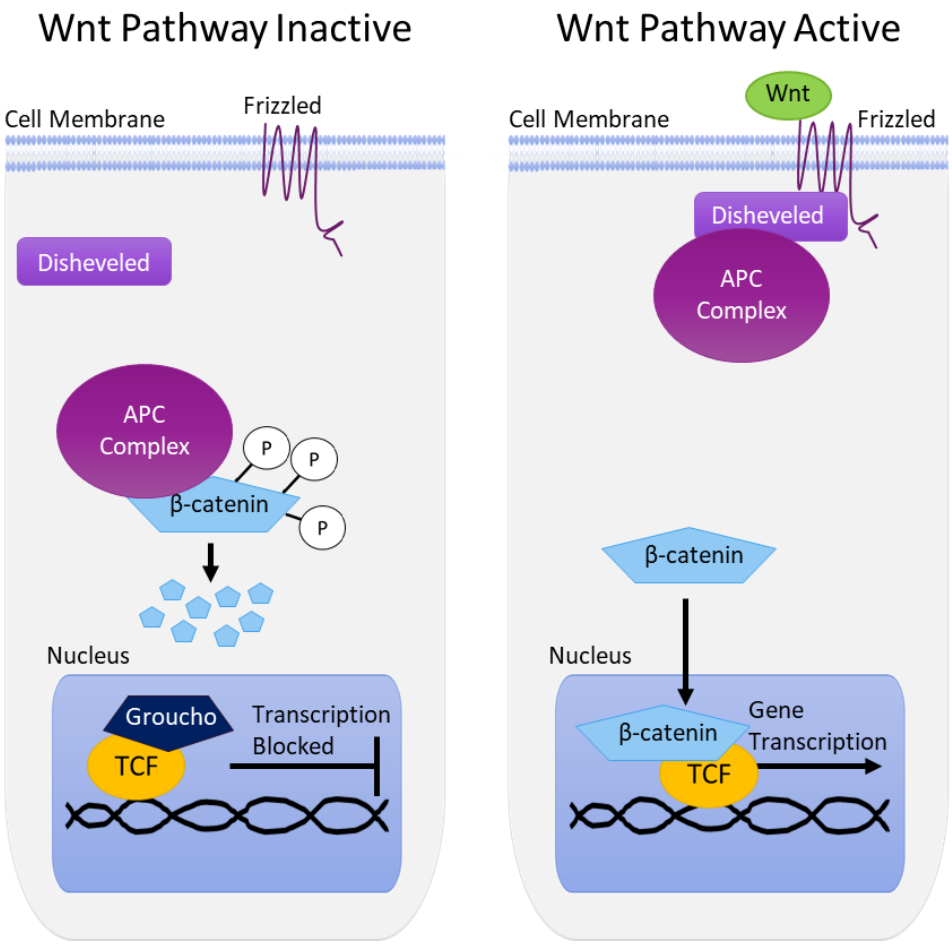

Figure 1.8. The Canonical Wnt Signaling pathway. The canonical Wnt pathway has both an inactive and an active state. In the inactive state, the Wnt ligand is not present, and β-catenin is tagged for degradation by the APC complex. In the presence of the Wnt ligand, the receptor Frizzled will recruit Disheveled and the APC complex, which will block it from interacting with β-catenin. β-catenin can then enter the nucleus, and, along with TCF, enacts changes to gene transcription.

This paper will focus primarily on the canonical pathway. The main players in the canonical Wnt pathway are, in order: the Wnt ligands, the Frizzled receptors, the Disheveled adaptor proteins, the APC destruction complex, and β-catenin (Figure 1.8). Wnt ligands are secreted, lipid-modified glycoproteins. There are five genes that encode Wnt ligands in *C. elegans*: *cwn-1*, *cwn-2*, *egl-20*, *lin-44*, and *mom-2*. These ligands exhibit regional differences along the anterior/posterior axis in terms of their expression. *cwn-1* and *cwn-2* are expressed more anteriorly than the remaining three ligands, *egl-20*, *mom-2*, and

lin-44, which are expressed in the posterior, with *lin-44* expressed most posteriorly [33]. It should be noted that this expression pattern is specifically seen in the first larval stage, L1, of the worm, and it is certainly possible that there are other times during the life of the animals when this expression pattern is not as exact as described here.

When a Wnt ligand binds to a Frizzled receptor, it leads to recruitment of the Disheveled proteins, which will inhibit the APC complex, preventing phosphorylation and subsequent degradation of β-catenin. This allows β-catenin to enter the nucleus and act as a transcription factor to regulate gene expression alongside the transcription factor TCF (*pop-1* in *C. elegans* [34]) (for review see [30, 35]). *C. elegans* in particular have four functional β-catenins, *bar-1*, *wrm-1*, *sys-1*, and *hmp-2*, which all retain some redundancy, but also maintain their own unique functions *in vivo* [36]. *bar-1* is the β-catenin that is known to most often interact directly with *pop-1*, the *C. elegans* homolog of TCF [37]. Thus, in general, and for our purposes, *bar-1* is the β-catenin that is activated at the end of the canonical Wnt pathway in *C. elegans*.

In *C. elegans*, Wnts are known to regulate axon guidance. In the D-type neuron DD6, the most posterior of the GABAergic D-type motor neurons during the L1 stage, loss of function (lof) mutations in the Wnt ligand *lin-44* lead to overgrowth of the DD6 dorsal axon [38]. This overgrowth was also seen in *egl-20* lof animals, but not in animals with mutations in *mom-2*, *cwn-1*, or *cwn-2*, the more anteriorly expressed Wnt ligands. Additionally, in *lin-44*; *egl-20* animals, the axons were significantly more overgrown than in either of the single mutants [38]. This suggests that it is localized, posterior Wnt signals that act as termination signals for this axon. Wnt and Frizzled also function to direct the anterior/posterior growth of the developing neurites of the AVM and PVM mechanosensory neurons, with *egl-20* acting as a posterior repellent to promote anterior growth [39]. As a final example, *lin-44* and *egl-20* also function to promote dendritic neurite outgrowth in the PQR sensory neuron, and both act through the *lin-17*

Frizzled receptor [40]. Thus, in multiple different types of neuron within the *C. elegans* nervous system, Wnts play a vital role in directing the growth, repulsion, and termination of the outgrowing neurites.

The Wnt pathways have also been (and were first) found to be involved in axon growth in mouse and *Drosophila* models (for review see [41-44]). As an example, dopaminergic neurons within the mouse ventral midbrain rely on Wnt5a and a noncanonical Rac1 pathway to first promote neurite elongation and then, after time and a shift in expression, to repress that same neurite elongation [45]. New research has even shown that the canonical Wnt pathway is involved in vertebrate axon guidance. Specifically, when LRP5/LRP6, a Wnt co-receptor that functions with Frizzled, or β-catenin were silenced, there was a significant increase in axon pathfinding errors in the DI1 neuron [46]. In the *Drosophila* ventral nerve cord, WNT5a functions noncanonically via a receptor complex of derailed/RYK and Src tyrosine kinases to promote proper growth of the anterior commissure [47]. It is interesting to note that in *D. melanogaster* [48] and *C. elegans* [49], derailed/RYK (*lin-18* in *C. elegans)* can function on its own as a receptor, while in vertebrate models, derailed/RYK appears to function as a co-receptor with Frizzled in Wnt signaling [50]. However, on a larger scale, the literature overall shows that both the canonical and noncanonical Wnt pathways are involved in the development of the nervous system, including, but not limited to, directing axon growth. Additionally, the manner in which the pathway is able to act in axon growth, specifically when directing both outgrowth and attenuation of growth, has yet to be fully described.

1.5 Hox genes in *C. elegans* development

Hox genes as a group are highly conserved. The Hox genes usually exist in clusters within the genome, and they function during development to specify segment identity and placement within the body. Notably, Hox genes often specifically pattern the anterior/posterior axis, and they are expressed along

that axis in the order that they are present within the gene cluster (for review see [51]). These clusters of genes are thought to have undergone their first duplication sometime between the divergence of sponges and hydra, and, since then, have continued to duplicate and diverge throughout evolutionary history (for review see [52]). Hox genes were first discovered in *D. melanogaster*, where mutations within the bithorax and antennapedia complexes lead to severe changes in segment identity [53-55]. Hox genes have a similar role in the *Drosophila* CNS, where they are involved in specification of embryonic and larval neuronal subtypes (for review see [56]). In the vertebrate nervous system, Hox genes are involved in specification of neurons within the hindbrain and spinal cord (for review see [57]). Interestingly, the Hox genes that act in the specification of the hindbrain and spinal cord are influenced by differential combinations of Wnt, retinoic acid (RA), and fibroblast growth factors (FGF) signaling, which ultimately patterns the hindbrain and spinal cord to generate the correct dorsal or ventral motor neurons [58]. Thus, even in vertebrates, there is a connection between Wnt signaling and the Hox genes in neuronal development.

C. elegans have an abbreviated Hox cluster, located on chromosome III and consisting of six Hox genes: *lin-39*, *ceh-13*, *mab-5*, *egl-5*, *php-3*, and *nob-1* (for review see [59]). These genes are, roughly, listed in the order in which they are expressed in the animal. With *ceh-13* [60] being the most anterior, and more importantly for this work, *egl-5* being expressed in the posterior [61], followed by *php-3* and *nob-1* [62] expressed most posteriorly in the tip of the tail. This is especially important to note, since Hox genes are expressed within specific regions of the body, and thus will only act as transcription factors in those specific regions where they are expressed. This lends them well to having a role in specification, since they can co-function with more generally expressed transcription factors, to induce spatially specific gene expression profiles, thus leading to unique cellular subtypes.

Hox genes are known to function in development within *C. elegans*. As an example, the Hox gene *egl-5* is required for the development of the HSN neurons in *C. elegans*. *egl-5* regulates the expression of the HAM-2 and UNC-86 transcription factors within the HSN, which are required for proper differentiation of the HSN neurons [63]. Further, *egl-5* aids in differentiating the HSNs from the PHBs. Here, *egl-5* is expressed with *ham-1* in the precursor cell for both the HSNs and the PHBs, but only has continued expression in the HSNs [64]. Additionally, *egl-5* has been shown to act as a terminal selector in the touch receptor neurons (TNRs). Specifically, *egl-5* works in concert with *unc-86* to drive the activation of *mec-3* in TRN fate identity [65]. This example succinctly shows both that Hox genes are involved in the development of the nervous system, and, relevantly, demonstrates a key quality of terminal selectors, in that they often work in conjunction with other transcription factors, *i.e*. *egl-5* and *unc-86*, to drive unique gene expression changes which confer specific neural identities.

During *C. elegans* development, Hox genes and Wnts are known to intersect. One such area is in the specification of the P12 cell fate. During P12 cell fate specification, there are two cells, one of which will adopt the P12 fate, and the other which will adopt the P11 fate. However, both precursor cells are capable of adopting either fate. In *egl-5* animals, the P12 cell fate fails to be adopted by the precursor cells, leaving animals with two P11 cells [66]. Further work reported that *mab-5*, another Hox gene, was involved in the promotion of the P11 fate through an antagonistic relationship with the P12 promotion factors, and that Wnt signaling via *bar-1*, in the absence of *egl-5* and *mab-5*, still promotes P12 fate specification, given that the *mab-5; egl-5; bar-1* mutant had significantly more incidents of P12 to P11 changes than the *mab-5; egl-5* double alone [67]. While there are other factors involved in P12 fate specification, such as the epidermal growth factor (EGF) pathway, along with *php-3* and *nob-1*, this is still a clear example of the Wnt pathway acting with *egl-5* in a developmental context to drive cell fate specification and differentiation. To list a few more examples, *bar-1* has also been shown to regulate the

Hox gene *lin-39* during vulval development in the *C. elegans* hermaphrodite [68]. Wnts also activate the Hox gene *mab-5* in the formation of rays in the male tail [69], and in the Q cells of the nervous system, the Wnt ligand *egl-20* (and the β-catenin *bar-1*) is essential for proper expression of *mab-5* in the QL neuroblast [70]. Together, these provide a small sample of the developmental contexts in which Hox genes and the Wnt signaling pathway intersect.

Thus, given what is known about Wnts and Hox genes, and what is still unknown about the factors that govern axon guidance, we sought to examine their role in axon growth in the D-type GABAergic motor neurons. We hypothesized that *egl-5* was a downstream factor of Wnt signaling, and, later, that this system was also acting in the role of a terminal selector for specifying and maintaining the identity of VD13, the most posterior D-type neuron. Functioning in a way similar to that of a terminal selector is not an unheard-of role for Wnts or Hox genes. Wnts have been shown to regulate other genes required for proper axon pathfinding. In the zebrafish dorsal retina, continuous Wnt signaling is required to activate BMP to maintain the identity of the dorsal retinal domain [71]. Additionally, as mentioned above, *egl-5* has been shown in other contexts to function downstream of the Wnt pathway, and, in particular, may be a good candidate terminal selector, due to its role in development and the observation that once turned on in the nucleus, it rarely turns off, a key factor in the terminal sectors role in maintaining a cells identity throughout the life of the cell [61].

Here, we begin with Chapter III, where we show that the Wnt signaling pathway, via the Hox gene *egl-5*, appears to act as a terminal selector for the D-type GABAergic motor neuron, VD13. In Chapter IV, we further explore the specification of VD13 via the *lhIs97* transgene. Additionally, using our VD13 specific marker, we performed a mutagenesis screen for heat-sensitive alleles. Through this screen, we recovered eight potential candidates to further explore factors that are involved in specification and axon guidance. Finally, in Chapter V, we further explore the role that Wnt signaling has in instructing the

growth of VD13 during development, specifically of the ventral posterior neurite of DD6 and VD13. Overall, we show that the Wnt pathway functions in both specification and the guidance of axon growth, two key parts of neuronal development.

Chapter II: Methods

Sections 2.2, 2.3, 2.4, 2.7, and parts of 2.1 were published along with Chapter III on March 3, 2020 in *The Journal of Developmental Biology [72].*

2.1 Strains and Genetics

N2 (var. Bristol) was used as the wild-type reference strain in all experiments. Additionally, CB4856, a CB isolate of "Hawaiian strain" HA-8, was the wild type strain used for SNP mapping in the DNA sequencing performed in Chapter IV. Strains were maintained at 18–22°C, using standard maintenance techniques as described [73]. Alleles used in this report include LGI: *lin-44(n1792), lin-17(n671), pop-1(hu9)*, *bli-3(im10), mab-20(ev788)*, *unc-55 (e402*), *ncx-4(tm5106);* LGII: *mig-5(rh94), mig-5(tm2639), dsh-1(ok1445), dsh-2(or302)*, *plx-2(ev733)*, *cwn-1(ok546);* LGIII: *egl-5(n945);* LGIV: *egl-20(gk453010), egl-20(lq42)* [74], *egl-20(gk453010*), *egl-20(n585*), *cwn-2 (ok895*); LGV: *mom-2(or77*); LGX: *sdn-1(zh20)*, *bar-1(ga80).* The following integrated strains were used: LGII: *juIs76* [*Punc-25::gfp*]; LGV: *wgIs54* [*Pegl-5::egl-5::gfp*]; LGX: *lhIs97* [P*plx-2*::*mCherry*], *lhIs93* [*Punc-25::egl-5*], *oxIs12* [*Punc-47::GFP*]. The following extrachromosomal arrays were generated and used in this report: *lhEx609, lhEx610* [P*plx-2*::*rfp*], *lhEx555* [P*unc-25*::*egl-5 cDNA*], *lhEx608*. The *lhEx555* array was generated by injecting pEVL479 (P*unc-25::egl-5*) into wild-type animals at 2 ng/µl, along with pBA183 (P*myo-2::mCherry*) at 5 ng/µl. The *lhEx609, lhEx610* arrays were generated by injecting pEVL551 into wild-type animals at 5 ng/µl along with P*str-1::gfp* at 20 ng/µl. *lhEx609* was integrated into the genome using ultraviolet light and tetramethylpsoralen (UV/TMP), to generate *lhIs97,* and backcrossed to wild-type six times prior to use. The *lhEx608* array was generated by injecting a DSH-2 genomic PCR product along with pEVL387 [Punc-25::mCherry::unc-43 3' UTR) at 2 ng/ul (DSH-2).

2.2 Plasmid Construction

pBA102 (P*plx-2::cfp::unc-54 3'utr*) contains a segment of the *plx-2* promoter (nucleotides -3863 to -871 with respect to the start of translation). pBA102 was digested with *Bam*HI and religated to create a shortened *plx-2* promoter (contains nucleotides -1089 to -871, with respect the start of translation, to create pEVL530 (P*plx-2*::*cfp*::*unc-54* 3'UTR). pEVL387 (P*unc-25*::*mCherry*::*unc-43 3'UTR*) was digested using *Xma*I and *Spe*I and ligated to pEVL550 digested with *Xma*I and *Spe*I to generate pEVL531 (P*plx-2::mCherry*::*unc-43 3' utr*).

The *egl-5* cDNA was amplified from total RNA that had been converted to cDNA using random hexamer oligos and superscript III reverse transcriptase (Life Technologies). The cDNA was amplified using the following primers, *egl-5*F1 5'-ttggaaagcagtgagagtgag-3' and *egl-5* R1 5'-ggagggatcattgagaaacttgag-3' and inserted into a vector with the *unc-25* promoter and unc-54 3'UTR using LR Clonase (Life Technologies).

2.3 Fluorescence Microscopy

The complete set of GABAergic MNs was visualized using *juIs76,* while VD13 and the LUAs were scored using *lhIs97*. Scoring and imaging were done using an Olympus FV1000 laser-scanning confocal microscope with the Fluoview software. Animals with posterior neurites (Pdns) or spurious *lhIs97* expression in DD6 were not included in the shape analysis of VD13. Images were exported to ImageJ to be rotated and/or cropped for presentation. The ImageJ Image Calculator function was used to make the image of the intersection between *juIs76* and *lhIs97.*

2.4 Statistics

Fisher's exact test was used to evaluate statistical significance between genotypes, and calculated with Prism GraphPad (5.0) or GraphPad QuickCalcs (http://www.graphpad.com/quickcalcs/). All genotypes were scored on a minimum of two different days, and the results averaged between scoring sessions. We set a threshold of $P < 0.005$ to determine significance to account for multiple testing. The standard deviation of the population was used to calculate error bars for the reported VD13(+) expression in the varying genotypes, as well as in the axon growth data, was calculated using Microsoft Excel 2016.

2.5 Mutagenesis Screen

Ethyl methanesulfonate (EMS) mutagenesis was conducted as previously described [73]. *juIs76; lhIs97* animals were grown up using standard techniques, washed off of plates and then added to 50mM EMS and left at room temperature for four hours with agitation. After the incubation period, the worms were washed, EMS was inactivated, and then the worms were moved to NGM plates with *E. coli* and left overnight at 20°C. The next morning, five plates were started, each with five surviving young adults, and moved to 25°C. From those P0s we generated ~500 plates, each started with 4-5 F1s, for a total of ~2000 haploid genomes screened. F2s were screened for the VD13 (RFP-) phenotype, where the mCherry expression from our *lhIs97* marker was lost in VD13, but not the LUAs. Individuals which did show the VD13 (RFP-) phenotype were individually plated, so that the offspring could be monitored and further examined.

2.6 Library Prep and Genetic Mapping

To prepare for sequencing the eight candidate mutation lines (*lh39-lh46*) were crossed to Hawaiian (*CB4856*) males. Animals were then allowed to self-fertilize and homozygous, after which animals that continued to display the loss of expression (VD13-) phenotype were selected. These animals (total 9-24 per line) were allowed to self-fertilize, until plates were just overgrown. Animals were then washed off and their DNA was extracted. DNA was quantified utilizing a Qubit. Once extracted, the DNA per animal was calculated, and diluted so that the final, combined DNA per line was equalized per animal. We then attached Illumina primers via the Nextera Illumina Sequencing kit, DNA concentrations were rechecked via Qubit and Tapestation, then DNA libraries were pooled and submitted for sequencing at The University of Kansas Genome Sequencing Core. Raw FASTQ files were uploaded to https://usegalaxy.org/ and processed using the Galaxy platform [75]. Within Galaxy, the specific programs used were: fastp [76], Map with BWA-MEM [77], Samtools merge [78], RmDup [78], and FreeBayes [79]. The final VCF file was then exported from Galaxy to Microsoft Excel 2016, and the unique variants were selected for from each candidate line. The Integrated Genome Viewer [80] (https://software.broadinstitute.org/software/igv/home) was used to view .bam files to determine if variant SNPs were located in coding regions of genes, and ApE: A Plasmid Editor (https://jorgensen.biology.utah.edu/wayned/ape/) was used to determine the effects of those variant SNPs, to determine candidate mutations.

2.7 Data Availability

All strains, plasmids and genomic sequencing data described herein are fully available upon request.

Chapter III: The Hox Gene *egl-5* Acts as a Terminal Selector for VD13 Development via Wnt Signaling

This chapter was published on March 3, 2020 in *The Journal of Developmental Biology* [72].

Abstract

Nervous systems are comprised of diverse cell types that differ functionally and morphologically. During development, extrinsic signals, *e.g*., growth factors, can activate intrinsic programs, usually orchestrated by networks of transcription factors. Within that network, transcription factors that drive the specification of features specific to a limited number of cells are often referred to as terminal selectors. While we still have an incomplete view of how individual neurons within organisms become specified, reporters limited to a subset of neurons in a nervous system can facilitate the discovery of cell specification programs. We have identified a fluorescent reporter that labels VD13, the most posterior of the 19 inhibitory GABA (γ-amino butyric acid)-ergic motorneurons, and two additional neurons, LUAL and LUAR. Loss of function in multiple Wnt signaling genes resulted in an incompletely penetrant loss of the marker, selectively in VD13, but not the LUAs, even though other aspects of GABAergic specification in VD13 were normal. The posterior Hox gene, *egl-5,* was necessary for expression of our marker in VD13, and ectopic expression of *egl-5* in more anterior GABAergic neurons induced expression of the marker. These results suggest *egl-5* is a terminal selector of VD13, subsequent to GABAergic specification.

Introduction

Nervous systems are organized into functional units comprised of diverse cells. Knowing a cell's identity enables us to trace its lineage, describe the architecture and connectivity of networks and elucidate the physiology of organismal behaviors. The original attempt to systematically categorize neurons was by Ramon y Cajal, who beautifully illustrated conserved, distinguishing neuronal morphologies in different animals [81]. Today, neuroscientists categorize neurons using anatomical, morphological, molecular, or functional criteria, *e.g*., hippocampal, pyramidal, tyrosine hydroxylase or motor neuron, *etc.,* are different, but informative, labels for specific classes of neurons.

During development, neurons acquire differential features through iterative rounds of specification in a hierarchical fashion. These rounds are driven by both extrinsic cues, which provide spatial information to the cells, and intrinsic transcriptional programs orchestrated by transcription factors and terminal selectors. For example, motorneurons (MNs) within the vertebrate spinal cord are initially specified by Olig2 [82, 83], after which they organize into discrete motor columns along the anterior-posterior axis [84, 85], and then into subtypes or motor pools, which correspond to specific muscle regions within the limbs. Many different transcription factors exhibit selectivity for the different sub-divisions along the A/P axis and within the functional regions (for review see [86, 87]). Of these, Hox genes play a critical role in multiple events of MN specification along the A/P axis (for review see [88]).

Caenorhabditis elegans (*C. elegans*) have both excitatory (cholinergic) and inhibitory (γ-amino butyric acid/GABA-ergic) MNs. These MNs collaborate to control body wall muscles to produce smooth sinusoidal locomotion. MNs can be categorized based on when they form, the specific body regions innervated and their function. The loss of GABAergic MN function results in a "shrinker" phenotype, which enabled screens for genes that regulate GABAergic specification and function [89]. Two of those genes—*unc-25,* which encodes glutamatergic acid decarboxylase, the final biosynthetic step in GABA

synthesis, and *unc-47,* which encodes the vesicular GABA transporter—have provided differentiation markers that have also been used to further understand GABAergic specification [90, 91].

There are several genes that have been identified to play a role in GABAergic specification. *cdn-1* is necessary for the proper specification and differentiation of both GABAergic and cholinergic MNs [92]. *unc-30* functions downstream of *cdn-1* to specify the fate of the D-type GABAergic MNs [93, 94]. The Aristaless homolog, *arl-1, unc-62* and *unc-55* repress DD-like fates and promote the specification of VD fates [95-98]. Together, these provide a small subset of the genes that are involved in the specification of GABAergic MNs in *C. elegans.*

Here, we report a new marker specific for the most posterior GABAergic D-type MN, VD13, and a pair of bilaterally symmetrical neurons that we have tentatively identified as the LUA neurons, LUAL and LUAR. Using this marker, we observed developmental defects in the morphology of VD13 in animals with mutations in Wnt signaling genes, including animals where expression of the marker was lost from VD13, but not the LUAs. Expression was completely lost in VD13 in animals lacking the β-catenin, *bar-1*, and the Hox gene, *egl-5*. Additionally, we found redundant function in regulating expression for two disheveleds (*dsh-1* and *mig-5*) and two Wnt ligands (*lin-44* and *egl-20*). Our results indicate that Wnt signaling promotes *egl-5* to function as a terminal selector for the VD13 fate.

Results

3.1 Isolation of a VD13-Selective Marker

There are 19 GABAergic primary motorneurons (MNs) in the *C. elegans* locomotor circuit. The six dorsal D-type (DD) neurons form during embryogenesis [99]. These neurons are presynaptic to the ventral body wall muscles during the first larval stage (L1) [26]. However, during L1, the 13 ventral D-type (VD) neurons begin forming. The most anterior neuron, VD1, forms first, while the most posterior, VD13, forms last. During the L1 stage the DD neurons remodel to innervate the dorsal muscles, as VD neurons innervate ventral muscles [26, 100, 101].

Using GFP (green fluorescent protein) reporters under the control of GABA-specific promoters, several labs have investigated the development of the GABAergic MNs. Briefly, the D-type GABAergic MNs share a common morphology, a sideways H shape, with the cell body on the ventral midline. During development, the cell body extends an axonal-like process anteriorly, from which a commissural process forms, and bifurcates at the dorsal nerve cord, where anteriorly and posteriorly directed processes extend [102]. In general, the processes reach to the next D-type neuron of the same class to ultimately become tiled along the body (Figure 1).

We serendipitously isolated a reporter transgene active in VD13 and the bilaterally symmetrical LUA neurons. This transgene uses a fragment of DNA upstream of the *plx-2*/Plexin gene [103]. We created an integrated transgene, *lhIs97,* with this promoter fused to mCherry (Figure 1). In conjunction with a pan-GABAergic MN marker *juIs76* (P*unc-25::*GFP) [104], mCherry and GFP overlapped uniquely in VD13 (Figure 1). The cell-selective expression of the *lhIs97* transgene suggested VD13 was undergoing developmental events separate from other GABAergic MNs.

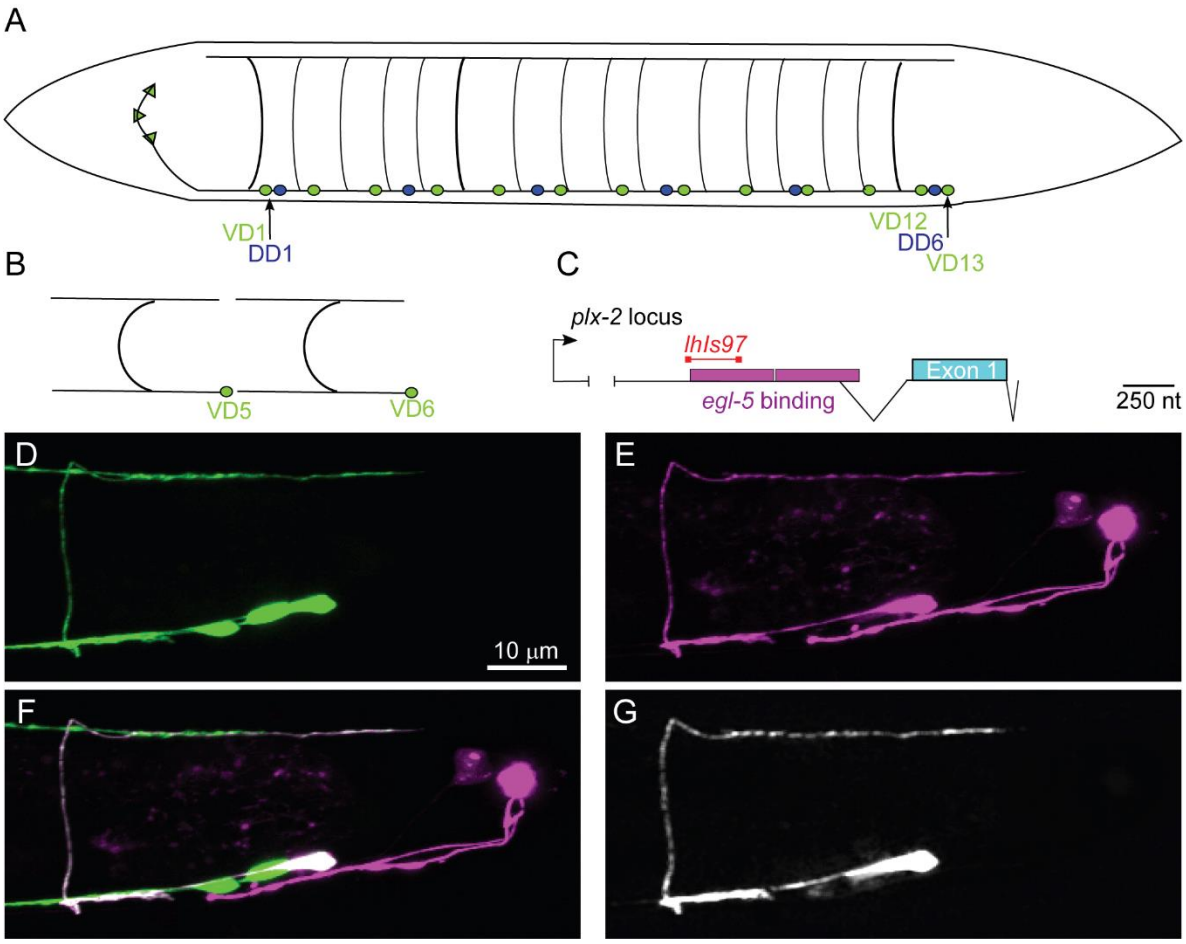

Figure 3.1. *lhIs97* is a VD13-selective GABAergic motorneuron (MN) marker. **A**) A schematic of the 19 GABAergic MNs. DD1 and VD1 are the most anterior and VD13 is the most posterior. **B**) The characteristic tiled H shape of the VD neurons is illustrated. **C**) A schematic of the *plx-2* locus. The region upstream of the *plx-2* first exon contains two *egl-5* binding sites [105]. RNASeq experiments have identified an intron in the 5' region (indicated by the branched line). The segment of the promoter used to generate the *lhIs97* marker is indicated in red. **D**–**G**) The posterior region of an *lhIs97* wild-type animal showing GABAergic GFP (**D**), *lhIs97*-expressed RFP (**E**), the merge of the two channels (**F**) and the overlap of the GFP and RFP channels, which is exclusive to VD13 (**G**).

In wild-type animals, we found that, rather than being "H" shaped, VD13 was most frequently "C" shaped (82 ± 1% of animals observed) (Table 1, Figure 2). In approximately 9% of animals, the cells had either a T shape where the cell extended an additional, anteriorly directed process in the dorsal nerve cord, or only an anterior process ("P" shaped). Interestingly, we also found that in 9% of animals no

VD13 commissural process was visible (“N” shaped), or it formed, but failed to reach the dorsal nerve cord (“O” shaped). We subsequently grouped these as either polarity defects (“T” or “P” shaped) or formation defects (“N” or “O” shaped).

Next, we examined animals with the starting extrachromosomal array, *lhEx609,* to determine whether these altered morphologies were caused by the insertion of the transgene. We found that the proportion of morphologies was largely consistent. That is, 73% of animals had a C shape. In total, 10% of animals lacked a visible VD13 commissure (“N” shaped), while a minority of animals had misrouted VD13 axons (“O” shaped). Failure of VD13 to form a commissure or to be misrouted is extremely rare in wild-type *juIs76* animals. Thus, we conclude that the P*plx-2* transgene itself can have a small effect on VD13 development. Overall, though, none of the animals we examined had an “H” shaped VD13, which is typical of the other GABAergic MNs. These data argue that the morphology of VD13 could be slightly variable but is principally “C” shaped in wild-type animals. The cell-selective expression of *lhIs97* also suggested that VD13 exhibits characteristics different from the other GABAergic MNs.

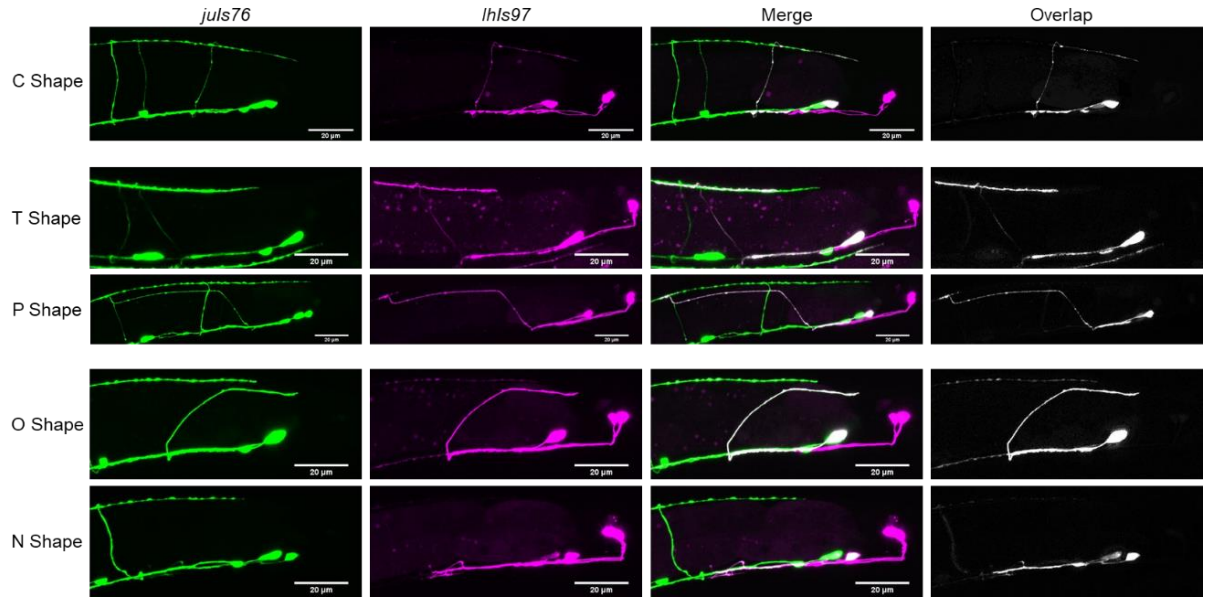

Figure 3.2. Different VD13 morphologies observed. The most common shape of VD13 in *juIs76; lhIs97* animals was a C shape. Aberrant morphology categories observed were either in the dorsal cord polarity ("T" or "P" shaped) or commissural outgrowth and guidance ("O" or "N" shaped). Note, the "C", "T", and "O" shaped morphology examples are wild-type animals, "N" shaped, *dsh-1* mutants, and "P" shaped from *egl-20* mutants.

3.2 VD13 Morphology is Dependent on Wnt-Signaling

Previous work has shown that canonical Wnt signaling regulates the development of posterior GABAergic neurons [38]. In *C. elegans*, there are five genes encoding Wnt ligands (*cwn-1, cwn-2, egl-20, lin-44,* and *mom-2*). Of those, *mom-2*, *egl-20*, and *lin-44* are expressed in the posterior of the animal where they are in a position to influence VD13 [33].

We visualized VD13 in animals lacking either *lin-44* or *egl-20*. We found that animals lacking *lin-44* or *egl-20* frequently had VD13 axons that grew past the normal termination point for VD13, similar to previous reports [38]. We also observed VD13 with posteriorly directed neurites (Pdns) emanating from the cell body, confirming these can come from VD13 [106]. Based on these observations we concluded that *lhIs97* was enabling us to confidently observe previously characterized defects in GABAergic neurons.

We then characterized the different neuronal morphologies in the Wnt ligand mutants (Table 1). We found that, in general, when *lin-44* was compared to the wild-type, the same distribution of shapes was found, with no significant differences. The loss of *egl-20* resulted in a significant increase in polarity defects, but not in the formation or completion of commissural outgrowth.

We next analyzed loss of function mutations in *lin-17/*Frizzled*, dsh-1/*Disheveled and *mig-5/*Disheveled, and we categorized the penetrance of the different shapes of VD13 neurons in these mutants (Table 1). In the *lin-17, mig-5* or *dsh-1* mutants, we found a significant increase in the penetrance of dorsal polarity defects, ("T" or "P" shaped neurons), suggesting the polarized growth of neurites in the dorsal nerve cord relied on the function of these proteins. Loss of function in *lin-17* or *dsh-1* had no discernable effect on commissure formation, while there was a significant increase in formation and outgrowth defects in animals lacking *mig-5*. Thus, we confirmed that loss of Wnt signaling genes affected VD13 development, where mutations in ligands versus downstream effectors can be distinct, as has been previously reported [38].

Table 3.1. VD13 morphology by genotype.

Genotype	**N**	**C Shape**	**Polarity (T/P)**	**Outgrowth (N/O)**
wild type (*lhIs97*)	161	82%	9%	9%
lin-44(n1792)	88	77%	18%	5%
			(*P* = 0.0446)	(*P* = 0.3135)
egl-20(gk453010)	159	64%	23%	14%
			(*P* = 0.003)	(*P* = 0.0769)
lin-17(n671)	40	48%	50%	3%
			(*P* < 0.0001)	(*P* = 0.6961)
mig-5(rh97)	85	36%	52%	12%

			(*P* < 0.0001)	(*P* = 0.0339)
dsh-1(ok1445)	177	24%	71%	5%
			(*P* < 0.0001)	(*P* = 0.2113)

3.3 Expression of *lhIs97* in VD13 is Dependent on Certain Wnt Pathway Genes

In the course of examining the morphology of VD13 in Wnt signaling mutants, we discovered that mutations in *lin-44, egl-20, lin-17* or *mig-5,* but not *dsh-1*, resulted in an occasional loss of RFP expression in VD13. These animals continued to exhibit expression in the LUA neurons, and VD13 was still present (as labeled by *juIs76*)*,* indicating the neurons were still being specified as GABAergic MNs (Figure 3). The penetrance of the *lhIs97* "off in VD13" phenotype was 22% in *lin-44,* <1% in *egl-20*, 30% in *lin-17* and 54% in *mig-5* animals (Figure 3).

To determine whether *dsh-1* was compensating for the absence of *mig-5,* we analyzed *dsh-1mig-5* double mutants. We found that in this background, *lhIs97* expression in VD13 was lost in 100% of animals analyzed (Figure 3). We next generated *lin-44; egl-20* double mutants, and these animals also exhibited a synergistic decrease, with only ~2% positive for RFP (98% lost expression) (Figure 3). These data indicate that *lin-44* and *egl-20* contributed to VD13 specification in parallel. Finally, we tested the dependence of RFP expression on *bar-1,* which encodes a β-catenin ortholog that functions downstream of *lin-44* in many contexts. We found that *lhIs97* was integrated on the X chromosome, near *bar-1,* and thus, we used the *lhEx610* transgene to examine *bar-1* mutants. Animals lacking *bar-1* also failed to demonstrate expression of the *Pplx-2* transgene in VD13, with 96% losing RFP expression in VD13 (Figure 3). Again, the LUA neurons were grossly unaffected and *juIs76* expression was intact. Overall, these results indicate that the canonical Wnt signaling pathway is critical for VD13 identity, subsequent to GABAergic MN specification.

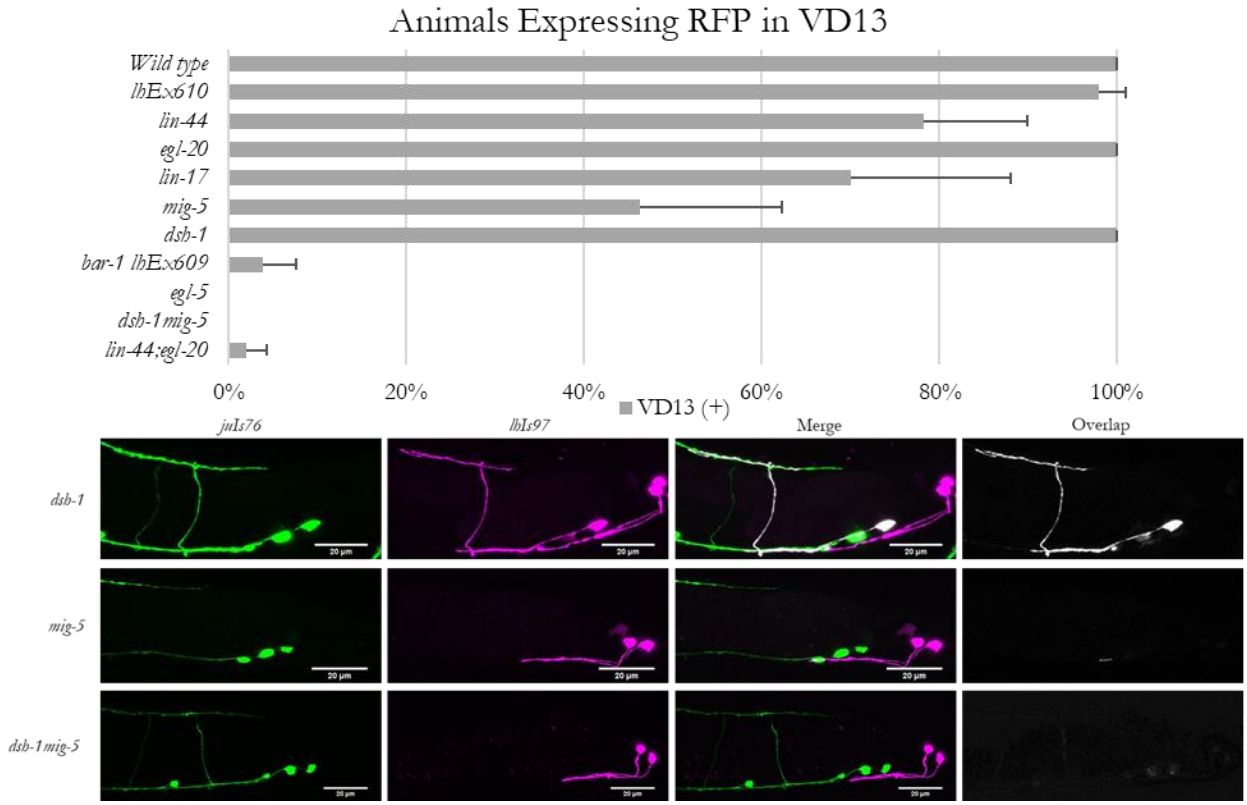

Figure 3.3. Expression of *lhIs97* is selectively lost in VD13 in Wnt loss of function animals. Animals were scored for the presence or absence of RFP in VD13. The percentage of animals (mean ± s.d.) that expressed RFP in each genetic background is presented in the graph. Below are examples of RFP expression being present in VD13 in *dsh-1* mutants, but absent in the majority of *mig-5* single mutants and all *dsh-1mig-5* double mutants.

3.4 *egl-5* is Necessary for *lhIs97* Expression in VD13

The severe perturbation of *lhIs97* expression in the *dsh-1mig-5* and *lin-44; egl-20* doubles led us to look at potential transcriptional targets of the Wnt pathway. Here, Hox genes were obvious candidates. *C. elegans* have an abbreviated Hox cluster with three genes: *lin-39, mab-5,* and *egl-5.* Of these, *egl-5* is the most posterior. The *plx-2* promoter was found to contain an *EGL-5* binding site by chromatin immunoprecipitation (ChIP) [105] (Figure 1). We found that *egl-5* was expressed in VD13 and the LUA neurons using an *EGL-5*::GFP translational fusion (*wgIs54)* (Figure 4). We noted that there were many

cells that expressed *EGL-5* but were not RFP positive in *lhIs97* animals. Thus, *egl-5* is not sufficient to activate RFP expression, but cells that express RFP also express *egl-5.*

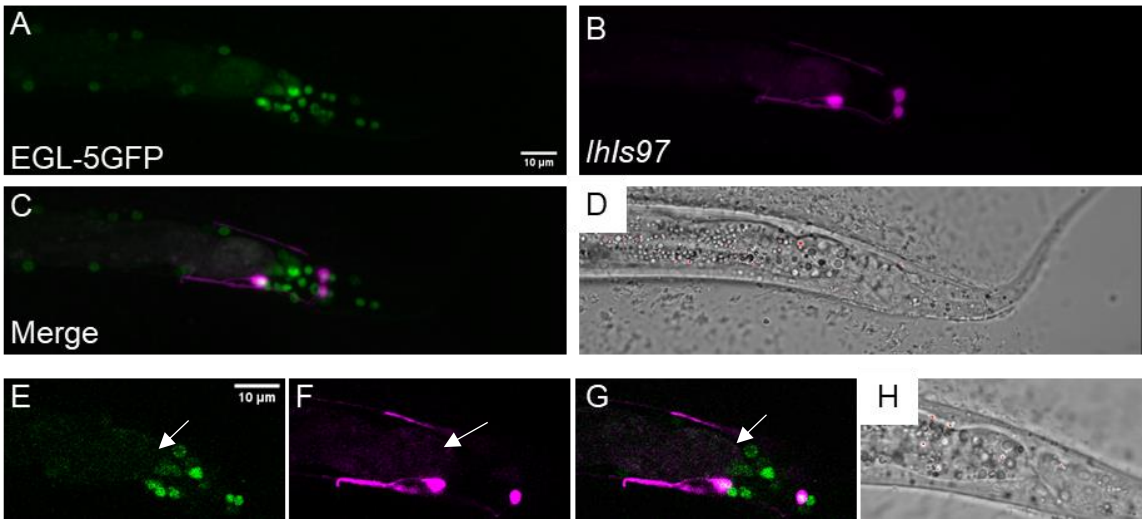

Figure 3.4. *egl-5* is expressed in VD13 and the LUA neurons. **A**) *EGL-5*::GFP, under the control of the *egl-5* promoter, was observed in the posterior of the animal. **B**) *lhIs97* expresses RFP in VD13 and the LUAs. **C**) The signal is co-incident in both cells, suggesting that *egl-5* is expressed in both VD13 and the LUAs. **D**) A transmitted light image of the region. **A**–**D**) A z-projection through the entire animal. **E**–**H**) A single plane image through the center of VD13. The arrow indicates VD13.

We crossed *lhIs97* into a loss of function mutation in *egl-5, n945,* and found that it led to total loss of expression of RFP in VD13 (Figure 5). As with the Wnt mutants, RFP expression was maintained in the LUA neurons and VD13 was still GFP positive by *juIs76* in *egl-5* mutants. Thus, despite the fact that *egl-5* was expressed in the LUAs, it was not essential for expression of RFP in these neurons.

We attempted to rescue *lhIs97* expression in VD13 by expressing *egl-5* using a GABAergic-specific promoter, *unc-25*. We found that, in addition to recovering RFP in VD13, expression of RFP was ectopically activated in all 19 of the GABAergic MNs (Figure 5). Overall, these results indicate that *egl-5* is both necessary and sufficient for activating the *plx-2* promoter in the GABAergic MNs. However, in non-GABAergic neurons, we do not find that the presence of *egl-5* is sufficient to activate RFP

expression from *lhIs97.* Finally, despite the ectopic *egl-5*-dependent expression of RFP in the anterior GABAergic MNs, we did not specifically note that these cells now adopted a C shape. This is not uncommon for Hox transformations, where it is apparently more frequently observed that posterior cells can be transformed to more anterior-like fates by misexpression of Hox genes, but rarely vice versa.

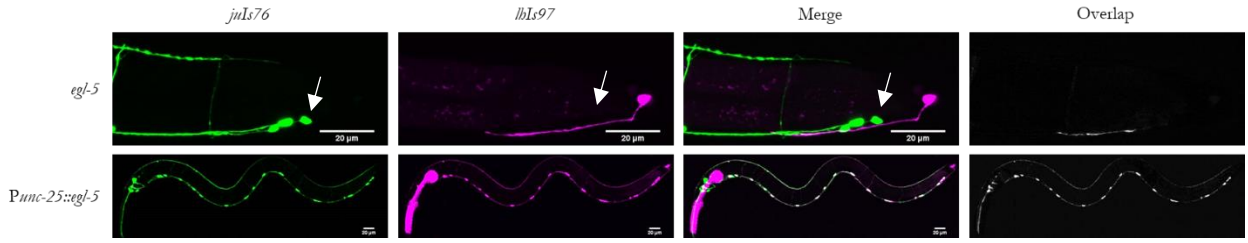

Figure 3.5. *egl-5* is necessary and sufficient for *lhIs97* expression in GABAergic neurons. Top row, *egl-5*(*n945*) mutants have lost RFP in VD13 (arrow). Bottom row, ectopic expression of *egl-5* in all GABAergic neurons results in RFP expression in these cells.

Discussion

In *C. elegans*, the loss of a single transcription factor can result in a complete loss of specific behaviors. For example, *ttx-3* results in thermotaxis defects, while the loss of *che-1* results in chemotaxis defects. Subsequent work has found that these transcription factors contribute to the unique identities of individual neurons that regulate these behaviors, which has led to the term "terminal selectors" being applied to these proteins [4, 96]. Terminal selectors bind to specific regions of promoters, activating gene expression in only a select set of cells. Part of the goal of understanding the acquisition of neuronal identity is to map terminal selectors to their responsive DNA segments.

Here, we have found a relatively short segment of DNA that is upstream of the *plx-2*/Plexin gene. This 218 bp fragment, when placed upstream of an mCherry reporter gene, results in the expression of RFP in only three of the 302 neurons in the *C. elegans* nervous system. Of these neurons, one is a GABAergic MN, VD13, and two are bilaterally symmetric interneurons (LUAL and LUAR). VD13 and the LUAs are apparently only related by their proximity to one another in the tail of the animal.

Interestingly, we found that mutations in genes in the Wnt signaling pathway, most specifically, the posterior Hox gene, *egl-5*, resulted in a loss of RFP expression, specifically in VD13, but not the LUAs. Importantly, this loss of identity was not associated with a loss of the GABAergic identity, as these cells still expressed the post-differentiation marker, *unc-25*. And, if we expressed *egl-5* in all GABAergic neurons, we observe robust RFP expression throughout the GABAergic MNs. Animals lacking *egl-5* did not exhibit any alteration in RFP expression in the LUAs, nor was RFP expressed everywhere *egl-5* is found in the animal. This suggests that the DNA segment contains a separate element that is activating expression in the LUAs, dependent on a different terminal selector. Altogether, these results suggest that within VD13, *EGL-5* is activating transcription from that DNA segment, suggesting this is a terminal

selector and DNA segment pair, and that this was occurring after VD13 was specified as a GABAergic MN.

This new marker will help us to better understand how GABAergic MNs develop and become individualized during development. Whether VD13 is unique in having another level of specification, or if other DD and VD neurons undergo additional layers of differentiation remains to be seen. In addition, using this promoter, we have shown that this combination of Wnt signaling is instructional for the morphology of VD13. The *lhIs97* reporter illuminates a "C" shaped neuron, versus the sideways H shape typical of the other D-type GABAergic MNs. The lack of anterior processes from the commissure in most of the animals examined suggests that the pattern of axon outgrowth in VD13 is distinct. Loss of *egl-20/*Wnt, *lin-17/*Frizzled and *mig-5* or *dsh-1/*Disheveled resulted in an increase in anterior projections along the dorsal cord. These results suggest that Wnt signaling is normally promoting growth in VD13 toward the posterior direction or inhibiting anterior growth. This is interesting in as much as Wnt ligands have been previously discovered as promoters of GABAergic axon termination in the posterior. This adds yet another layer of complexity in how this signaling pathway might affect neuronal development. The ectopic expression of *egl-5* throughout the GABAergic neurons did not obviously result in the adoption of the VD13 morphology, which suggests that either the morphology is independent of the *egl-5* program, or that anteriorizing factors, which instruct the formation of the H shape, are able to overcome ectopic *egl-5* expression.

This is not the only context where *egl-5* functions in this manner. Notably, *egl-5* functions in the touch receptor neurons (TRNs) to induce further morphological changes to define the PLM neuron, which differentiate them from the standard touch receptor AML neuron [107]. We do not see expression of our *egl-5*-dependent RFP reporter in the touch neurons, suggesting that *EGL-5* is regulating this via a different DNA contextual element in the TRNs. Thus, Wnt signaling and *egl-5* are used as terminal

selectors in multiple neuronal developmental contexts to differentiate neurons within established classes (*e.g*., mechanosensory, GABAergic, *etc.*).

Going forward, it is important to continue to define the interactions of the Wnt signaling pathway and *egl-5* in their role as terminal selectors. Namely, our results agree with previous work showing that the Wnt pathway can have some contradictory results when analyzing neural development. With regard to the expression of *lhIs97* in VD13, loss of the ligands and effectors appear to act equivalently. Conversely, with regard to the morphology of VD13, loss of the ligands is somewhat discrete when compared to the effectors. The consequences on morphology are consistent with other observations that Wnt ligand mutations result in axon termination errors, specifically observed as axon overgrowth. When analyzed, *lin-17/*Frizzled receptor mutants had both under and overgrowth, and the Disheveled adaptors, as well as the β-catenin *bar-1,* are exclusively undergrown [38]. In our hands, loss of Wnt ligands had only a modest effect on dorsal process polarity, while *lin-17, mig-5* and *dsh-1* had very strong effects. Within the specification of VD13, *lin-44; egl-20* double mutants were stronger than loss of *lin-17* alone, suggesting there are other Wnt receptors involved in this process. However, those double mutants were the same as removing *bar-1*, suggesting that *bar-1* is working downstream of both *lin-44* and *egl-20* in this event. Wnt signaling may then, somehow, be activating *bar-1* during early events (VD13 specification) but may function via a different mechanism during axon termination. Further defining this relationship and exploring factors downstream of *egl-5* will allow us to better define the manner in which these terminal selectors function to modulate gene expression during neural development.

Overall, though, our observations suggest that Wnt signaling is contributing to many different aspects of neuronal development for these neurons. The ability to use a cell-selective marker to interrogate those functions will enable new mechanistic questions to be asked. Unfortunately, due to the fact that loss of function in some Wnt signaling genes renders our single cell marker unusable, we cannot examine the

morphology of VD13 alone in the *lin-44, egl-20,* or *egl-5* mutants. However, knowing that there is an additional layer of specification that occurs in VD13 may enable us to find other markers that may be transcriptionally independent of Wnt signaling and permit us to visualize VD13 in those backgrounds.

Chapter IV: Further Exploring VD13 Specification via *lhIs97*

Abstract

During development, neurons undergo rounds of specification, a process which gradually assigns them a specific function. As such, specification is controlled via extrinsic and intrinsic factors, which work together to enact regulation of genomic transcription to ensure that a neuron is assigned its correct identity. Here, we utilize our previously described marker, *lhIs97*, which selectively marks the most posterior D-type GABAergic motor neuron, VD13, and the bilaterally symmetrical LUA neurons, to further examine the factors that are necessary for the specification of VD13. We look at one of the VD differentiation markers, *unc-55*, as well as the *lhIs97* promoter, *plx-2* and its ligand, *mab-20,* and find that they are not required for expression of *lhIs97* in VD13. Additionally, we find that the heparan sulfate proteoglycan, syndecan (*sdn-1* in *C. elegans*), is not involved in the specification of VD13, but may be involved in the differentiation of DD6 and VD13. Finally, we use our selective marker to perform a mutagenesis screen for conditionally expressed alleles, specifically those that are temperature sensitive. We find eight potential candidates. Each of these candidate lines has varying penetrance of *lhIs97*, which suggests that these eight lines may have mutations in conditionally expressed genes that are involved in the specification and axon guidance of VD13. Additionally, we begin to characterize those candidates, based on their expression of *lhIs97* in VD13, their VD13 morphology, and their axon growth, and find defects in all of these areas of their development in a select number of our candidate lines.

Introduction

One of the crucial elements of neuronal specification is the type of neurotransmitter that the neuron will use in transmitting signals. In vertebrates, GABAergic neurons exist in multiple locations within the brain, such as the cortex, the cerebellum, *etc*. In addition to this, there is not just one type of GABAergic neuron in these locations. This can be seen in the cerebellar cortex, where a population of Pax-2 expressing progenitor cells gives rise to the GABAergic neurons, and then these neurons are further differentiated via external and internal cues (For review, see [108]). Thus, these neurons, while all utilizing the neurotransmitter GABA, must have other identifying features that are involved in their specific specification.

The different types of GABAergic neurons can be distinguished in a number of ways. As an example, within the hippocampus there are multiple types of GABAergic interneurons, which innervate the pyramidal neurons that are also located within the hippocampus. These GABAergic interneurons can be distinguished in multiple ways, such as by their expression patterns, *i.e.* cholecystokinin versus parvalbumin, as well as which domains of the pyramidal neurons they innervate, their firing patterns, *etc*. [109]. So, multiple types of GABAergic neurons can exist in the same region and must be differentially specified so that they are assigned the correct subtype, and thus the correct function. Additionally, across both vertebrates and nematodes, which also utilize the neurotransmitter GABA, there appear to be conserved factors in GABAergic specification, such as the LIM homeodomain factors [110-112]. Thus, *C. elegans* provides an ideal system in which to continue to study the role of specification factors in development, given their relatively small nervous system and well characterized population of GABAergic neurons.

There are 26 GABAergic neurons in *C. elegans*, 19 of which are the D-type motor neurons [26]. As previously mentioned, these neurons are, in part, first specified as GABAergic via the activity of the

transcription factor *cdn-1*. *cdn-1* is required for activation of *unc-30* in the D-type neurons [92]. *unc-30* then goes on transcriptionally promote the expression of *unc-25* and *unc-47*, both of which are required for GABAergic specification and function, since they respectively synthesize GABA and function as its transporter [90, 93, 94].

Subsequent to specification as GABAergic, these neurons will be further differentiated to form two distinct classes of neurons that span the anterior/posterior axis: the dorsal D (DD) and the ventral D (VD) motorneurons. The DD neurons form first, during embryogenesis, and innervate both the dorsal and ventral body wall muscles until the VD neurons begin to form during the L1 larval stage. During this time of VD outgrowth, the DD neurons must rewire to only innervate the dorsal muscles. This rewiring of the DD neurons will allow the VD neurons to develop to properly innervate the ventral muscles. During this process, given that these two sets of neurons must innervate different muscles, it is important that these neurons be differentiated from one another. Previous work has shown that *unc-55* is necessary for the VD neurons to differentiate from the DD neurons [113], and *unc-62* is required for the proper expression of *unc-55* in the VD neurons [98]. In addition to *unc-62* and *unc-55*, the Aristaless paralog *arl-1* is required for the differentiation of the VD neurons, and appears to function in parallel to *unc-55* in defining the VD differentiation from the DD neurons [95, 96]. Thus, there are multiple genes that are involved in the differentiation of the VD neurons.

arl-1 is not the only gene to function in parallel to *unc-62* and *unc-55* during the specification and growth of the D-type neurons. The heparan sulfate proteoglycan, syndecan (*sdn-1* in *C. elegans*), has been shown to function in other aspects of neurite growth, such as in the outgrowth of the AIY interneurons, along with ephrin *efn-4* [114]. Additionally, *sdn-1* appears to function in axon guidance for the HSN, PVQ, and D-type motor neurons [115]. As the previous work examined the commissures of the D-type motor neurons, work from our lab furthered showed *sdn-1* is also involved in regulation of axon

outgrowth (unpublished [116], preprint [117]). Thus, we sought to further elucidate the effect that loss of *sdn-1* had on axon growth by examining animals with both *sdn-1* loss and *lhIs97*, our VD13 marker.

In an effort to continue to define additional genes acting either downstream of, or in parallel to, the Wnt pathway in VD13 specification and axon growth, we performed a mutagenesis screen. We utilized the loss of expression (VD13-) of *lhIs97* as our marker for potential candidates in this pathway. Additionally, we used this screen to look for temperature sensitive alleles. Temperature sensitive mutations are a form of conditional gene expression, though they can also affect protein function as well as protein stability. As such, temperature sensitive mutations are incredibly useful in genetics, as they allow for the temporal control of mutations. Temporal control of a mutation can allow for the study of otherwise lethal mutations, which would be highly valuable to us, as mutations in the Wnt pathway, such as in the Disheveled *dsh-2*, are maternal effect lethal.

As an example of temperature sensitive genes, the heat shock proteins (or 'molecular chaperones') are differentially expressed based on the presence or absence of a cellular stressor, including, but not limited to, heat. One of the first heat shock proteins to be studied was hsp70. Hsp70 is highly conserved, and responds to stress by binding to unfolded proteins, either for segregation or to disrupt aggregating proteins via binding and ATP hydrolysis (for review see [118]). Hsps also have both endogenous and conditional roles within the nervous system. For example, in the brain, hsp70 is conditionally expressed in response to stressors such as hypothermia, and hsp27 is conditionally expressed in both the central and peripheral nervous systems following damage to neurons (for review see [119]).

For our specific work, we aimed to generate temperature sensitive mutations where a loss of expression of the target gene is only triggered upon exposure to an extreme temperature, either 15°C or 25°C. These experiments would be similar to the seminal research done on conditionally active mutations in *C.*

elegans, such as those which characterized the formation of the vulva [120] and the temperature sensitivity aspect of the decision to switch to the dauer stage (a decision which takes in to account temperature, in addition to food supply and pheromone presence), in which development arrests between the L1 and L2 larval stages [121]. Generating lines with temperature sensitive mutations would permit for raising of strains at WT temperatures, where the mutation was not active. Experimentally, we could then raise animals at the conditionally active temperature until the L2 stage, when the VD neurons are fully developed and then move the animals back to room temperature, or vice versa. This would allow us to tease apart if there is a temporal aspect to these genes. Specifically, are these genes needed during the development of the neuron alone, *i.e.* they are no longer needed once the neuron has finished developing at the end of the L2 larval stage. Or is the expression of these genes also needed throughout the life of the neuron to maintain its specification. Thus, conditionally active mutations within our system, the posterior GABAergic D-type motor neurons, would be highly beneficial in understanding this system.

Here, we show that *unc-55*, *plx-2*, and *mab-20* are not required for expression of our marker, *lhIs97*, in VD13 or the LUAs. We report that *sdn-1* does not significantly affect the expression of *lhIs97* in VD13. *sdn-1* does, however, cause a significant increase in misexpression in DD6. We also report eight potential candidate genes from our EMS mutagenesis screen. Of these eight genes, five appear to be temperature sensitive. *lh40*, appears to be due to a premature stop codon in *sma-9*. Together, these data provide further insight into the genes involved in the specification and growth of VD13. Further, we have identified numerous potential causative mutations in each of our eight lines, and, through further characterization, these candidates may identify novel genes, or allow for the use of conditionally active mutations to further our understanding of how these genes function in the growth and development of VD13.

Results

4.1 *unc-55*, *plx-2*, and *mab-20* are not required for *lhIs97* expression in VD13

To further explore the specification of VD13, we sought to see if VD13 needed to be specified as a VD neuron to express *lhIs97*. *unc-55*, *unc-62*, and *alr-1* are all involved in the differentiation of the VD neurons from the DD neurons, thus, we planned on generating lines of animals with mutations in each of these genes, along with our VD13 marker, *lhIs97*. While we are still generating animals with *unc-62; lhIs97* and *arl-1; lhIs97*, we were able to generate *unc-55; lhIs97* animals. We found that *unc-55* animals had no significant change to RFP expression in VD13 (100% VD13+). This suggests that VD13 does not require *unc-55* to express *lhIs97*. Additionally, *unc-55* had minimal effect on the morphology of VD13, with 78% of animals with a C shaped neuron (p=0.5762, Fisher's Exact Test), as this was not significantly different from the 89% of animals with a C shaped neuron seen in WT (*juIs76; lhIs97*) animals.

Since our *lhIs97* marker is expressed via a fragment of the *plx-2* promoter, we looked to see if loss of *plx-2* would disrupt expression of the marker or lead to growth defects in VD13. Plexins are a class of transmembrane receptors, which mainly function in development, including in axon guidance, along with the signaling molecule semaphorin (for review see [122]). *plx-2* and *plx-1* are the plexin homologs in *C. elegans*. We found that there was no loss of expression in *plx-2* animals of *lhIs97* (100% VD13+). Additionally, as a whole, VD13 in a majority of *plx-2* animals had a morphology (92% C shaped, p=0.3886, Fisher's Exact Test) similar to WT animals with only the *juIs76; lhIs97* markers (Figure 4.1). Thus, loss of *plx-2* does not appear to have an effect on *lhIs97* expression or VD13 morphology.

Plexins are cell-surface receptors for ligands, including semaphorins. Semaphorins have previously been shown to be involved in a manner of developmental processes, including cellular migration and adhesion [123], morphogenesis [124], and axon guidance [125]. *C. elegans* have three semaphorin genes: *mab-20*, *smp-1*, and *smp-2*. Previous work in *C. elegans* has shown that *mab-20* and *plx-2*

interact, as well as that *mab-20* can interact with other receptors, such as the Ephrin, *efn-4* [103]. Similar to *plx-2* animals, *mab-20* animals did not lose expression of the *lhIs97* marker (100% VD13+) and were largely C-shaped (90%, p=0.53, Fisher's Exact Test), similar to WT animals (Figure 4.1). Thus, neither *plx-2* nor *mab-20* are required for *lhIs97* expression or for development of proper morphology of VD13.

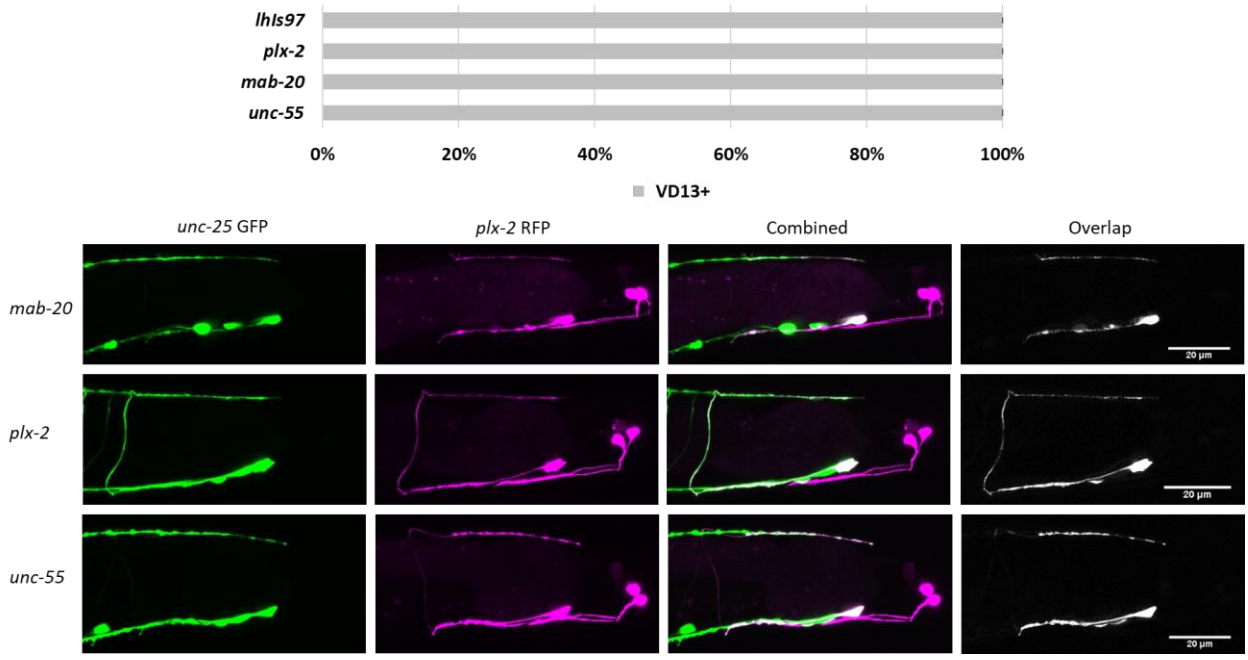

Figure 4.1 *unc-55*, *plx-2,* and *mab-20* have no RFP expression loss in VD13. Similar to WT animals, animals with loss of *unc-55*, *plx-2*, and *mab-20* do not lose expression in VD13 (100% VD13+) and have no significant change in VD13 morphology.

4.2 *sdn-1* loss increases the expression of *lhIs97* in DD6

Previous work in our lab has suggested that the heparan sulfate proteoglycan *sdn-1* functions in parallel with Wnt signaling to direct axon growth. Thus, we wanted to see if *sdn-1* also played a role in the specification of the posterior D-type motor neurons, specifically VD13 and DD6. Using our VD13 marker, *lhIs97*, we found that in 45% of *sdn-1* animals, there is expression in both VD13 and DD6, compared to only 14% VD13+/DD6+ *lhEx610* animals (p=0.0001, Fisher's Exact Test). Though there is no statistically

significant difference in VD13+ expression between *snd-1* and *lhEx610* animals (Figure 4.2). This suggests that while *sdn-1* is not involved in the specification of VD13, it may somehow be involved in the differentiation between DD6 and VD13.

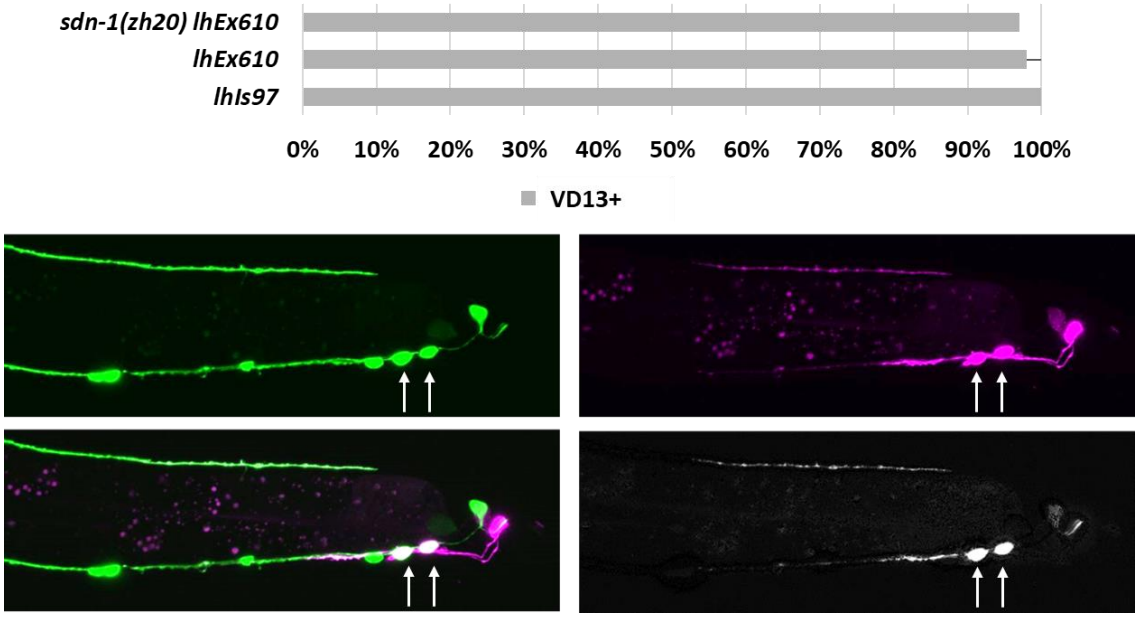

Figure 4.2. Loss of *sdn-1* does not affect expression of the *lhIs97* marker in VD13. RFP expression loss in VD13 was only nominally different from the array (*lhEx610*) alone. Loss of *sdn-1* led to increased expression of the transgenic array in DD6 (pictured). Arrows point to DD6 and VD13.

4.3 *lhIs97* in the male *C. elegans*

C. elegans most commonly exist as hermaphrodites, which self-fertilize by first producing sperm during their early life, and then switching over to developing eggs and a vulva. While hermaphrodites have the XX sex chromosomes, *C. elegans* can also exist as males. Males have XO for their sex chromosomes, and typically only arise in nature due to chromosome nondisjunction [126]. Males are physically very different from hermaphrodites, as they are much thinner, and develop a hook at the end of their tails, along with a host of other differences, including in the differentiation of their neurons [127]. Given that many of these differences occur in the posterior of the animal, as that is where the male tail rays and

hook develop, we wanted to look at if there was any effect on VD13 with our *lhIs97* marker in male animals. In *juIs76; lhIs97* WT males, we found there was no loss of expression in VD13. *lhIs97* also appears to potentially mark some neurons between DD6/VD13 and the more posterior LUAs, LUAL and LUAR (Figure 4.3). This would not be uncommon, given that males have more neurons than hermaphrodites, and the majority of these additional neurons are located within the posterior of the animal. Thus, *lhIs97* may be a good marker for studying not only the D-type neurons in male animals, but in studying other neurons within the tail.

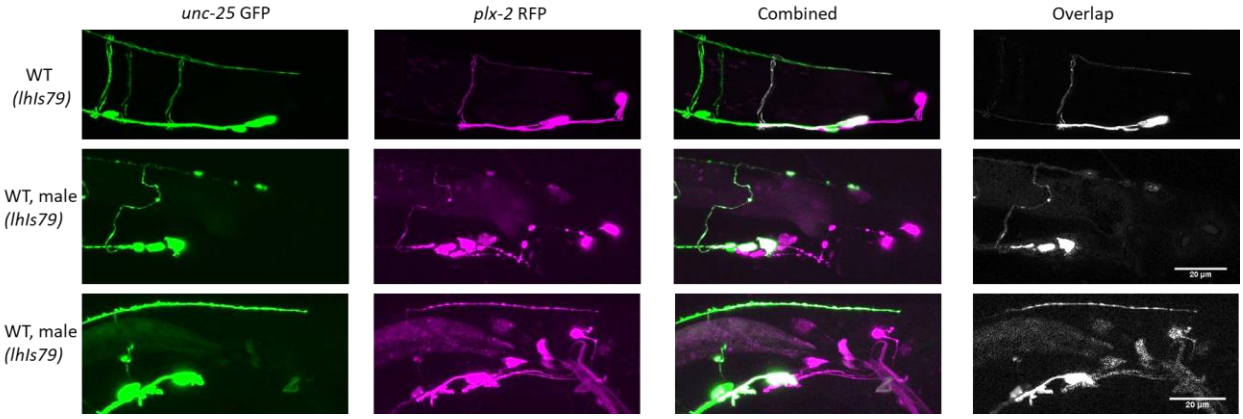

Figure 4.3. *lhIs97* in the *C. elegans* male. There is no loss of expression of *lhIs97* in VD13 in males. Additionally, there is some overexpression of *lhIs97* in DD6 in some male animals as well as possible over expression of *lhIs97* in other neurons in the tail, which are not the previously reported DD6, VD13, or the LUAs.

4.4 Generation of temperature-sensitive *lhIs97* expression loss lines

Finally, while we were unable to score the morphology of *egl-5* and *bar-1* mutants, due to the VD13- expression phenotype in those animals, this phenotype also presented us with a unique opportunity to screen for additional genes involved in VD13 specification. We performed a mutagenesis screen at 25°C, specifically looking for animals which were VD13- for RFP expression of *lhIs97*. Our goal was to not only

recover mutations in novel genes involved in axon growth and neuronal specification, but to also recover temperature sensitive mutations potentially in Wnt pathway or *egl-5* genes.

At the end of our screen, we identified eight new alleles, *lh39-lh46*, which display incompletely penetrant loss of RFP in VD13 at 25°C. Of these, five (*lh39*, *lh40*, *lh41*, *lh42*, and *lh46*), had lower expression in VD13 at 25°C compared to at 20°C (Table 4.1). We also scored our animals at 15°C, to check for temperature sensitivity to cold. One of our candidate lines, *lh41*, had a decrease in VD13+ expression at 15°C (p=0.0328, Fisher's exact test) (Table 4.1). Surprisingly, as was seen in our *sdn-1; lhIs97* animals, there was overexpression of our *lhIs97* marker in DD6 in *lh43* and *lh44*, with 69% and 47% of animals having expression in both VD13 and DD6, respectively. Together, these numbers suggest that at least five of our candidate lines have mutations in genes that are involved in the expression of our *lhIs97* marker in VD13, and thus may also be involved in the specification of VD13.

Table 4.1. Comparison of VD13+ expression at 15°C, 20°C, and 25°C in candidate strains.

Genotype	**N**	**% expression 15°C**	**% expression 20°C**	**% expression 25°C**
wild type (*lhIs97*)	≥30		100%	100%
lh39	≥30	100% (P=1.0000)	98%	71% (P <0.0001)
lh40	≥30	30% (P=1.0000)	33%	13% (P=0.0238)
lh41	≥30	86% (P=0.0328)	98%	85% (P=0.0316)
lh42	≥30	87% (P=0.3847)	93%	69% (P=0.0017)
lh43	≥30	100%	100%	96%

		(P=1.0000)		(P=0.2051)
lh44	≥30	100%	100%	94%
		(P=1.0000)		(P=0.0592)
lh45	≥30	100%	98%	91%
		(P=1.0000)		(P=0.1534)
lh46	≥30	97%	100%	87%
		(P=0.4970)		(P=0.006)

P values are compared to '% expression 20C' for each of the individual strains.

We scored the morphology of all eight of our candidate lines starting at 20°C (Table 4.2). To recap from Chapter III, we scored morphology in three categories. 'C shaped' neurons are ostensibly the WT shape, as they are the most commonly found in *juIs76; lhIs97* animals. 'T' and 'P' shaped neurons are those that reach the dorsal nerve cord, but then grow towards the anterior of the animal, and are thus combined together as polarity defects. 'N' and 'O' neurons are those that either fail to extend from the ventral nerve cord, or extend, but fail to reach the dorsal nerve cord, and thus have been combined together as outgrowth defects.

We found that of our candidates, two, *lh40* and *lh41*, have significant defects in polarity. Given the loss of expression, as well as the defects in morphology in VD13, which often translate to defects in growth overall, it is reassuring that these candidates appear to be involved in both specification and, potentially, in directing the growth of VD13, even at 20°C. Additionally, note that three of our lines have low N values. This is due to two reasons. For *lh40*, there is a very low expression (33%) in VD13. Additionally, for *lh42* and *lh46*, while expression could be seen in VD13, the expression was too faint to score the

morphology of the axon in most animals. Finally, *lh43* had high levels of overexpression in DD6, thus leading to low numbers of animals which could actually be scored.

Table 4.2. Morphology of VD13 in candidate strains at 20°C.

Genotype	**N**	**C Shape**	**Polarity (T/P)**	**Outgrowth (N/O)**
wild type (*lhIs97*)	161	82%	9%	9%
lh40	15	20%	73% (P=0.0001)	7% (P=1.0000)
lh41	122	61%	32% (P=0.0001)	7% (P=0.39)
lh42	14	64%	7% (P=1.0000)	29% (P= 0.0494)
lh43	36	89%	3% (P=0.3100)	8% (P=1.0000)
lh44	46	100%	0% (P=0.0429)	0% (P=0.026)
lh45	45	91%	4% (P=0.5311)	4% (P= 0.3741)
lh46	13	69%	8% (P=1.0000)	23% (P=0.1372)

P values are compared to WT (*lhIs97*).

Additionally, we have begun to score the morphology of our candidate lines at 25°C, to look for morphology differences that may occur due to the potential temperature sensitive condition of the

mutation. These morphological defects would be in addition to the differences in *lhIs97* VD13+ expression seen at 25°C (Table 4.3). Surprisingly, our WT strain, *jusIs76; lhIs97*, had a greater difference in morphology between 20°C and 25°C than did our candidate line *lh41*. Though, a part of this difference may be due to the large difference between the n values for this line at 20°C and 25°C.

The remainder of the strains will need to continue to be scored, especially *lh39*, *lh40*, *lh42*, and lh46, as these have significant differences in VD13+ expression between 20°C and 25°C. Similarly to what we reported for these lines at 20°C, scorable animals, and thus n values for these lines are very low, given the faint expression in VD13 which prevents scoring, or the simple lack of expression which is more common at 25°C. Overall, it will be exciting to see if there are greater morphological difference in the other lines than what was observed in *lh41*.

Table 4.3. Comparison morphology of VD13 in wild type (*lhIs97*) and candidate strain *lh41* at 20C and 25°C.

Genotype	**N**	**C Shape**	**Polarity (T/P)**	**Outgrowth (N/O)**
wild type (*lhIs97*) 20°C	161	82%	9%	9%
wild type (*lhIs97*) 25°C	37	56%	33%	11%
			(P=0.0004)	(P=0.7561)
lh41 20°C	122	61%	32%	7%
lh41 25°C	91	66%	28%	6%
			(P=0.6239)	(P=1.0000)

P values are compared to morphology data at 20°C for each strain.

It should also be noted that, in addition to having defects in VD13+ expression, four of our candidate lines, *lh40*, *lh41*, *lh42*, and *lh46,* also have significant defects in axon growth as well as the loss of expression in VD13 (Figure 4.4). Specifically, we recorded axon growth defects in *lh40*, *lh41*, *lh42*, and

lh46 where the dorsal posterior axon fails to properly extend to be parallel with the ventral cell body. These axons are referred to as 'undergrown'. Here, we find that *lh40* has the highest incidence of undergrown axons out of our candidate lines, with 94% of animals having axons that fail to reach the VD13 cell body (p=0.0001, Fisher's exact test). Additionally, 74% of animals with *lh46* have undergrown axons (p=0.0001, Fisher's exact test). Finally, *lh41* and *lh42* have undergrown axons in 59% and 63% of animals, respectively (p=0.0001, Fisher's exact test). Axon growth defects, as we see in *lh40*, *lh41*, *lh42*, and *lh46* are similar to undergrowth defects seen in *egl-5*, *bar-1*, and *dsh-1mig-5* animals (more on this is Chapter V). Thus, it is highly promising that we do see axon growth defects in our candidate lines, as this suggests that the mutations in these lines are in genes that may indeed be involved in directing axon growth in VD13, in addition to potentially being involved in specification.

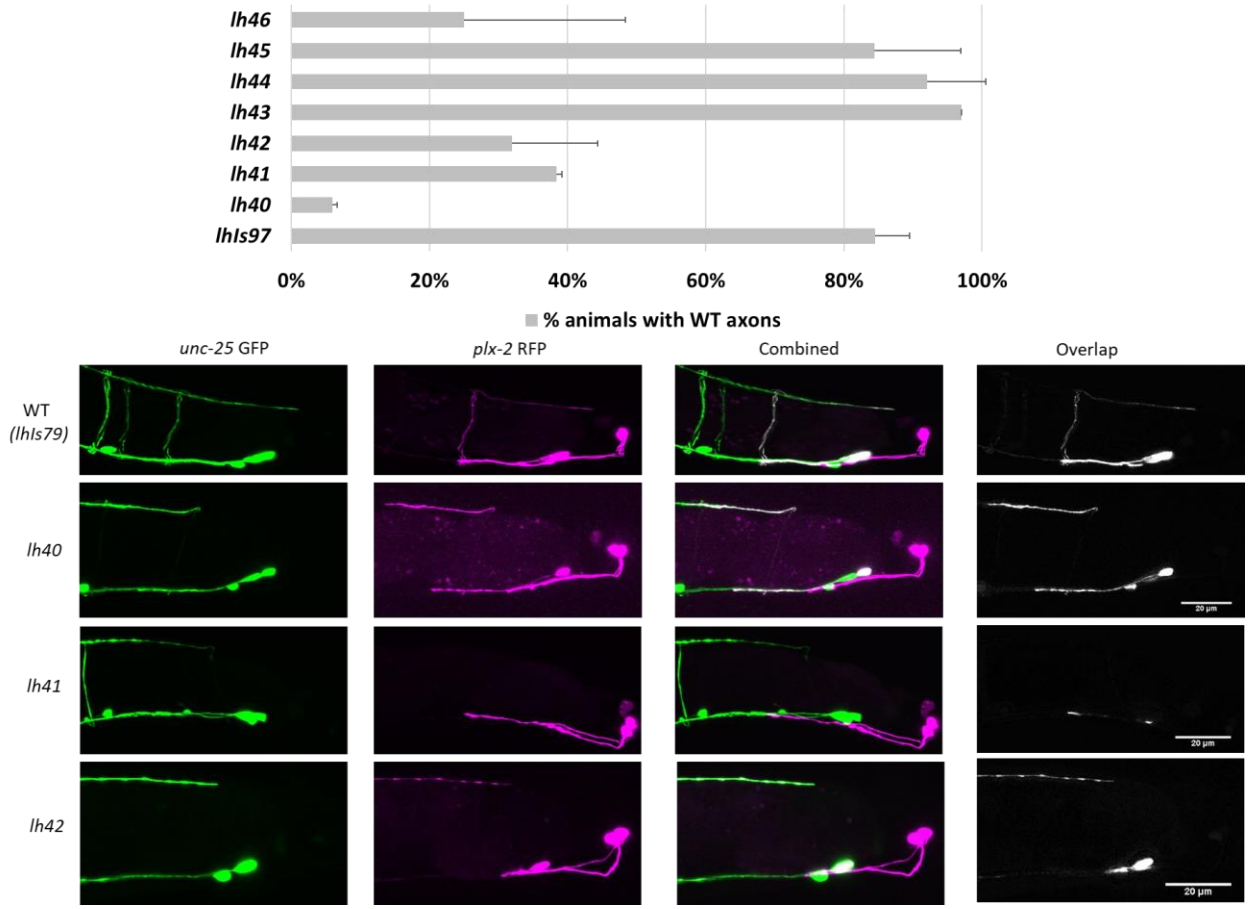

Figure 4.4. *lh40*, *lh41*, *lh42*, and *lh46* have significant defects in axon growth. The same four lines that we find have significant temperature sensitive mutations also have significant defects in axon growth. The figure above shows the percentage of animals for each line which have WT length axons. Each of these lines have undergrowth defects, with 94%, 59%, 63%, and 74% of *lh40*, *lh41*, *lh42*, and *lh46* animals having undergrown axons, respectively.

Finally, we genome sequenced each of our eight candidate lines. We then used a combination of programs on the Galaxy platform, as well as Excel, to map the data, and filter for unique variants for each of the eight candidate lines. Through this process, we were able to narrow down each line to a set of potential mutations, utilizing both the Integrated Genome Viewer as well as ApE: A Plasmid Editor. To point out one example, *lh40* is likely a premature stop codon in the *sma-9* gene (Figure 4.5). This premature stop codon originates from a C to T single nucleotide polymorphism at position X:10781069. *sma-9* has, at least, 11 isoforms, due to alternative splicing at both the 5' and 3' end, and these isoforms

have been categorized into different classes, depending on their splicing (Class I, II III for 5' end splicing and Class A, B, C for 3' end splicing) [128]. The SNP in *lh40* affects 10/11 of the *sma-9* isoforms.

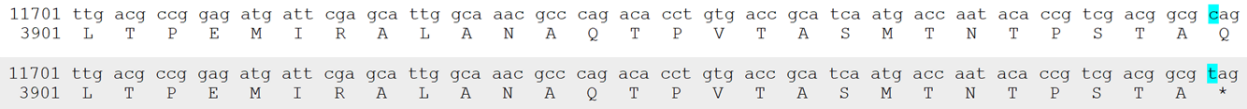

Figure 4.5 *lh40* likely results from a premature stop codon at position X:10781069 in the *sma-9* gene. Highlighted in teal is the SNP where a C has changed to a T, creating a premature stop codon, which affects 10/11 *sma-9* isoforms.

Additionally, we have been able to narrow down the possible mutations in all of our other candidate lines. Looking for a lower-than-expected ratio of CB4856 haplotypes in the sequencing we were able to assign our mutations to the most likely linkage group. (For *lh39-lh41*, see Table 4.4 and for *lh42-lh46* see Table 4.5). To mention some of the most interesting mutations: *lh39* has a G to A change in *Y56A3A.2*. *lh40*, as previously mentioned, is likely a premature stop codon in *sma-9*. *lh41* has a potential splice site mutation in *bar-1*, as well as a C to T mutation in *mls-2* and *lh43* has a similar C to T mutation in *tln-1*. *lh42* has a G to A change in *twk-8*, and *lh45* has a similar mutation in *nhr-110* and *ntr-1*. Finally, *lh46* has potential mutations in *C17E4.10* and *Y51H4A.13*, both of which are enriched in multiple cells, including neurons. Many of these potential causative mutations occur in genes which have known DNA binding, RNA binding, or transcription regulatory activity. Given this, and their known expression in neurons, these genes are promising candidates to be involved in the specification and development of VD13.

Table 4.4 Candidate mutations in VD13 differentiation screen for *lh39*, *lh40*, and *lh41* (ranked in order of interest)

	Maps to LG	Rank	Position	Ref	Alt	Gene	Effect	Description	Depth	Allele Balance
lh39	**III**									
	III	1	11855671	G	A	*Y56A3A.2*	L283F	Predicted to have metalloendopeptidase activity. Is an ortholog of human MBTPS2 (membrane bound transcription factor peptidase, site 2).	49	57%
	III	2	10232982	G	A	*Y70G10A.2*	S232L	Weakly related to Jagged ligands, expressed in male tail	36	61%
	III	3	10183195	G	A	*mua-3*	E3746K	Transmembrane cell adhesion receptor mua-3, at very end of protein, animals are not muscle attachment defective	34	56%
	III	4	5866804	G	A	*F01F1.15*	3' UTR	Is an ortholog of human CNPY2 (canopy FGF signaling	24	63%
	III	5	11401419	C	T	*Y47D3B.3*	5' UTR	Predicted to encode a protein with the following domain: Abnormal cell migration protein 18-like.	43	65%
	III	6	8983572	C	T	*pde-2*	promoter	Predicted to have 3',5'-cyclic-nucleotide phosphodiesterase activity and protein homodimerization activity. Is expressed in AFDL and AFDR.	38	66%
lh40	**X**									
	X	1	10781069	C	T	*sma-9*	Q1916Stop	Exhibits transcription coactivator activity and transcription corepressor activity. Is involved in several processes, including nematode male tail tip morphogenesis; positive regulation of mesodermal cell fate specification; and transforming growth factor beta receptor signaling pathway.encodes 11 isoforms, stop codon affects most isoforms (10/11)	21	100%
	X	2	5501144	G	A	*T23F2.2*	L649F	Is predicted to have cytoskeletal protein binding activity.	20	100%
	X	3	7071773	G	A	*B0403.6*	F157I	Uncharacterized protein	26	100%
	X	4	10417116	C	T	*cdk-11.2*	R630K	Is predicted to have cyclin-dependent protein serine/threonine kinase activity. Is involved in positive regulation of embryonic development. Animals are not Emb	30	97%
	X	6	5116303	G	A	*apl-1*	silent	Amyloid precursor-like.	36	97%
	X	6	7091422	G	A	*C36B7.5*	silent	Predicted to have the following domains: Thrombospondin type 1 domain; Thrombospondin type-1 (TSP1) repeat.	26	96%
	X	6	11930385	C	T	*dot-1.4*	silent	Is predicted to have histone methyltransferase activity (H3-K79 specific). Is an ortholog of human DOT1L (DOT1 like histone lysine methyltransferase).	20	95%
	X	6	12470094	C	T	*myo-2*	silent	Expressed specifically in the pharynx	32	97%
lh41	**X**	(most likely X may be II, but a lot less likely)								
	X	1	7167373	C	T	*bar-1*	splice site	Affects +1 site, likely a mutation causing change, exon 15-16 splicing	46	96%
	X	2	4761307	C	T	*mls-2*	A84T	Exhibits RNA polymerase II regulatory region sequence-specific DNA binding activity. Is expressed in somatic nervous system. Is an ortholog of human HMX1 (H6 family homeobox 1).	56	98%
	X	3	4831846	C	T	*R08E3.1*	silent	Predicted to have Notch biding activity	33	100%
	X	4	13330551	G	A	*sir-2.2*	E181K	Is predicted to have NAD+ binding activity; NAD-dependent protein deacetylase activity; and zinc ion binding activity. Is involved in innate immune response. Localizes to mitochondrion.	53	98%
	II	5	7124047	CGGCA	CGGGCA	*fust-2*	Q85H	May be sequencing error, all reads very close to end, not a lot of coverage in other lines as well	5	100%
	II	6	3431610	C	T	*skpo-2*	D719N	Is predicted to have peroxidase activity. Human ortholog(s) of this gene are implicated in Alzheimer's disease 1 and anterior segment dysgenesis 7. Is an ortholog of human EPX.	55	89%
	II	7	4258530	C	T	*clec-135*	M67V	Is predicted to have carbohydrate binding activity.	55	85%
	II	8	6695200	C	T	*C18H9.5*	G18E	Is predicted to have transmembrane transporter	29	83%
	II	9	2623978	T	A	*D2062.4*	F57Y	Male-based (RNASeq)	29	86%
	II	10	2194062	C	T	*C33C12.10*	Q16R	Uncharacterized protein	45	80%

Table 4.5 Candidate mutations in VD13 differentiation screen for *lh42*, *lh43*, *lh44*, *lh45*, and *lh46* (ranked in order of interest)

	Maps to LG	Rank	Position	Ref	Alt	Gene	Effect	Description	Depth	Allele Balance
lh42	**IV**									
	IV	1	9085078	G	A	*twk-8*	E501K	Is predicted to have potassium ion leak channel activity. Is expressed in body wall musculature and nervous system	15	100%
	IV	2	6207201	A	T	*ugt-24*	L434M	Predicted to have UDP-glycosyltransferase activity.	22	95%
lh43	**I**	(mapping confidence low, high percentage of CB throughout LGs)								
	I	1	1740135	C	T	*tln-1*	R2508C	Talin homolog, mutation is in I/LWEQ domain	108	94%
	I	2	702607	C	T	*hgap-1*	S1101F	Predicted to have GTPase activator activity. Mutation is just adjacent to GAP domain.	108	97%
	I	3	6562945	C	T	*tmed-3*	P63S	Transmembrane emp24 domain-containing protein 7; TMP21-related; and GOLD domain superfamily. Mutation in epm24 domain, residue frequently P, but not fixed	36	91%
	I	4	191782	C	T	*atm-1*	T651I	Predicted to have protein serine/threonine kinase activity. Is involved in response to ionizing radiation. Localizes to chromatin. Mutation is not in any identifiable domains	62	94%
lh44	**IV**	(mapping confidence low, high percentage of CB throughout LGs)								
	IV	1	6373895	G	A	*hrpf-2*	P>L	Predicted to have RNA binding activity.An ortholog of human HNRNPF (heterogeneous nuclear ribonucleoprotein F).	30	79%
lh45	**I or V**	(mapping confidence low, high percentage of CB throughout LGs)								
	V	1	1623445	C	T	*nhr-110*	G226S	Is predicted to have DNA-binding transcription factor activity; sequence-specific DNA binding activity; and zinc ion binding activity. Mutation in hormone binding domain, but not highly conserved residue	17	94%
	I	2	12621313	C	T	*ntr-1*	intron	Predicted to have G protein-coupled receptor activity. Is expressed in intestine and neurons. Mutation is unlikely to affect splicing	17	94%
lh46	**Unclear**	(mapping confidence low, high percentage of CB throughout LGs)								
	I		9436671	T	C	*C17E4.10*	V162A	Is enriched in germ line; hypodermis; neurons; and ventral nerve cord based on tiling array;	21	81%
	IV		16643753	C	T	Y51H4A.13	G169E	Is enriched in neurons based on tiling array and RNA-seq studies. Mutation is in Zc3h12a-like Ribonuclease NYN domain.	19	74%

Discussion

In *C. elegans*, neuronal specific florescent markers have been invaluable in studying the development of the nervous system. Here, we utilize our new, VD13 specific marker, *lhIs97*, to examine known factors involved in specification and axon growth, such as *unc-55* and *sdn-1*, as well as further examine new, potential factors involved in these processes, such as *mab-20* and *plx-2*. While *unc-55*, *mab-20*, and *plx-2* were not shown to affect expression of *lhIs97* in VD13, we did find that *sdn-1* had significant off target effects. These effects lead to our marker not only being expressed in VD13 and the LUAs, but in DD6 as well. While we did see DD6 expression in our WT and array lines, the percentage of animals with DD6+/VD13+ expression in *sdn-1* animals was significantly higher. Thus, *sdn-1* may be involved in the differentiation of DD6 and VD13, and loss of *sdn-1* leads to overexpression of *lhIs97* in DD6.

Additionally, we began a new mutagenesis screen. Our screen was a forward genetic screen, where we mutagenized whole worms with Ethyl methanesulfonate (EMS). EMS is a strong mutagen, which has been highly used and is well characterized. EMS is known to most often cause nucleotide substitutions in the form of G/C to A/T mutations [129]. Once mutagenized, we then screened the progeny for animals which lost expression of our mCherry marker, *lhIs97*, in VD13, but not in the LUAs. Mutagenesis screens have long been a technique to understand genetics and to identify new genes that may be involved in a process. Additionally, screens of this nature have been widely used in *C. elegans* research studies. One such example is in the Million Mutations Project, which sought to provide the *C. elegans* community with a wide array of mutant strains for each gene in the *C. elegans* genome, by using multiple mutagenesis protocols, including EMS [130]. Thus, we had reason to believe that an EMS screen, combined with the VD13- loss of expression phenotype, would be a viable screening tool to use to look for other genes that are involved in the specification of VD13.

We were able to successfully generate and identify eight candidate lines, each with varying levels of expression loss, and five, most promisingly, that appear to be temperature sensitive. In *C. elegans*, conditionally active genes have been highly valuable in research. These genes have been used to study everything from aging [131, 132] to the development of the nervous system [131]. Heat shock protein promoters have additionally been utilized to control gene expression, such as in the case of *bar-1*, where a heat shock promoter was used to drive *bar-1* expression by stabilizing *bar-1* without the presence of a Wnt ligand [133].

In this work, conditionally active alleles of genes would be incredibly useful for further elucidating when genes/proteins are required for specifying VD13 (or perhaps maintaining that specification). As an example, we previously discussed how, in an *egl-5* lof background, *lhIs97* RFP+ expression was lost from VD13. This left us unable to look at the axon morphology behind the undergrowth phenotype. A conditionally active *egl-5* mutation would potentially allow for us to separately control the role of *egl-5* in VD13 specification and axon growth. As a hypothetical example, if animals were grown at room temperature, then *egl-5* would be 'on' to specify VD13, and *lhIs97* RFP would also be expressed. Then, we could conditionally inactivate *egl-5* during the axon growth phase to study axon morphology. Alternatively, if *egl-5* is indeed a terminal selector for VD13, then it's continued expression would be necessary for VD13 maintenance of identity, so conditional loss of *egl-5* might be able to further support the claim that *egl-5* is a terminal selector in this developmental instance.

As we have been processing the data from our DNA sequencing, we have identified a number of candidate genes in which mutations have occurred in each of our candidate lines that were recovered from our mutagenesis screen. Most excitingly, we have recovered multiple potential mutations occurring in genes that are known to have DNA binding abilities or are linked to changes in gene expression. Mutations in genes that possesses these qualities are most exciting for us, as genes that can

function as, or similarly to, transcription factors are ideal candidates to be involved in the specification and direction of axon growth, as both specification and axon growth require changes within gene expression during development. As an example, we highly suspect that *lh40* has a causative mutation in the *sma-9* gene, as the mutation here leads to a premature stop codon. *sma-9* is a zinc finger transcription factor, and it is the *C. elegans* homologue to the *Drosophila* Schnurri and the vertebrate Smads. The Smads function as a transcription factor in the transforming growth factor β (TGF-β) and bone morphogenic proteins (BMPs) pathways (for review, see [134]). Similar to β-catenin in the canonical Wnt pathway, Smads are activated after a ligand binds to a receptor. Once activated, Smads then enter the nucleus to influence changes in gene expression, often with a co-activator or co-repressor, depending on the change to gene expression. In *C. elegans*, *sma-9* has been shown to be involved in regulating body size and male ray formation [128], dorsal-ventral patterning [135], amyloid beta aggregation [136], *etc*. Thus, it is an ideal candidate to be involved in the growth and specification of VD13.

As second example, one of the potential causative mutations for *lh41* is *mls-2*. In *C. elegans*, *mls-2* has been shown to be involved in development of cephalic sheath (CEPsh) glia. Specifically, *mls-2* is involved in CEPsh glia differentiation, as well as in development of other neurons within the head, which interact with the CEPsh glia [137]. During the development of these neurons, *mls-2* functions to guide axon growth in the AFD neurons. *mls-2* specifically functions through the CEPsh glia, thus acting non-cell-autonomously, as rescue of *mls-2* in the AFD neurons alone was not sufficient to rescue growth defects in those same neurons [137]. *mls-2* is also required for the specification of the AWC neurons, via activation of *ceh-36*, as loss of *mls-2* leads to loss of *ceh-36* expression, and thus defects in the morphology of the AWC neurons [138]. Thus, similarly to our *bar-1* and *egl-5* known factors, new DNA

binding genes that have been shown to function in neurons, like *sma-9* and *mls-2,* are exciting potential candidates for further defining how specification is achieved in VD13.

In terms of the breadth, we can also be fairly certain that we did not reach full saturation with our mutagenesis screen. Given that all of the strains recovered retain some expression of *lhIs97* in VD13, this means we likely did not recover strains with null mutations in *egl-5* or *bar-1*, as null mutants for either exhibit no, or very low, RFP expression in VD13. While *lh41* does have a potential splice site mutation in *bar-1*, we would need to do further genotyping to see if there is indeed a mutation in *bar-1*, and what the effect on *bar-1* expression is given the presence of that mutation, as *lh41* does still have VD13+ expression. Additionally, we did not recover any mutants that look similar to *lin-44*, which would both have loss of expression (VD13-), and have significantly overgrown axons. Since we did not achieve full saturation with this screen for all genes involved in VD13 specification, another screen of the same nature may provide additional novel genes or novel, conditionally expressed alleles of known genes. Until that time, there are still many potential genes that may come out of our candidate lines, and we will continue to categorize those lines, their mutations, and their potential role in the development of VD13.

Chapter V: The Wnt Signaling Pathway Instructs the Growth and Termination of Axons in the D-type GABAergic Motorneurons

Abstract

Neurons are varied in morphology, and it is this variation in morphology that aids them in sending signals to a diverse set of targets. The neuronal morphology is made up of processes, such as axons and dendrites, which will extend from the neuronal cell body during development as neurites, before being properly polarized to send signals. Thus, to properly function, a neuron must be able to grow its neurites into the correct morphology. However, neurons are not born with the innate knowledge of how or where to extend their neurites to attain their proper morphology. Instead, as they extend neurites during development, those neurites are given instructional cues, in the form of guidance molecules, which act as both attractants and repellants to direct the growth of the neurite. Given the vast number of subtypes of neurons, and the highly differential morphology that those subtypes can adopt, it is not a surprise that there is still much that is unknown about how neurites are directed in their growth. Previous work from vertebrates to invertebrates has suggested that for many neuronal subtypes, the Wnt signaling pathway is involved in directing axon growth (among other aspects of neuronal development). To study the role of the Wnt pathway in axon growth, we utilize the nematode *C. elegans*. These animals have only 302 neurons, and are genetically highly manipulatable, making them ideal model organisms. Previous work has shown that, in concert with work done on other model organisms, Wnt signaling is involved in axon growth in the D-type motorneurons. Previous work in the D-type GABAergic motorneurons has shown that canonical Wnt signaling is involved in the outgrowth of the most posterior neurons, DD6 and VD13. We have expanded on that work, to show that Wnt signaling is involved in both outgrowth and repulsion of the dorsal posterior axon of DD6 and VD13.

Introduction

Previously, we introduced concepts about how, during development, neurons will extend neurites, that receive proper growth/termination signals, which ultimately guide those neurites to their target location, where they will form synapses. However, the initial growth of a neuron is not the only period during its life when it will need to grow. Many neurons form early within development when the organism is not yet fully grown. Thus, after their initial growth period, neurons must also be able to elongate, stretch and grow with the organism, to continue to properly function and innervate the correct targets. Recent *in vitro* studies have found that mechanical forces acting on, or 'stretching', an axon, will lead to the growth of that axon [9, 139]. Additionally, the ability for axons to stretch, and not snap, is likely dependent upon mass, potentially in the form of membrane, cytoplasm, *etc*. which is being added not just at the growth cone, but all along the axon via transport by microtubules [139, 140]. The matter of how axons elongate, especially after the growth cone is gone and synapses have already been formed, is still an expanding field of inquiry (for review see [141, 142]).

While the above studies looked at neurons *in vitro*, we can utilize *C. elegans* to study the continued growth of neurons *in vivo*. *C. elegans* have a period of embryogenesis, within an egg. They then hatch as L1 larvae, and progress through three more larval stages, L2-L4, during which they continue to grow larger and develop until their final larval molt into an adult animal. In the D-type GABAergic motor neurons, there is a great need for the neurons to be able to continue to grow with the animal. The DDs form during embryogenesis, *i.e.* they are fully formed when the animal hatches as an L1 Larvae. The VDs begin forming in the L1 stage, and are finished by the end of L2 [143]. This means that both the DDs and the VDs must continue to grow with the animal as it progresses through its remaining larval stages, during which the animal nearly quadruples in size.

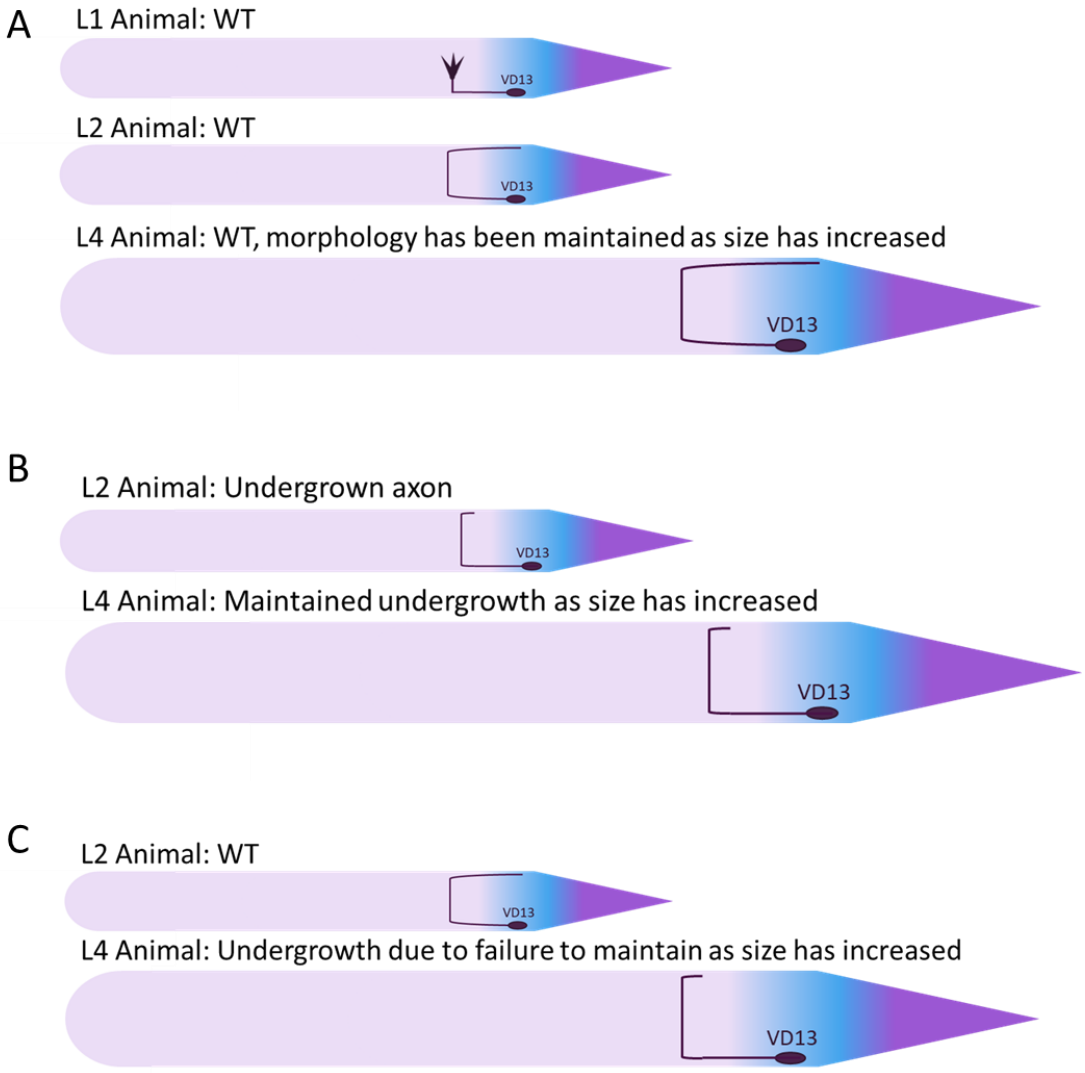

Figure 5.1. The VD and DD neurons continue to grow with the animal after they are formed. The DD neurons are fully formed when the embryo hatches as an L1 larvae, and the VD neurons are fully formed by the L2 larval stage. Thus, the initial growth of these neurons takes place early on in the life of the worm, and the neurons must then continue to hold their shape as they grow with the worm through the next two larval stages and into adulthood.

Since the VD and DD neurons undergo both an initial growth to form their shape, and then a continued growth to remain consistent in size with the rest of the growing animal, a question remains whether axon growth defects seen in L4 animals are due to initial growth defects or due to failure to continue growing with the animal (Figure 5.1 A). In this scenario, there are two possible routes for axon growth deficiency to be observed in the L4 stage of the animal. Scenario 1: During the initial growth in L1, the

dorsal axon failed to properly extend to be in line with the cell body. Then, this undergrowth was maintained, as the neuron grew to keep in size with the animal, but the original morphology was maintained (Figure 5.1 B). Scenario 2: During the L1 stage, the axon developed the proper morphology, however, during the homeostasis growth phase, the morphology was not kept, as the growth was misdirected, and thus the axon did not fully extend to keep up with the expanding animal, leading to a growth defect in the L4 stage (Figure 5.1 C). It is likely that Scenario 1 is what is occurring within these neurons, as we can see growth defects in the DD neurons in L1 animals, before the VD neurons have formed, that appear to continue into adulthood. However, it is beneficial to be able to study these neurons at different stages, so that we can begin to be able to understand both the processes that direct the initial outgrowth and morphology of the neuron, as well as those that direct the continued growth of the neurons as the animal continues to grow and mature.

Additionally, even during the initial growth of the D-type GABAergic motor neurons, there is not always an obvious growth cone. When these neurons grow, the ventral cell body extends a neurite anteriorly. The anterior growth of this neurite does not have an obvious growth cone. This neurite will eventually stall its growth, bifurcate, and send a commissure dorsally. As the commissure is guided towards the dorsal nerve cord, there is a visible growth cone, however, once the growth cone reaches the dorsal nerve cord, it flattens. Here, the neurite will again stall and bifurcate, and send a process posteriorly, with no visible growth cone (Figure 5.2). Thus, it is essential to understanding how axons grow to understand not only how growth is promoted at the growth cone, but how neurites are able to grow, and have that growth directed, when there is no visible growth cone.

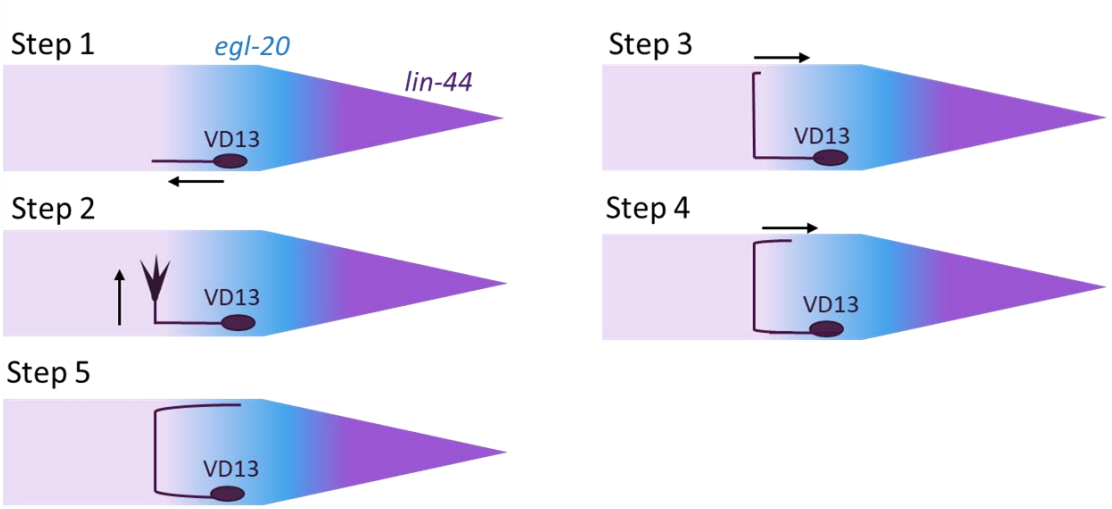

Figure 5.2. Neurites are not always directed by a growth cone. During the growth of the DD and VD neurons, a growth cone is only present during the extension of the neurite from the ventral to the dorsal cord. There is no visible growth cone for the extension along either the ventral or dorsal nerve cord, thus, while growth cones are one way to direct and extend a growing protrusion, there must be other ways of extending a neurite when no growth cone is present. Steps 1-4 represent the initial outgrowth of the neurite from the ventral cell body, to extension of a commissure to the dorsal verve cord, and then extension of the posterior dorsal neurite. Step 5 represents how the neuron, fully formed in the L2 larval stage, must now grow, and hold its shape as the worm grows.

A known director of axon growth is the Wnt signaling pathway. The Wnt pathway consists of the canonical and noncanonical pathways (for review see [30]). In the canonical pathway, the Wnt ligand binds to the transmembrane receptor Frizzled, sometimes with the co-receptor LRP5/6. This activates the effector protein Disheveled, which will disrupt the APC destruction complex (consisting of, generally, axin, GSK3B, and APC). This disruption leaves cytoplasmic β-catenin untagged for degradation, and thus, β-catenin can enter the nucleus to interact with the TCF and influence gene expression.

Canonical Wnt signaling is not only involved in changes in gene expression. Recent work has shown that the pathway can also directly interact with, and influence, microtubule dynamics in axon growth (for review see [144]). Specifically, canonical Wnt signaling can influence microtubule dynamics via the interactions of Disheveled with various members of the APC complex, including, GSK3B [145], axin [146]

and APC [147]. Disheveled is able to inhibit GSK3B to stabilize microtubules in the axon independently of TCF and β-catenin. Thus, Disheveled appears to not transcriptionally affect microtubules dynamics, but to interact with GSK3B, axin, and microtubule binding proteins, such as Map-1B [146]. The role of Wnt in axon microtubule dynamics can also act through β-catenin, and yet not need to influence transcription [147]. Additionally, Wnt signaling mediates the amount of APC at the growing plus end of microtubules in the growth cone, leading to a 'looped end' phenotype in the microtubules, and a loss of directional growth [147]. Thus, it is possible for canonical Wnt signaling to function in axon guidance by both influencing changes in gene expression and through directly influencing microtubule dynamics.

Previous work has shown that the Wnt pathway functions in the D-type GABAergic motorneurons to guide the growth of their posterior dorsal axon. Specifically, the most posteriorly expressed Wnt ligands, *egl-20* and *lin-44*, function as repellants, or termination signals for the most posterior D-type motor neurons, DD6 and VD13 [38] (Figure 5.3). Previous work has shown that both *egl-20* and *lin-44* mutants have overgrown axons, and animals missing both ligands (*lin-44; egl-20*) have axons which overextend farther than either of the single mutants. Additionally, overexpression of *lin-44* via its endogenous promoter, or mis-localized expression of *lin-44* via the *egl-20* promoter lead to premature termination of the axon. This suggests that both *egl-20* and *lin-44* are necessary for the proper growth of this axon, acting as posterior termination signals.

Figure 5.3. *lin-44* and *egl-20* are involved in outgrowth in VD13. In a WT animal *egl-20* is expressed near the cell body and termination point of VD13, while *lin-44* is expressed more posteriorly. Loss of both *egl-20* and *lin-44* leads to overgrowth, with *lin-44* axons being slightly more overgrown than *egl-20* axons, and in *lin-44; egl-20* double mutants, the axons are more overgrown than in either of the single mutants.

As the Wnt ligands are only the beginning of the pathway, Maro et al. went on to look at the receptor for Wnt, Frizzled. The *C. elegans* genome encodes four Frizzled receptors: *lin-17*, *mig-1*, *mom-5*, and *cfz-2*. Of these receptors, only *lin-17* displayed axon guidance defects [38]. Interestingly though, unlike the Wnt ligands, a sampled pool of animals lacking *lin-17* displayed a percentage of both undergrown *and* overgrown axons, which is an unexpected result, given that the ligands need a receptor to signal through, and thus a similar phenotype would be expected. This phenotype was not statistically significant compared to *lin-44*; *lin-17* double mutants [38]. Even mutations in other, noncanonical Wnt receptors, *lin-18* or *cam-1*, displayed only minor overextension. Additionally, the *lin-17* phenotype could be rescued by cell autonomous expression of *lin-17* via a GABAergic specific promoter [38]. Thus, in the D-type neurons, *lin-44* appears to act through the *lin-17* frizzled receptor. However, it is important to note that since there are three other Frizzled homologs, there could be some form of compensation

when looking at single or double mutants. Additionally, given the discrepancies in phenotype, there appears to be more going on than simple Wnt pathway activation via *lin-44*/Wnt binding to *lin-17*/Frizzled.

Downstream of the Frizzled receptor lies Disheveled. In Wnt signaling, Disheveled is recruited by Frizzled after Frizzled is activated by a Wnt ligand. Disheveled is an effector protein, which contains three important domains: DIX, PDZ, and DEP. The DEP domain is suspected to be involved in interaction with upstream regulators of Disheveled in the Wnt pathway [148] . The DEP domain is also involved in Wnt activation of the JNK pathway [149], while the PDZ domain is involved in the canonical β-catenin pathway [150]. Along with the PDZ domain, the DIX domain is also involved in canonical signaling, as axin, an integral scaffolding protein in the APC complex, also contains a DIX domain, allowing for interactions between the two proteins [151, 152]. Thus, through its different domains, Disheveled is able to function in both the canonical and noncanonical Wnt pathways.

In the canonical pathway, Disheveled functions to disrupt the APC destruction complex, allowing β-catenin to go undegraded. How exactly Disheveled disrupts the APC complex is still mostly unknown. It has been predicted that Disheveled is interacting in some manner with the APC complex, to disrupt its tagging of β-catenin for degradation. As Disheveled is known to be able to bind to axin, this interaction of Disheveled and axin may prevent axin, and thus APC and GSK3B, from being able to effectively bind and phosphorylate β-catenin. Additionally, GSK3B, alongside axin, may be recruited by Disheveled to the plasma membrane, to phosphorylate the Frizzled co-receptor LRP6 [153]. This recruitment may again disrupt the complex, by moving some or all of its components to the plasma membrane, thus leaving the cytoplasmic β-catenin ‘out of reach’ and thus unavailable for tagging for degradation.

C. elegans has three genes encoding Disheveleds: *dsh-1*, *dsh-2*, and *mig-5*. Maro et al. found that in the D-type neurons, *mig-5* and *dsh-1* mutant animals had undergrown axons, while *dsh-2* had no effect [38]. Similarly, to the Frizzleds, it is possible that the Disheveleds are able to compensate in some capacity when only one is lost. Additionally, this is again the exact opposite phenotype to what is seen when the Wnt ligand is lost, which is not expected when looking at the canonical pathway.

In the canonical Wnt pathway, after Disheveled is activated by Frizzled, it goes on to disrupt the APC complex. This disruption leaves β-catenin undegraded, so it can enter the nucleus and interact with TCF to intact changes in gene expression. Maro et al. found that *gsk-3* and *pry-1* mutant animals, which are the *C. elegans* homologs of GSK3B and axin, have overextended axons [38]. This is identical to the loss of the Wnt ligands, which does not support an antagonistic relationship, like in the canonical Wnt pathway. Additionally, *bar-1*/β-catenin and *pop-1*/TFC, mutant animals have undergrown axons. While it is reassuring that the phenotype of the ACP complex genes and the transcription factors is opposite, due to their antagonistic relationship, it is still unclear how the Wnt pathway is acting in these neurons to promote both outgrowth and termination.

Here, we show that *bar-1* is epistatic to *lin-44* and *egl-20* in axon growth. Additionally, the Hox gene *egl-5* functions cell autonomously in axon outgrowth. Finally, of the *C. elegans* Disheveleds, *dsh-1* and *mig-5*, but not *dsh-2*, are required for outgrowth of the axon. Together, these results suggest that the Wnt pathway may be functioning in two opposing ways: both to promote outgrowth of the axon, via the Disheveleds, *dsh-1* and *mig-5*, *bar-1*, and potentially *egl-5*, and to attenuate that growth, via the Wnts and their respective Frizzled receptors.

Results

5.1 Wnt Signaling in Axon Growth

During growth, axons respond to different environmental cues. These cues can be generalized, such as to a specific type of neuron, or be highly specific, depending on the type of guidance that is occurring. As such, many neurons can grow through a similar point, such as the spinal cord, or the dorsal/ventral nerve cord in *C. elegans*, but these neurons will respond differentially to different cues. Thus, these guidance cues can guide the growth, termination, and placement of each specific neuron. As an example, the most posterior D-type motor neurons, DD6 and VD13, terminate in the posterior of the animal, just before the anus. However, there are numerous other neurons which grow past the DD and VD termination point, to reside in the posterior nerve cluster (Figure 5.4). Given this, it has been hypothesized that there must be some cues that DD6 and VD13 are differentially able to respond to, so that they can receive the cue to terminate their axons, while the other neurons grow past unabated.

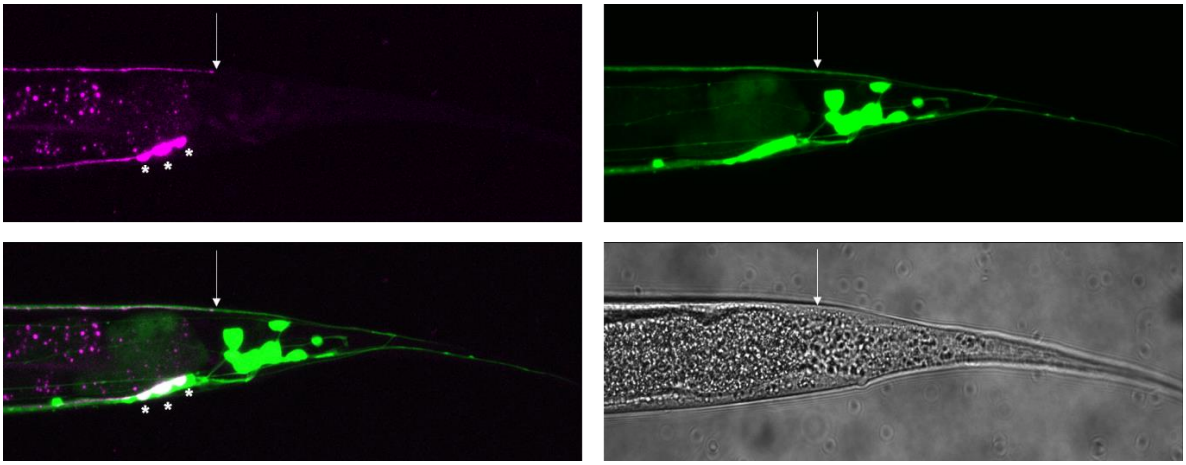

Figure 5.4. DD6 and VD13 have a unique termination point in the posterior of *C. elegans*. The dorsal posterior axon of VD13 terminates slightly beyond the location of the dorsal cell body (arrow, RFP). Additional neurons (GFP) do not terminate at that location, and instead terminate more posteriorly in the tail.

One guidance cue that has been studied in the context of axon growth in the D-type neurons is the canonical Wnt signaling pathway. Previous work has shown that disrupting Wnt signaling leads to a

combination of under and overgrowth of the dorsal posterior axon of the most posterior D-type motor neurons, DD6 and VD13 (Figure 5.5). And similar work has shown that the specific locations of the Wnt ligands along the anterior/posterior axis is important for the proper outgrowth of neurites [38, 154]. Thus, given the previous work suggesting that Wnt signaling is not only acting as a guidance factor for axon growth in DD6 and VD13, but acting in a way not fully indicative of the canonical pathway, we sought to further elucidate just how the pathway was instructing axon growth.

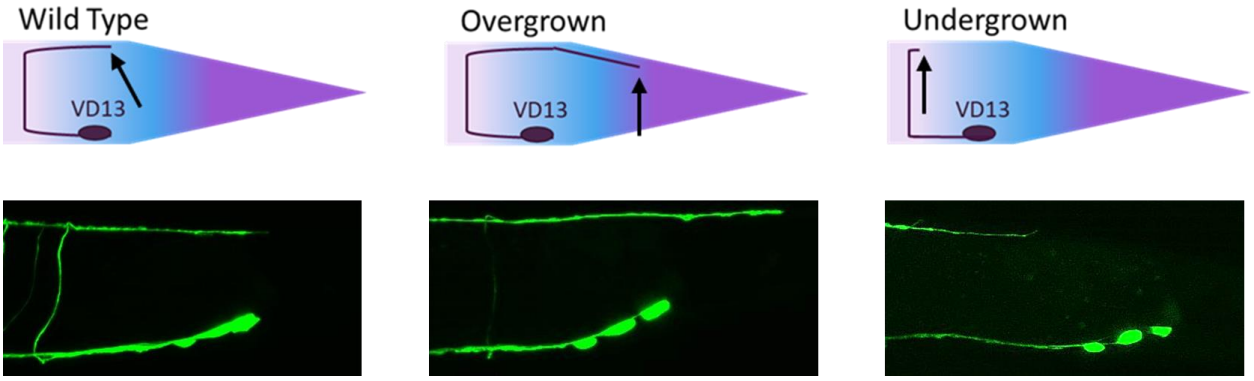

Figure 5.5. Visual representation of a WT, overgrown, and undergrown axon in VD13. The dorsal axon of VD13 terminates inline or just slightly beyond the cell body. Overgrown axons grow beyond this point, reaching past the cell body towards the posterior. Undergrown axons fail to reach the cell body of VD13. Arrows point to the termination point of the dorsal axon.

As previously mentioned, there are five Wnt ligands in *C. elegans*, and they are expressed in discrete regions along the anterior/posterior axis [33]. *lin-44* and *egl-20* are only expressed in the posterior of the animal, with some additional expression from *cwn-1* and *mom-2*, though those also have more anterior expression. Finally, *cwn-2* is the most anteriorly expressed, and there is little Wnt expression in the head of the animal, given the expression of the Wnt antagonist *sfrp-1*.

Work in our lab has shown similar results to those previously reported by Maro et al. [38], where *cwn-2* and the *cwn-2; cwn-1* double have little effect on axon outgrowth in DD6 and VD13 (94% and 87% of animals with WT length axons, respectively, p=0.0794, p=0.0048, Fisher's Exact Test). Additionally, we

have also found that *lin-44*, *egl-20*, and *lin-44*; *egl-20* animals have a significant number of overgrown axons (68%, 62% and 41% of animals with overgrown axons, respectively, p=0.0001, Fisher's Exact Test).

Additional work in our lab looked at the Frizzled, *mom-2*, which is maternal effect lethal. We found that *mom-2* does have some effect on axon growth. Additionally, we looked at double mutants of *mom-2* with the other posterior Wnt ligands, *egl-20* and *lin-44*. Here we found that *mom-2* did not appear to exacerbate the overgrowth phenotype of either of the single Wnt ligand mutants, with *lin-44; mom-2* and *egl-20; mom-2* 82% and 20% of animals with overgrown axons, respectively (Figure 5.6).

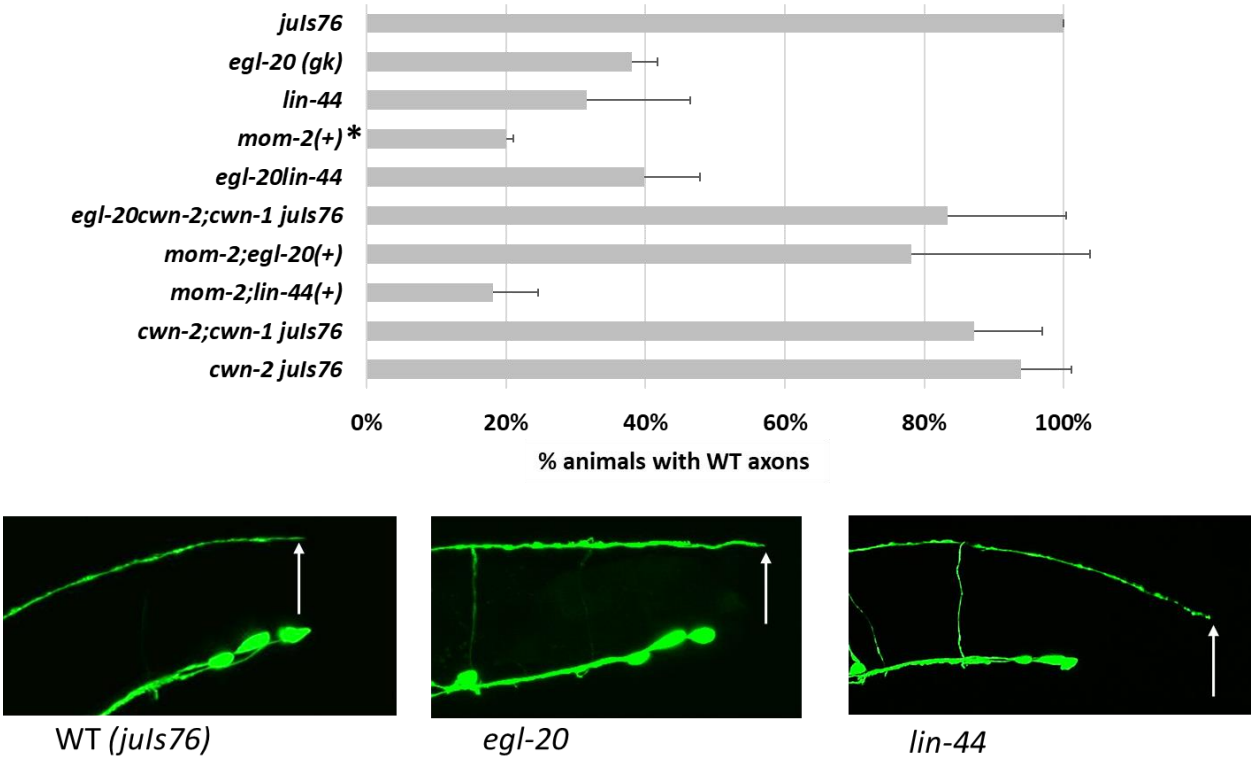

Figure 5.6. The posterior Wnt ligands are involved in axon growth in VD13. *egl-20*, *lin-44*, and *mom-2* each have significant defects in axon growth, as do the double mutants *lin-44; egl-20*, *mom-2; egl-20*, *mom-2; lin-44*, and the triple mutant *egl-20 cwn-2; cwn-1*. Animals with *cwn-2* as a single mutant and as a double mutant with *cwn-1* do not have significant defects in axon growth. Arrows point to the termination point of the dorsal axon. Bars with an '*' denote data that has been previously reported, and is currently available at bioRxiv [117].

Previous work from our lab had again found similar results to Maro et al., where *bar-1* animals have an undergrown dorsal axon 96% of the time [38, 117]. This is unusual to see, given that *bar-1* is one of the *C. elegans* β-catenins, and is expected to be activated at the end of the canonical pathway. Thus, loss of *bar-1* would be expected to have a similar phenotype to other necessary upstream factors in the canonical Wnt pathway. Namely, an overgrown axon. However, these results taken together are similar to what was seen in Chapter III.

In Chapter III, we reported that *lin-44*, *dsh-1mig-5,* and *bar-1* all have a loss of expression of our marker, *lhIs97* in VD13 (Figure 3.3). This suggests that these genes may be functioning similarly in terms of VD13 development. Thus, we wanted to specifically examine the relationship between *bar-1* and the Wnt ligands, *lin-44* and *egl-20*, and how they function in both promoting outgrowth and axon growth termination. We generated double mutants of *bar-1* with *egl-20* and *lin-44*. Here, we found that *bar-1* appears to function in an epistatic manner with *egl-20* and *lin-44*. Specifically, while *egl-20* and *lin-44* mutant animals have no undergrown axons, in double mutants with *bar-1*, there is a significant decrease in the number of animals with overgrown axons (62% to 1% in *egl-20; bar-1* and 68% to 10% in *lin-44; bar-1*) as well as a significant increase in the number of animals with undergrown axons (89% in *egl-20; bar-1* and 65% in *lin-44; bar-1*) (Figure 5.7) [117].

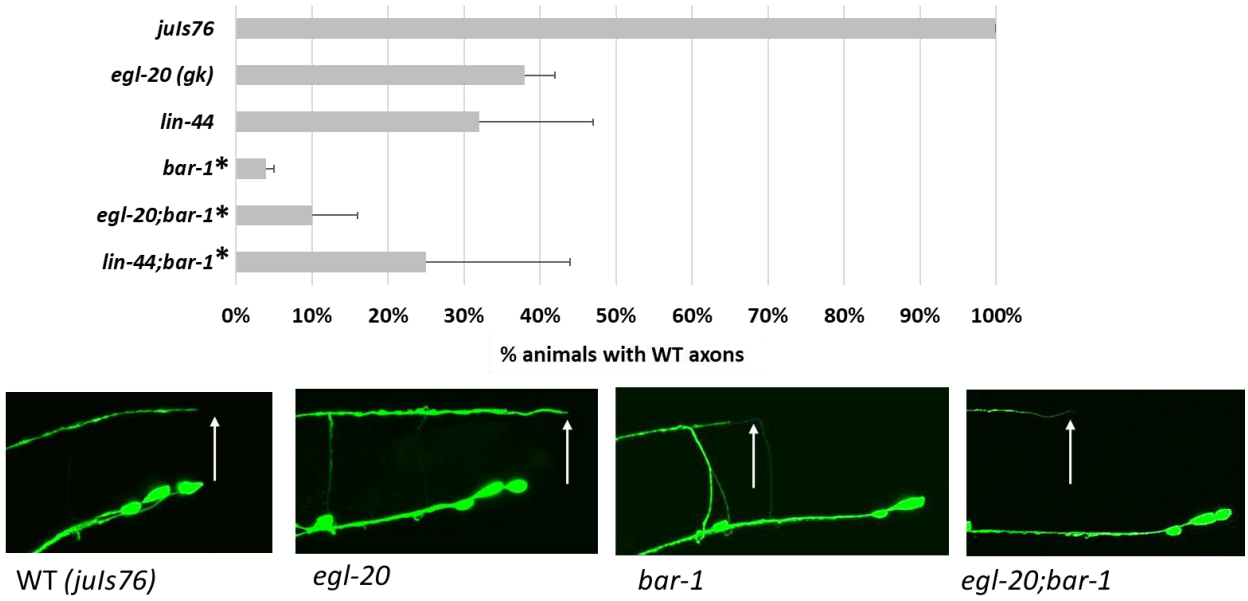

Figure 5.7. In axon growth, *bar-1* is epistatic to *egl-20* and *lin-44*. e*gl-20* and *lin-44* animals have overgrown axons (62% and 68% respectively), with neither mutant having any undergrown axons (0%). *bar-1* animals have undergrown axons (96%). Animals with both *egl-20; bar-1* and *lin-44; bar-1* have undergrown axons in 89% and 65% of animals, respectively, with only 1% and 10% of animals having overgrown axons. Arrows point to the termination point of the dorsal axon. Bars with an '*' denote data that has been previously reported, and is currently available at bioRxiv [117].

Maro et al. found similar results, where *bar-1*; *lin-17* double mutants had intermediate phenotypes between the two, where, compared to *lin-17* single mutants, the number of overgrown axons decreased, and the number of undergrown axons increased, though not to the same extent as *bar-1* animals [38]. This suggests that either the Wnt ligands are working through other transcription factors, the Wnts are working through other, non-transcriptional pathways, or there is still compensation occurring, given that there are multiple Wnts and Frizzleds, but only one β-catenin that is typically activated at the end of the canonical Wnt pathway in *C. elegans*. As such, we looked more in depth at the Frizzleds, and found that *mom-5* has no effect on axon growth, similar to what was reported in Maro et al. [38]. Additionally, we generated the triple mutant *mom-5*; *mig-1*; *lin-17* and found that there was still both under (33%) and overgrowth (8%) with only 58% of animals having WT length axons. However,

it should be noted that, for these animals, our n=12. Since the triple mutant is lethal, it had to be kept over a balancer, and animals that did come off of the balancer were rare, and often died before they could be scored. Thus, further work must be done to look at the Frizzleds, and perhaps generate the quadruple mutant to truly see what happens to axon growth when all of the Frizzleds are lost from the posterior neurons.

5.2 *egl-5* is necessary for outgrowth of VD13

Given that *bar-1* and *egl-5* mutant animals have similar phenotypes (96% and 86% undergrown, respectively) we sought to see if *egl-5* was necessary for outgrowth, and if it was acting cell autonomously. Thus, we generated an *egl-5* rescue construct, *lhIs93*, which cell autonomously expressed *egl-5* via the *unc-25* promoter. Given that *unc-25* is GABA specific, this meant that our rescue construct was only expressed in the GABAergic neurons. We found that *egl-5* undergrowth can be rescued by expressing *egl-5* cell autonomously (Figure 5.8). 83% of *egl-5* mutant animals with the rescue construct had WT axon lengths, versus only 14% of *egl-5* mutant animals with no rescue (p=0.0001, Fisher's Exact Test). Thus, *egl-5* is both necessary and sufficient to rescue axon outgrowth in the most posterior D-type motor neurons.

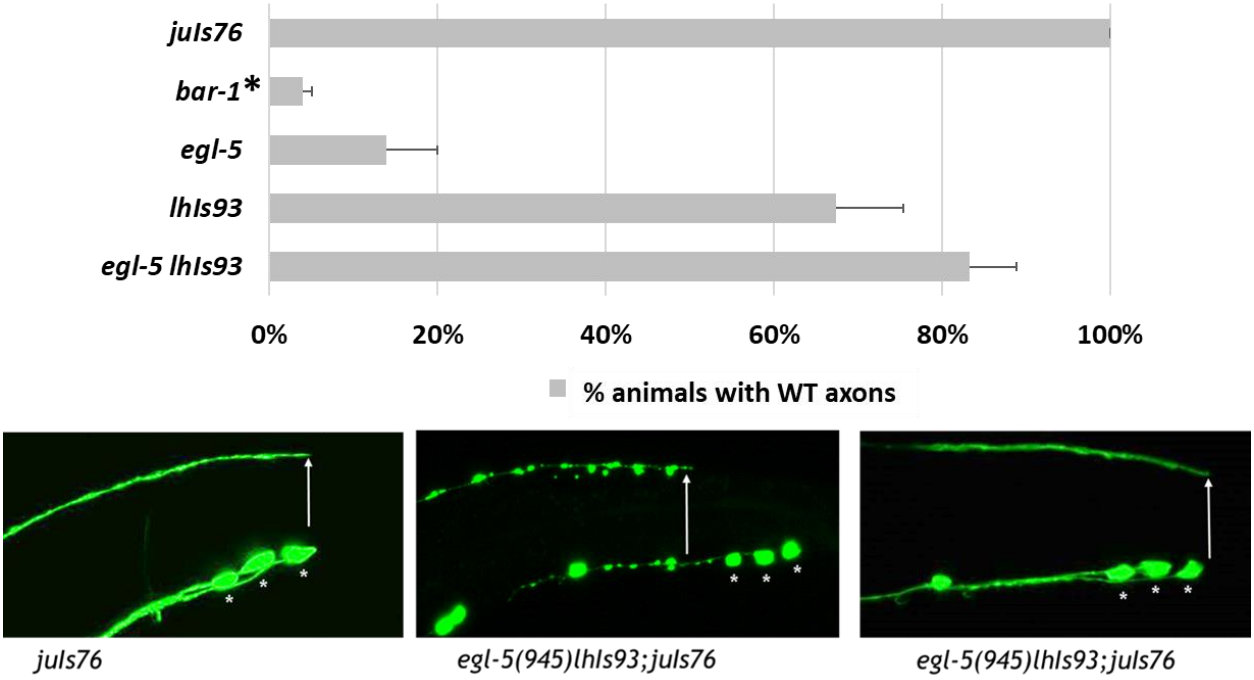

Figure 5.8. *egl-5* is necessary for outgrowth in VD13. 86% of *egl-5* animals have undergrown axons. These look highly similar to the 96% of *bar-1* animals which have undergrown axons. In both *egl-5* and *bar-1* animals, the dorsal axons fail to extend posteriorly beyond the point where the commissure from the ventral cord reaches the dorsal cord. Rescue of *egl-5* via the *unc-25* GABAergic specific promoter led to significant rescue of the undergrowth defect, with only 11% of animals with undergrown axons. Arrows point to the termination point of the dorsal axon. Bars with an '*' denote data that has been previously reported, and is currently available at bioRxiv [117].

5.3 *dsh-1* and *mig-5*, but not *dsh-2* promote outgrowth of VD13

To continue looking at how the Wnt pathway may be acting in both axon outgrowth and termination, we next looked at the Disheveleds. Previous work has shown that *dsh-1* and *mig-5* single mutants look similar to the *lin-17* Frizzled single mutants. These animals have both undergrown and overgrown axons, with only 69% of *dsh-1* animals and 24% of *mig-5* animals having WT length axons. Similar to the Frizzleds, we predicted that the Disheveleds may be compensating for each other, thus, we generated the *dsh-1*; *mig-5* double mutants. Unlike the Frizzleds, however, the *dsh-1*; *mig-5* animals are WT 63% of

the time, and only exhibit undergrown axons (Figure 5.9). Thus, it appears that the disheveleds may indeed be compensating for loss in the single mutants. To further examine this, we generated a *dsh-1*; *dsh-2* double mutant as well as the *dsh-1mig-5*; *dsh-2* triple mutant. Given that *dsh-2* is lethal, both of these strains had a cell autonomous *dsh-2* rescue via an endogenous *dsh-2* promoter. We then scored our animals using the *oxIs-12* [*Punc-47::gfp*] promoter. We found there was no significant difference between the *dsh-1*; *dsh-2* double mutants with the *dsh-2* rescue and the *dsh-1* single mutant animals (p=0.7397, Fisher's Exact Test) (Figure 5.9). This suggests that while *dsh-1* and *mig-5* are acting in axon growth, likely in axon outgrowth, *dsh-2* does not appear to be necessary.

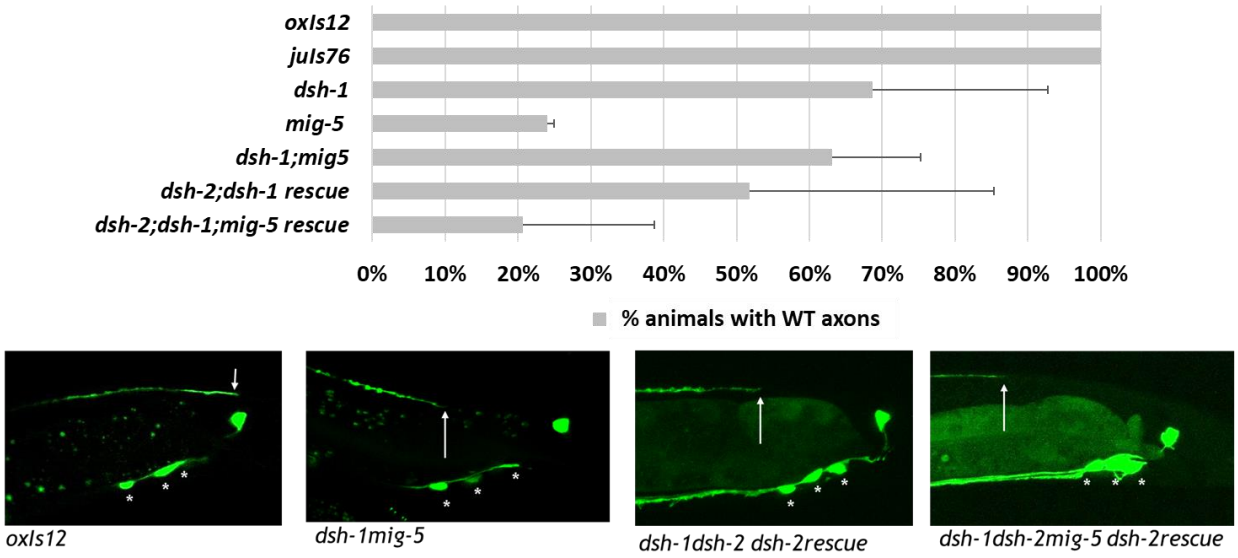

Figure 5.9. *dsh-1* and *mig-5*, but not *dsh-2*, promote outgrowth of VD13. The *dsh-1* and *mig-5* animals have significantly low percentage of WT axons, with only 69% and 24% of animals with WT axons, respectively. Defects in these animals consist of both overgrown and undergrown axons. The *dsh-1; mig-5* double mutant is undergrown in 37% of animals, with no overgrowth. To test for compensation, we sought to rescue the *dsh-2; dsh-1* double mutant as well as the *dsh-1; dsh-1; mig-5* triple mutant with a *dsh-2* rescue construct with the *oxIs-12* promoter. There was no significant difference between the *dsh-1; dsh-2* animals with the rescue complex and *dsh-1* animals (p=0.7397, Fisher's Exact Test). Arrows point to the termination point of the dorsal axon.

5.4 *plx-2, mab-20, and bli-3(im10)* do not affect axon outgrowth, while *pop-1* and *ncx-4* have some effect on axon growth

Given that our VD13 specific marker is expressed via a fragment of the *plx-2* promoter, we hypothesized that loss of *plx-2* may affect axon outgrowth. We found that *plx-2* mutant animals did not have significant defects in axon growth (98% WT) (Figure 5.10). This is similar to previous work, which also found little obvious defects in *plx-2* mutants [103]. We additionally looked at neuron growth in *mab-20* animals. Similar to its ligand, *mab-20* animals did not have defects in axon growth (96% WT) (Figure 5.10). Thus, there may be some compensation occurring, either via the other *plx-1*, or through other receptors that can function similarly to the plexin receptors and semaphorin ligands.

We additionally looked at *pop-1*, which is the TCF homolog of *C. elegans*. When Wnt signaling is inactive, TCF/LEF is in the nucleus, where it binds to repressor proteins, such as Groucho, to prevent transcription of target genes. However, when Wnt signaling is active, β-catenin enters the nucleus and interacts with TCF/LEF, leading to the unbinding of the repressor proteins, and to genomic transcription. Thus, we wanted to look at if *pop-1*, similar to *bar-1*, was required for axon growth. We found that 24% of *pop-1(hu9)* animals did have significantly undergrown axons (76% WT, P=0.0001, Fisher's Exact Test) (Figure 5.10). While the undergrowth of *pop-1* animals is not as penetrant as in *bar-1* mutants (96%), the posterior axons in *pop-1* animals still follow a similar pattern, where *pop-1* appears to be involved in promoting the outgrowth of the axon from the commissure.

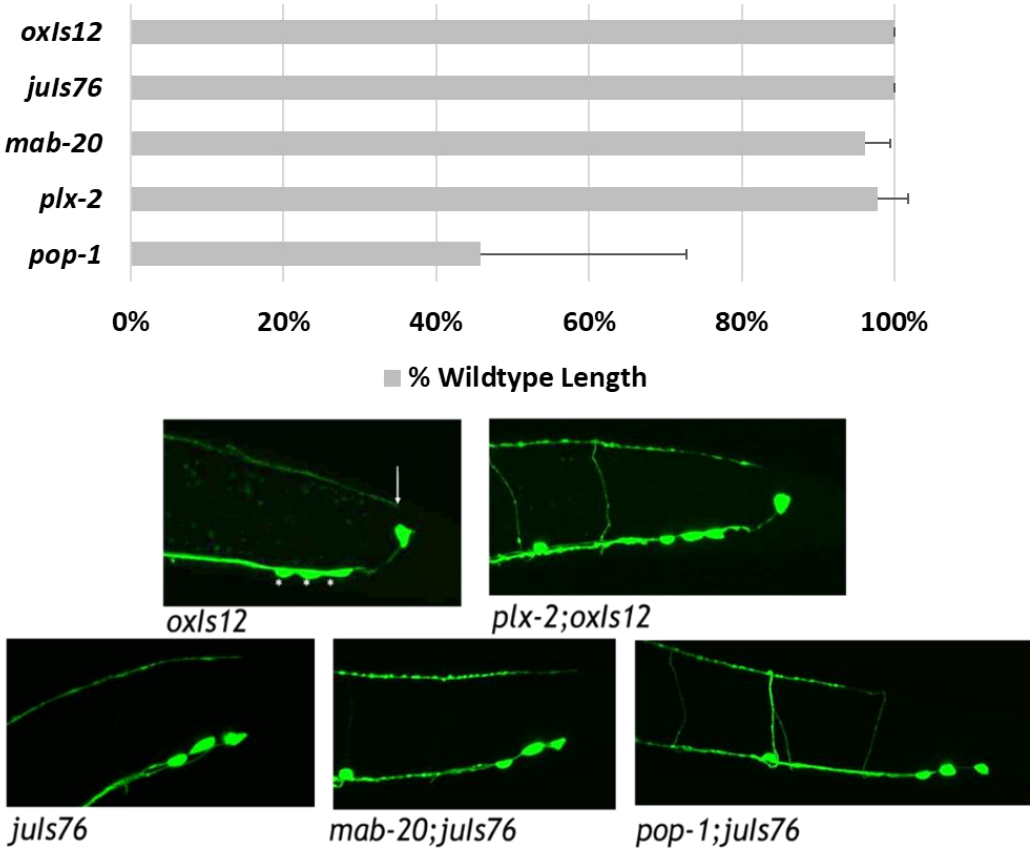

Figure 5.10. *pop-1*, the C. elegans TCF homolog, functions in axon outgrowth. Similar to previous studies, we found that there were defects in axon growth in *pop-1* animals, with only 76% of animals with WT axons. We additionally looked at *plx-2*, since our *lhIs97* VD13 marker is expressed via a fragment of the *plx-2* promoter, as well as the ligand for *plx-2*, *mab-20*. We found that there was no significant effect on axon growth in either *mab-20* or *plx-2* animals, which had WT length axons in 96% and 98% of animals, respectively. Arrows point to the termination point of the dorsal axon.

Finally, we looked at *bli-3* and *ncx-4*. Both *bli-3* and *ncx-4* were previously found to have a synthetic lethality phenotype with *sdn-1* [155]. Synthetic lethality is when a double mutant has a significantly higher embryonic lethality than either of the single mutants. A phenotype of synthetic lethality suggests that the two genes may be working in parallel pathways in development, as loss of either one of the genes can be compensated for, but loss of both leads to a synthetically elevated lethality. Given that previous work in our lab has also shown that *sdn-1* functions in parallel to the Wnt pathway in axon

outgrowth of the D-type neurons, we hypothesized that *bli-3* or *ncx-4* may also be playing a role in axon growth.

bli-3 is a dual oxidase, that has been implicated in stress response in *C. elegans*, where it encourages the formation of reactive oxygen species. The formation of these reactive oxygen species by *bli-3* can be both positive and negative. In the case of the dopaminergic neuron response to stress by manganese, these reactive oxygen species are toxic, and lead to stress [156]. Whereas, in response to pathogen infection, the generation of these reactive oxygen species can actually be protective, by activating downstream factors, such as *skn-1* [157]. In *bli-3*(*im10*) animals, we found that there was no significant change in axon growth (96% WT) (Figure 5.11). However, while *bli-3(im10)* confers a loss of function in the peroxidase domain, it is not a *bli-3* null allele. So, our results suggest that the specific *bli-3(im10)* allele is likely not involved in directing the growth of the D-type neurons, but other alleles of *bli-3* may provide different results or additional information on its role in the development of VD13.

ncx-4 is one of many Ncx genes in *C. elegans*, which function as sodium/calcium exchangers. *ncx-4* is specifically one of seven sodium/calcium exchanges that also requires potassium. Additionally, *ncx-4* is expressed only in neurons, and is, amongst other places, specifically expressed in the ventral and dorsal nerve cords, as well as in motorneurons [158]. Thus, *ncx-4* is a good potential candidate to be involved in axon guidance. *ncx-4* can be differentially spliced into two isoforms, isoform A and isoform B (Wormbase). Isoform A is much larger than isoform B, with the final proteins being 596 and 154 amino acids, respectively (Wormbase). Thus, we generated and scored multiple lines out of our cross to see if there were any differences between lines, potentially due to the changes in splicing. Out of eight *ncx-4* lines, there were two lines which had significant changes in axon growth (Figure 5.11). Two of our *ncx-4* lines were undergrown in 23% and 17% of animals, respectively ($p=0.0001$, $p=0.1538$ Fisher's Exact Test), though only the first was statistically significant. While the third line was both undergrown in 9%

of animals and overgrown in 17% of animals. However, in this third line, only the overgrowth phenotype was significantly different from the WT phenotype (p=0.0003, Fisher's Exact Test). This suggests that *ncx-4* may be acting in axon growth in the D-type neurons. Additionally, it suggests that there may be one isoform of *ncx-4* in particular that is move involved in axon guidance. Our lab has recently obtained a deletion mutation of *ncx-4*, so we can continue to further follow-up on the function of *ncx-4* in the development of VD13.

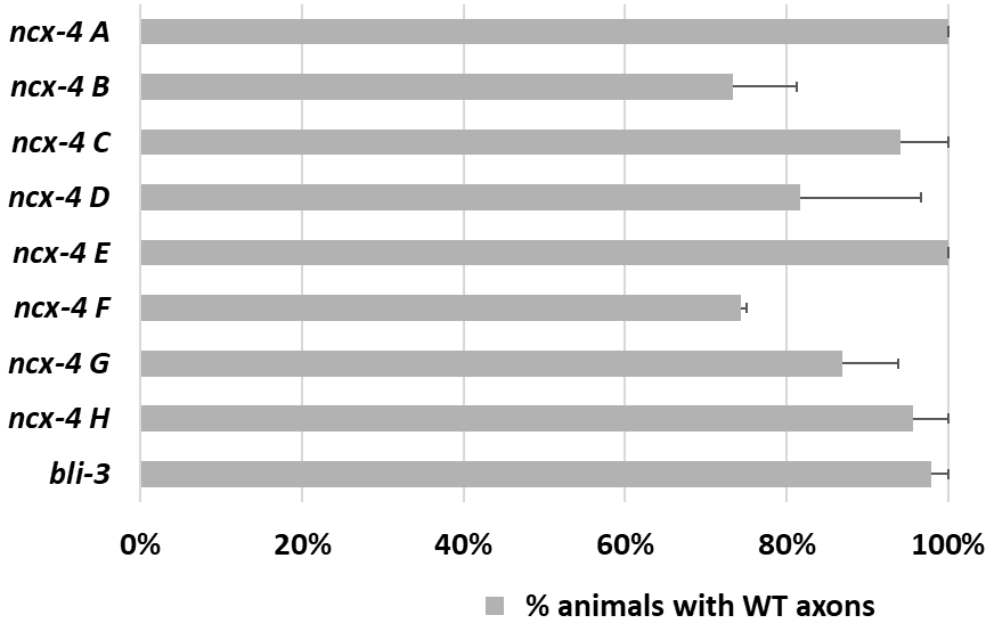

Figure 5.11. *ncx-4*, but not *bli-3(im10)*, is potentially involved in axon outgrowth in VD13. We found no significant change to axon growth in *bli-3*(*im10*) animals, with 98% of animals with WT length axons. Out of our eight ncx-4 lines, we found three that had significant effect on axon growth. These three lines, B, D, and F had animals with WT length axons in 73%, 82%, and 74% of animals, respectively.

Altogether, we found that, on their own, neither *plx-2*, *mab-20*, or *bli-3* had any significant effect on axon growth. Some *ncx-4* strains from our crosses had minor axon guidance defects, as did *pop-1* (similar to those in Maro et al. [38]). Thus, going forward, it may be important, specifically for *plx-2* and *mab-20*, to generate double or triple mutants with *plx-1* to see if there is compensation occurring

between these genes in axon growth. Since *plx-1* does not bind to *mab-20*, it is possible that knocking out both the *plx-2*/*mab-20* signaling, as well as the potential *plx-1*/*smp-1* signaling would provide insight into their function in axon growth. However, given that *mab-20* can interact with non-plexin receptors, we may still see some compensatory events. Additionally, it may be informative to look at axon growth in double mutants with *ncx-4* and either *sdn-1*, or the Wnt pathway members, to determine if it is indeed working in parallel or in concert with those systems to direct axon growth.

Discussion

In this chapter, we began to look further into the role that the Wnt pathway plays in the axon guidance of the most posterior GABAergic D-type motorneurons, DD6 and VD13. We have shown here that the posteriorly expressed Hox gene, *egl-5*, acts cell autonomously to promote outgrowth of the posterior dorsal neurite. We were also able to confirm that *egl-5* is necessary and sufficient for the proper guidance of the posterior axon. Through use of our GABAergic specific *egl-5* rescue construct, we hope to further show that cell-autonomous rescue of *egl-5* is sufficient to compensate for the loss of *bar-1* in *bar-1* animals, as this would highly suggest that not only is *egl-5* indeed involved in directing the growth of these posterior axons, but that it is also activated at the end of the canonical Wnt pathway, which typically functions through *bar-1*/β-catenin in *C. elegans*. Given that *egl-5* is a Hox gene, and thus a known transcription factor, it is also likely that there are other factors which function downstream from *bar-1* and *egl-5* that have yet to be identified.

Additionally, we have shown here that there indeed does seem to be compensatory ability between the Disheveleds, particularly *dsh-1* and *mig-5*. However, the third Dishevelled, *dsh-2,* does not appear to be involved in axon guidance in these neurons. This is not an unusual role for *dsh-1* and *mig-5*, which have been shown to function together in other aspects of axon growth. Specifically, in the PLM neurons, *dsh-1* and *mig-5* function to attenuate Wnt and Frizzled signaling, to promote posterior neurite outgrowth [159]. We see a similar pattern in our system, where the Disheveleds appear to be involved in outgrowth, while both of the Wnt ligands, *lin-44* and *egl-20*, appear to be involved in attenuating growth. It is possible that the disheveleds, though *bar-1* and *egl-5*, are functioning in a similar manner as they do in the PLM neurons, where they are somehow attenuating the signal from the Wnts and Frizzleds in the posterior D-type motorneurons, to promote the outgrowth of the axon.

The attenuation of Wnt and Frizzled signaling by Disheveled, and thus the other downstream members of the Wnt pathway, may explain the discrepancies that we, and other previous works, have seen. Specifically, here we have agreed with previous findings that, in the GABAergic motor neurons of *C. elegans*, the Wnt pathway appears to act in both a canonical and noncanonical manner. This is especially evident in the discrepancies between animals with mutations in the Wnt ligands, namely *egl-20* or *lin-44*, and the β-catenin, *bar-1*. Since the Wnt ligands are needed to ensure that β-catenin is not degraded by the APC complex, we would expect to see a similar phenotype in animals which are mutant for either the Wnt ligands or β-catenin. As an example, we see similar phenotypes in *bar-1*/β-catenin and *pop-1*/TCF animals, both of which have a significant percentage of animals with undergrown axons. This is what would be expected since *pop-1* is inactive when *bar-1* is not present in the nucleus. When *bar-1* does enter the nucleus, it will bind to *pop-1*, and enact changes to gene transcription. Thus, animals with a loss of *bar-1* or *pop-1* should and do have a similar phenotype. However, when looking at the Wnt ligands and *bar-1*, we see the exact opposite phenotype. Animals with Wnt ligand mutations have overgrown axons, and animals with *bar-1* mutation have undergrown axons. This suggests that, in terms of axon guidance, the Wnt pathway is not acting in solely a canonical manner.

Additionally, this data is similar to what we recorded with our *lhIs97* VD13 marker. Using this marker, we noticed decreases in expression, specifically in VD13, in *lin-44*, *bar-1, egl-5*, and *dsh-1mig-5* animals. Notably, we did not see any decrease of expression in the other posterior Wnt ligand, *egl-20*. However, in terms of *C. elegans* development, *bar-1* activation at the end of a *lin-44* Wnt activated pathway, while *egl-20* Wnt functions in a similar, but different pathway, is not unique. During the development of the vulva, *lin-44*, via the receptors *lin-17* and *lin-18*, activates a canonical Wnt pathway, in which *bar-1* is not degraded, and enters the nucleus as a transcription factor [160]. *egl-20*, however, functions through *cam-1* and *vang-1*, which are not traditional canonical Wnt signaling components. These instead are

attributed to the noncanonical pathways [160]. Both are involved in defining the polarity of the vulva, but act through separate Wnt ligand activated pathways. Thus, in the growth and specification of VD13, we may be seeing discrepancies based on both the canonical and noncanonical Wnt pathways involvement.

This is not the only place in *C. elegans* where the canonical Wnt pathway seems to act in a counterintuitive, noncanonical manner. In the outgrowth of the AVG neuron, the first axon in the ventral nerve cord, posterior neurite growth is instructed by two Wnt ligands, *lin-44* and *egl-20*, acting through both canonical Frizzled receptors and noncanonical receptors. Here *lin-44* functions to promote outgrowth of the AVG neuron, and *rpm-1* functions to attenuate *egl-20* signaling, to prevent overgrowth of the axon [161]. This is highly apparent, as animals with the *lin-44; egl-20* double, as well as animals with the *lin-44; egl-20; rpm-1* triple all have the *lin-44* undergrown phenotype, whereas the overgrowth phenotype is only seen in *rpm-1* animals. In zebrafish, the patterning and growth of the dorsal spinal cord are both controlled by canonical Wnt signaling, however, the canonical pathway acts temporally, and through two different transcriptions factors: Tcf7 for patterning and Tcf3 for growth [162]. Additionally, previous work in our lab has shown that cadherins, such as *fmi-1*/*flamingo*, function in parallel to the canonical Wnt receptor Frizzled *lin-17* and the Disheveled *dsh-1* in regulating growth of the VD neurons [106]. *sdn-1* also functions in parallel to Wnt signaling to direct the growth of the posterior D-type neurons [117]. Thus, there are multiple reasons why we may be seeing so many differences in phenotypes between members of the same pathway. Namely, the two main Wnt ligands involved in axon growth, *lin-44* and *egl-20*, may be acting through different receptors, both Frizzleds and non-Frizzleds, and thus may be able to act both as outgrowth signals as well as growth attenuation signals, to properly pattern the VD13 axon. Additionally, as has been shown in other work, the Dishevelleds may also be functioning to attenuate the signal from the Wnts and Frizzleds, and together,

these different factors may all be working together, though sometimes antagonistically, to properly direct the growth of the posterior axon.

Since the Wnt ligands are known to act not only through multiple receptors and pathways, but also through non-transcriptional means to guide all manner of developmental processes involved in neuronal specification, growth, *etc*. it is possible that, as we delve deeper into the double and triple mutants, that we may be presented with a clearer picture, as we are simply seeing the results of multiple disruptions to the development of these neurons, that culminates in axon guidance defects. Additionally, further work with other known receptors of the Wnt ligands, such as *lin-18*, *rpm-1*, *cam-1*, *etc*. may provide us with additional information as we continue to tease apart the complexities of the development of the posterior GABAergic motorneuron, VD13.

Chapter VI: Conclusions & Future Research

Conclusion

Building a nervous system is a highly complex and costly matter. As such, an organism must carefully balance resources to both build a correctly connected neural network, and to also try to conserve as many resources as possible (for review see [163]). Thus, organisms have combined highly complex networks of signals and receptors, which ultimately influence changes in gene transcription, into a system that is specialized to specify, grow, and maintain the complexity of their nervous systems. Given how complex the nervous system is, there is much still to be discovered about how the neurons that make up that system are individually specified and directed in their initial growth, their continued growth with the organism, their maintenance, and their potential regrowth after injury.

To begin to tease apart one small part of the puzzle of neurogenesis and development, we utilize the model organism *C. elegans*. Specifically, we have utilized two of the 302 neurons in the *C. elegans* nervous system. These two neurons are the most posterior neurons of the D-type GABAergic motor neurons, DD6 and VD13. Given that the D-type neurons are laid out like tiles along the body of the animal, these most posterior neurons give us an excellent system to study axon guidance, as there is no more posterior neuron to block our view of their posterior axons. Additionally, we have found that the most posterior neuron, VD13, is an ideal candidate for studying specification, specifically by using our new VD13 specific marker, *lhIs97*. Thus, with our system and our marker in hand, we began to look at the role that the Wnt signaling pathway plays in the development of VD13, and, more specifically, the role that the Hox gene *egl-5*, in conjunction with the Wnt signaling pathway, plays in specification and axon guidance.

egl-5 is required for correct neural identity in multiple posterior neurons in *C. elegans*. In neurons such as the HSN and our VD13, continual expression of *egl-5* is necessary to promote the acquisition and

maintenance of the correct neuronal identity. We have begun to show the evidence for the role of *egl-5* in VD13, as loss of *egl-5* leads to axon growth defects in 86% of animals, as well as loss of our VD13 specific marker, *lhIs97*. Additionally, cell-autonomous rescue of *egl-5* is sufficient to rescue both of these defects. As such, *egl-5* fits the proposed description of a 'terminal selector'. A terminal selector is a term that can be assigned to a protein, or, more often, multiple proteins, that work together to assign the final, terminal identity to a neuron. These terminal selectors are thus often transcription factors, though that is not always the case, and their continued expression is required to maintain the terminal identity of a neuron.

Continuing to define how neuronal selection works, especially when it comes to the terminal identity of neurons, is an incredibly exciting goal. To further explore how the terminal identity of VD13 is defined, we performed a mutagenesis screen, and generated eight candidate lines. Each of these lines has some loss of *lhIs97* expression, specifically at 25°C. Performing a screen at an elevated temperature was intentional, as we hoped to recover temperature sensitive mutations. Mutations that are conditionally active under a certain temperature are highly valuable, especially when working with pathways and genes that are critical for development, and thus can be lethal to the animal. Conditionally active mutations would thus allow for temporal control of the mutation and allow us to both work with potentially lethal mutations, as well as control when during the development of the animal these mutations are active. Excitingly, we have multiple candidate genes for each of our candidate lines, which include genes such as *sma-9* and *mls-2*, which are known to interact with DNA and enact changes to gene expression.

Finally, we have begun to further detail how the Wnt signaling pathway is involved in directing axon growth in VD13. Wnt signaling has been shown to be involved in promoting both outgrowth of the dorsal posterior neuron in VD13, as well as in attenuating that growth, and promoting termination at

the correct location. When genes at the beginning of the Wnt pathway are disrupted, such as the Wnt ligands and Frizzled, we find that there is an overgrowth phenotype, suggesting that these are involved in directing axon growth termination. Additionally, loss of later factors in the pathway, such as *bar-1*, the β-catenin, lead to undergrowth. Thus, we sought to further define how these factors were acting separately and together to direct axon growth.

We describe how, of the three *C. elegans* Disheveleds, *dsh-1* and *mig-5* function to promote outgrowth of the axon in VD13. The final Disheveled, *dsh-2*, does not appear to be necessary in axon growth in VD13. We additionally find that some isoforms of *ncx-4* may be involved in directing axon outgrowth. Additionally, four of the candidates from out mutagenesis screen, *lh40*, *lh41*, *lh42*, and *lh46* all have undergrowth phenotypes. These phenotypes are similar to those seen in factors which act at the end of the Wnt pathways, such as the Disheveleds, *dsh-1* and *mig-5*, as well as *bar-1*, and *egl-5.* Additionally, we see this phenotype in genes that function in parallel to the Wnt pathways, such as *sdn-1*. Thus, the mutations within these lines may also be functioning downstream of, or in parallel to, the Wnt pathway in directing the outgrowth of VD13. Further work defining the receptors, and thus the specific pathway that the Wnt ligands are functioning through, may further define if there is more than just the canonical Wnt pathway functioning in directing the growth of this neuron.

Thus, throughout this work, we have sought to expand our knowledge on how the Wnt signaling pathway is involved in both specification and axon growth of the D-type GABAergic motor neuron, VD13. We have also provided multiple avenues for this work to be built upon, both through further mutagenesis screens, further categorization of the mutations recovered from the candidate lines, and through further defining how the Wnt signaling pathway may act in both a canonical and non-canonical role in directing the axon growth of VD13.

Limitations & Considerations for Future Research

Working with highly conserved molecules that are vital for multiple areas of development is always going to lead to some limitations. This is most obviously a limitation in our work on further elucidating the roll of Disheveled in axon growth, since loss of *dsh-2* is maternal effect lethal. Future work on this project will look into generating mosaic animals with transgenic arrays, where we would look for those animals that lose transgenic rescue in the D-type neurons, specifically VD13, but retain enough expression that the loss of that mutation is not lethal. We have tried this previously, but all of our arrays were too highly transmitting to form working mosaic animals. In the future, there are a few ways that we could reapproach this question. The first would be to reinject our rescue arrays at lower and varying concentrations, to try to obtain mosaic animals to further examine the role of the Dishevelеds in axon growth. Secondly, future work in the lab could utilize cell-specific knock out techniques, such as CRISPR, to knock out *dsh-2* in the D-type neurons of our *dsh-1mig-5* animals. Both of these could provide solutions to our issues in scoring *dsh-2* animals, and help to provide answers on which of the dishevelеds are acting in this system, and the effects on the development of VD13 when all three of the dishevelеds are lost in the D-type GABAergic motor neurons.

In previous work, both from Maro et al. [38] and from our own lab, we have found that multiple Wnt signaling pathways are acting in the same system, *i.e.* in directing the axon growth and termination of the most posterior D-type GABAergic motor neurons, DD6 and VD13. This has made determining the role that these genes specifically play in axon growth hard to elucidate. Thus, going forward, it is imperative to generate mutants in which different combinations of Wnt and Frizzled ligands are lost to try and determine which pathways they are working through, and if there is additional signaling beyond *lin-44* working through *lin-17*. Additionally, looking at the interactions between the dishevelеds and the APC complex genes may provide additional information, like what has been found in vertebrates, where

these genes are bypassing transcriptional activation, and instead directly influencing the growth of axons via changes to microtubules.

Additionally, while our VD13 marker, *lhIs97*, was incredibly useful in starting to look at how the loss of Wnt pathway members actually effect the morphology and specification of VD13, we also had fully penetrant loss of *lhIs97* expression (VD13-) in *bar-1* and *egl-5* animals. This renders us unable to study the morphology of VD13 when these two genes are lost, which is unfortunate, since both are necessary for proper outgrowth of VD13. Thus, going forward, it would be imperative to find conditionally active mutations of these genes. This may allow us to further study the morphology of animals with mutations in these genes, or further confirm that they are indeed involved in specification as terminal selector genes.

However, while it is possible to screen animals in the mutagenesis screen for loss of *lhIs97* expression under a standard fluorescent microscope, it is incredibly time consuming, and can be difficult, given that it is only one cell in the posterior of the animal. Thus, since we know we did not reach full saturation with our initial screen, going forward we would want to adjust the protocol of the screen, to make it more obvious, and thus easier, to screen for animals that are lacking expression in VD13. This would both make the screen more efficient and make it easier to reach potential saturation on the genes that are involved in *lhIs97* expression in VD13.

Finally, we look to further defining genes that function downstream of the canonical Wnt pathway and the Hox gene *egl-5* in directing axon growth and specification. This will be accomplished in two ways: through research, into other areas in which *bar-1* and *egl-5* function in a similar developmental context, to look for potential genes that may also be involved in the D-type neurons. Genes such as *bli-3*, *col-38*, *col-49*, *etc*. have come out of pervious study, in which 14 genes were found to have altered expression

in *bar-1* mutants and increased expression in animals with a conditionally active *bar-1* transgene [133]. In addition to genes that are downstream of the Wnt pathway, the genes that come out of the mutagenesis may be alleles of current Wnt pathway genes, or alleles of genes in other adjacent pathways that we know are involved in D-type growth and specification, such as the heparan sulfate proteoglycan *sdn-1*. However, we may potentially uncover novel genes that have not yet been specified as being involved in the D-type neurons, such as in the case of *lh40*, which we highly expect to be *sma-9*. Now that we have identified potential genes from most of our candidate lines, we can confirm the mutations within these genes via complementation tests, and PCR or sequencing, as well as continue on with epistasis experiments to place them within the context of the known regulators of specification and growth of VD13.

In the overall scope of this research, we will continue to define the genes that are involved in the critical steps of development for motor neurons, specifically those like the D-type GABAergic motor neuron, which form long, pseudounipolar axons that form multiple synaptic connections along their length. Motor neurons are critical to an organism's function, and thus understanding their development gives us a deeper knowledge of neuronal biology and provides us with an additional depth of knowledge on how these neurons functions and develop.

REFERENCES

1. Clevers, H., *Wnt/beta-catenin signaling in development and disease.* Cell, 2006. **127**(3): p. 469-80.

2. van Amerongen, R. and R. Nusse, *Towards an integrated view of Wnt signaling in development.* Development, 2009. **136**(19): p. 3205-14.

3. Hobert, O., *Specification of the nervous system*, in *WormBook*, T.C.e.R. Community, Editor., WormBook.

4. Hobert, O., *Terminal Selectors of Neuronal Identity.* Curr Top Dev Biol, 2016. **116**: p. 455-75.

5. Sarafi-Reinach, T.R., et al., *The lin-11 LIM homeobox gene specifies olfactory and chemosensory neuron fates in C. elegans.* Development, 2001. **128**(17): p. 3269-81.

6. Gordon, P.M. and O. Hobert, *A competition mechanism for a homeotic neuron identity transformation in C. elegans.* Dev Cell, 2015. **34**(2): p. 206-19.

7. Gabilondo, H., et al., *Neuronal Cell Fate Specification by the Convergence of Different Spatiotemporal Cues on a Common Terminal Selector Cascade.* PLoS Biol, 2016. **14**(5): p. e1002450.

8. Serrano-Saiz, E., et al., *Modular control of glutamatergic neuronal identity in C. elegans by distinct homeodomain proteins.* Cell, 2013. **155**(3): p. 659-73.

9. Pfister, B.J., et al., *Extreme stretch growth of integrated axons.* J Neurosci, 2004. **24**(36): p. 7978-83.

10. Dent, E.W., S.L. Gupton, and F.B. Gertler, *The growth cone cytoskeleton in axon outgrowth and guidance.* Cold Spring Harb Perspect Biol, 2011. **3**(3).

11. Huber, A.B., et al., *Signaling at the growth cone: ligand-receptor complexes and the control of axon growth and guidance.* Annu Rev Neurosci, 2003. **26**: p. 509-63.

12. Mallavarapu, A. and T. Mitchison, *Regulated actin cytoskeleton assembly at filopodium tips controls their extension and retraction.* J Cell Biol, 1999. **146**(5): p. 1097-106.

13. Goldberg, J.L., *How does an axon grow?* Genes Dev, 2003. **17**(8): p. 941-58.

14. Ishii, N., et al., *UNC-6, a laminin-related protein, guides cell and pioneer axon migrations in C. elegans.* Neuron, 1992. **9**(5): p. 873-81.

15. Kennedy, T.E., et al., *Netrins are diffusible chemotropic factors for commissural axons in the embryonic spinal cord.* Cell, 1994. **78**(3): p. 425-35.

16. Serafini, T., et al., *The netrins define a family of axon outgrowth-promoting proteins homologous to C. elegans UNC-6.* Cell, 1994. **78**(3): p. 409-24.

17. Colamarino, S.A. and M. Tessier-Lavigne, *The axonal chemoattractant netrin-1 is also a chemorepellent for trochlear motor axons.* Cell, 1995. **81**(4): p. 621-9.

18. Hedgecock, E.M., J.G. Culotti, and D.H. Hall, *The unc-5, unc-6, and unc-40 genes guide circumferential migrations of pioneer axons and mesodermal cells on the epidermis in C. elegans.* Neuron, 1990. **4**(1): p. 61-85.

19. O'Donnell, M., R.K. Chance, and G.J. Bashaw, *Axon growth and guidance: receptor regulation and signal transduction.* Annu Rev Neurosci, 2009. **32**: p. 383-412.

20. Burden, S.J., *The formation of neuromuscular synapses.* Genes Dev, 1998. **12**(2): p. 133-48.

21. Akins, M.R. and T. Biederer, *Cell-cell interactions in synaptogenesis.* Curr Opin Neurobiol, 2006. **16**(1): p. 83-9.

22. Benson, D.L., D.R. Colman, and G.W. Huntley, *Molecules, maps and synapse specificity.* Nat Rev Neurosci, 2001. **2**(12): p. 899-909.

23. White, J.G., et al., *The structure of the ventral nerve cord of Caenorhabditis elegans.* Philos Trans R Soc Lond B Biol Sci, 1976. **275**(938): p. 327-48.

24. Klassen, M.P. and K. Shen, *Wnt signaling positions neuromuscular connectivity by inhibiting synapse formation in C. elegans.* Cell, 2007. **130**(4): p. 704-16.

25. Chisholm, A.D., et al., *The Genetics of Axon Guidance and Axon Regeneration in Caenorhabditis elegans.* Genetics, 2016. **204**(3): p. 849-882.

26. White, J.G., et al., *The structure of the nervous system of the nematode Caenorhabditis elegans.* Philos Trans R Soc Lond B Biol Sci, 1986. **314**(1165): p. 1-340.

27. McIntire, S.L., et al., *The GABAergic nervous system of Caenorhabditis elegans.* Nature, 1993. **364**(6435): p. 337-41.

28. Altun, Z.F., Hall, D.H. *Handbook of C. elegans Anatomy*. In WormAtlas 2017; Available from: http://www.wormatlas.org/hermaphrodite/hermaphroditehomepage.htm.

29. Altun, Z.F., Herndon, L.A., Wolkow, C.A., Crocker, C., Lints, R. and Hall, D.H. *WormAtlas*. 2002-2017; Available from: http://www.wormatlas.org.

30. Eisenmann, D., *Wnt signaling*, in *WormBook*, T.C.e.R. Community, Editor., WormBook.

31. Montcouquiol, M., E.B. Crenshaw, 3rd, and M.W. Kelley, *Noncanonical Wnt signaling and neural polarity.* Annu Rev Neurosci, 2006. **29**: p. 363-86.

32. Veeman, M.T., J.D. Axelrod, and R.T. Moon, *A second canon. Functions and mechanisms of beta-catenin-independent Wnt signaling.* Dev Cell, 2003. **5**(3): p. 367-77.

33. Harterink, M., et al., *Neuroblast migration along the anteroposterior axis of C. elegans is controlled by opposing gradients of Wnts and a secreted Frizzled-related protein.* Development, 2011. **138**(14): p. 2915-24.

34. Herman, M., *C. elegans POP-1/TCF functions in a canonical Wnt pathway that controls cell migration and in a noncanonical Wnt pathway that controls cell polarity.* Development, 2001. **128**(4): p. 581-90.

35. MacDonald, B.T., K. Tamai, and X. He, *Wnt/beta-catenin signaling: components, mechanisms, and diseases.* Dev Cell, 2009. **17**(1): p. 9-26.

36. Natarajan, L., N.E. Witwer, and D.M. Eisenmann, *The divergent Caenorhabditis elegans beta-catenin proteins BAR-1, WRM-1 and HMP-2 make distinct protein interactions but retain functional redundancy in vivo.* Genetics, 2001. **159**(1): p. 159-72.

37. Korswagen, H.C., M.A. Herman, and H.C. Clevers, *Distinct beta-catenins mediate adhesion and signalling functions in C. elegans.* Nature, 2000. **406**(6795): p. 527-32.

38. Maro, G.S., M.P. Klassen, and K. Shen, *A beta-catenin-dependent Wnt pathway mediates anteroposterior axon guidance in C. elegans motor neurons.* PLoS One, 2009. **4**(3): p. e4690.

39. Pan, C.L., et al., *Multiple Wnts and frizzled receptors regulate anteriorly directed cell and growth cone migrations in Caenorhabditis elegans.* Dev Cell, 2006. **10**(3): p. 367-77.

40. Kirszenblat, L., D. Pattabiraman, and M.A. Hilliard, *LIN-44/Wnt directs dendrite outgrowth through LIN-17/Frizzled in C. elegans Neurons.* PLoS Biol, 2011. **9**(9): p. e1001157.

41. Aviles, E.C., N.H. Wilson, and E.T. Stoeckli, *Sonic hedgehog and Wnt: antagonists in morphogenesis but collaborators in axon guidance.* Front Cell Neurosci, 2013. **7**: p. 86.

42. Bovolenta, P., J. Rodriguez, and P. Esteve, *Frizzled/RYK mediated signalling in axon guidance.* Development, 2006. **133**(22): p. 4399-408.

43. Farias, G.G., et al., *Wnt signaling modulates pre- and postsynaptic maturation: therapeutic considerations.* Dev Dyn, 2010. **239**(1): p. 94-101.

44. Schnorrer, F. and B.J. Dickson, *Axon guidance: morphogens show the way.* Curr Biol, 2004. **14**(1): p. R19-21.

45. Blakely, B.D., et al., *Wnt5a regulates midbrain dopaminergic axon growth and guidance.* PLoS One, 2011. **6**(3): p. e18373.

46. Aviles, E.C. and E.T. Stoeckli, *Canonical wnt signaling is required for commissural axon guidance.* Dev Neurobiol, 2016. **76**(2): p. 190-208.

47. Wouda, R.R., et al., *Src family kinases are required for WNT5 signaling through the Derailed/RYK receptor in the Drosophila embryonic central nervous system.* Development, 2008. **135**(13): p. 2277-87.

48. Yoshikawa, S., et al., *Wnt-mediated axon guidance via the Drosophila Derailed receptor.* Nature, 2003. **422**(6932): p. 583-8.

49. Inoue, T., et al., *C. elegans LIN-18 is a Ryk ortholog and functions in parallel to LIN-17/Frizzled in Wnt signaling.* Cell, 2004. **118**(6): p. 795-806.

50. Lu, W., et al., *Mammalian Ryk is a Wnt coreceptor required for stimulation of neurite outgrowth.* Cell, 2004. **119**(1): p. 97-108.

51. Mallo, M., D.M. Wellik, and J. Deschamps, *Hox genes and regional patterning of the vertebrate body plan.* Dev Biol, 2010. **344**(1): p. 7-15.

52. Lappin, T.R., et al., *HOX genes: seductive science, mysterious mechanisms.* Ulster Med J, 2006. **75**(1): p. 23-31.

53. Kaufman, T.C., R. Lewis, and B. Wakimoto, *Cytogenetic Analysis of Chromosome 3 in DROSOPHILA MELANOGASTER: The Homoeotic Gene Complex in Polytene Chromosome Interval 84a-B.* Genetics, 1980. **94**(1): p. 115-33.

54. Lewis, E.B., *A gene complex controlling segmentation in Drosophila.* Nature, 1978. **276**(5688): p. 565-70.

55. Lewis, R.A., et al., *Genetic Analysis of the Antennapedia Gene Complex (Ant-C) and Adjacent Chromosomal Regions of DROSOPHILA MELANOGASTER. II. Polytene Chromosome Segments 84A-84B1,2.* Genetics, 1980. **95**(2): p. 383-97.

56. Philippidou, P. and J.S. Dasen, *Hox genes: choreographers in neural development, architects of circuit organization.* Neuron, 2013. **80**(1): p. 12-34.

57. Alexander, T., C. Nolte, and R. Krumlauf, *Hox genes and segmentation of the hindbrain and axial skeleton.* Annu Rev Cell Dev Biol, 2009. **25**: p. 431-56.

58. Nordstrom, U., et al., *An early role for WNT signaling in specifying neural patterns of Cdx and Hox gene expression and motor neuron subtype identity.* PLoS Biol, 2006. **4**(8): p. e252.

59. Aboobaker, A. and M. Blaxter, *Hox gene evolution in nematodes: novelty conserved.* Curr Opin Genet Dev, 2003. **13**(6): p. 593-8.

60. Brunschwig, K., et al., *Anterior organization of the Caenorhabditis elegans embryo by the labial-like Hox gene ceh-13.* Development, 1999. **126**(7): p. 1537-46.

61. Ferreira, H.B., et al., *Patterning of Caenorhabditis elegans posterior structures by the Abdominal-B homolog, egl-5.* Dev Biol, 1999. **207**(1): p. 215-28.

62. Van Auken, K., et al., *Caenorhabditis elegans embryonic axial patterning requires two recently discovered posterior-group Hox genes.* Proc Natl Acad Sci U S A, 2000. **97**(9): p. 4499-503.

63. Baum, P.D., et al., *The Caenorhabditis elegans gene ham-2 links Hox patterning to migration of the HSN motor neuron.* Genes Dev, 1999. **13**(4): p. 472-83.

64. Singhvi, A., C.A. Frank, and G. Garriga, *The T-box gene tbx-2, the homeobox gene egl-5 and the asymmetric cell division gene ham-1 specify neural fate in the HSN/PHB lineage.* Genetics, 2008. **179**(2): p. 887-98.

65. Zheng, C., F.Q. Jin, and M. Chalfie, *Hox Proteins Act as Transcriptional Guarantors to Ensure Terminal Differentiation.* Cell Rep, 2015. **13**(7): p. 1343-52.

66. Chisholm, A., *Control of cell fate in the tail region of C. elegans by the gene egl-5.* Development, 1991. **111**(4): p. 921-32.

67. Li, X., et al., *HOM-C genes, Wnt signaling and axial patterning in the C. elegans posterior ventral epidermis.* Dev Biol, 2009. **332**(1): p. 156-65.

68. Eisenmann, D.M., et al., *The beta-catenin homolog BAR-1 and LET-60 Ras coordinately regulate the Hox gene lin-39 during Caenorhabditis elegans vulval development.* Development, 1998. **125**(18): p. 3667-80.

69. Hunter, C.P., et al., *Hox gene expression in a single Caenorhabditis elegans cell is regulated by a caudal homolog and intercellular signals that inhibit wnt signaling.* Development, 1999. **126**(4): p. 805-14.

70. Maloof, J.N., et al., *A Wnt signaling pathway controls hox gene expression and neuroblast migration in C. elegans.* Development, 1999. **126**(1): p. 37-49.

71. Veien, E.S., et al., *Canonical Wnt signaling is required for the maintenance of dorsal retinal identity.* Development, 2008. **135**(24): p. 4101-11.

72. Kurland, M., et al., *The Hox Gene egl-5 Acts as a Terminal Selector for VD13 Development via Wnt Signaling.* J Dev Biol, 2020. **8**(1).

73. Brenner, S., *The genetics of Caenorhabditis elegans.* Genetics, 1974. **77**(1): p. 71-94.

74. Josephson, M.P., et al., *EGL-20/Wnt and MAB-5/Hox Act Sequentially to Inhibit Anterior Migration of Neuroblasts in C. elegans.* PLoS One, 2016. **11**(2): p. e0148658.

75. Afgan, E., et al., *The Galaxy platform for accessible, reproducible and collaborative biomedical analyses: 2018 update.* Nucleic Acids Res, 2018. **46**(W1): p. W537-W544.

76. Chen, S., et al., *fastp: an ultra-fast all-in-one FASTQ preprocessor.* Bioinformatics, 2018. **34**(17): p. i884-i890.

77. Li, H. and R. Durbin, *Fast and accurate short read alignment with Burrows-Wheeler transform.* Bioinformatics, 2009. **25**(14): p. 1754-60.

78. Li, H., et al., *The Sequence Alignment/Map format and SAMtools.* Bioinformatics, 2009. **25**(16): p. 2078-9.

79. Tange., O., *GNU Parallel - The Command-Line Power Tool.* ;;Login: The USENIX Magazine, 2011. **36**(1): p. 42-47.

80. Robinson, J.T., et al., *Integrative genomics viewer.* Nat Biotechnol, 2011. **29**(1): p. 24-6.

81. Ramón y Cajal, S., *Histologie du système nerveux de l'homme & des vertébrés*. Éd. française rev. & mise à jour ed. 1909, Madrid,: Consejo Superior de Investigaciones Científicas, Instituto Ramón y Cajal.

82. Marquardt, T. and S.L. Pfaff, *Cracking the transcriptional code for cell specification in the neural tube.* Cell, 2001. **106**(6): p. 651-4.

83. Mizuguchi, R., et al., *Combinatorial roles of olig2 and neurogenin2 in the coordinated induction of pan-neuronal and subtype-specific properties of motoneurons.* Neuron, 2001. **31**(5): p. 757-71.

84. Landmesser, L., *The development of motor projection patterns in the chick hind limb.* J Physiol, 1978. **284**: p. 391-414.

85. Landmesser, L., *The distribution of motoneurones supplying chick hind limb muscles.* J Physiol, 1978. **284**: p. 371-89.

86. Osseward, P.J., 2nd and S.L. Pfaff, *Cell type and circuit modules in the spinal cord.* Curr Opin Neurobiol, 2019. **56**: p. 175-184.

87. Cave, C. and S. Sockanathan, *Transcription factor mechanisms guiding motor neuron differentiation and diversification.* Curr Opin Neurobiol, 2018. **53**: p. 1-7.

88. Dasen, J.S. and T.M. Jessell, *Hox networks and the origins of motor neuron diversity.* Curr Top Dev Biol, 2009. **88**: p. 169-200.

89. McIntire, S.L., E. Jorgensen, and H.R. Horvitz, *Genes required for GABA function in Caenorhabditis elegans.* Nature, 1993. **364**(6435): p. 334-7.

90. Jin, Y., et al., *The Caenorhabditis elegans gene unc-25 encodes glutamic acid decarboxylase and is required for synaptic transmission but not synaptic development.* J Neurosci, 1999. **19**(2): p. 539-48.

91. McIntire, S.L., et al., *Identification and characterization of the vesicular GABA transporter.* Nature, 1997. **389**(6653): p. 870-6.

92. Hallam, S., et al., *The C. elegans NeuroD homolog cnd-1 functions in multiple aspects of motor neuron fate specification.* Development, 2000. **127**(19): p. 4239-52.

93. Jin, Y., R. Hoskins, and H.R. Horvitz, *Control of type-D GABAergic neuron differentiation by C. elegans UNC-30 homeodomain protein.* Nature, 1994. **372**(6508): p. 780-3.

94. Eastman, C., H.R. Horvitz, and Y. Jin, *Coordinated transcriptional regulation of the unc-25 glutamic acid decarboxylase and the unc-47 GABA vesicular transporter by the Caenorhabditis elegans UNC-30 homeodomain protein.* J Neurosci, 1999. **19**(15): p. 6225-34.

95. Melkman, T. and P. Sengupta, *Regulation of chemosensory and GABAergic motor neuron development by the C. elegans Aristaless/Arx homolog alr-1.* Development, 2005. **132**(8): p. 1935-49.

96. Topalidou, I. and M. Chalfie, *Shared gene expression in distinct neurons expressing common selector genes.* Proc Natl Acad Sci U S A, 2011. **108**(48): p. 19258-63.

97. Zhou, H.M. and W.W. Walthall, *UNC-55, an orphan nuclear hormone receptor, orchestrates synaptic specificity among two classes of motor neurons in Caenorhabditis elegans.* J Neurosci, 1998. **18**(24): p. 10438-44.

98. Campbell, R.F. and W.W. Walthall, *Meis/UNC-62 isoform dependent regulation of CoupTF-II/UNC-55 and GABAergic motor neuron subtype differentiation.* Dev Biol, 2016. **419**(2): p. 250-261.

99. Durbin, R.M., *Studies on the Development and Organisation of the Nervous System of Caenorhabditis elegans*. 1987, Kings College: Cambridge. p. 150.

100. Howell, K., J.G. White, and O. Hobert, *Spatiotemporal control of a novel synaptic organizer molecule.* Nature, 2015. **523**(7558): p. 83-7.

101. Hallam, S.J. and Y. Jin, *lin-14 regulates the timing of synaptic remodelling in Caenorhabditis elegans.* Nature, 1998. **395**(6697): p. 78-82.

102. Ackley, B.D., *Wnt signaling and planar cell polarity genes regulate axon guidance along the anteroposterior axis in C. elegans.* Dev Neurobiol, 2013.

103. Nakao, F., et al., *The PLEXIN PLX-2 and the ephrin EFN-4 have distinct roles in MAB-20/Semaphorin 2A signaling in Caenorhabditis elegans morphogenesis.* Genetics, 2007. **176**(3): p. 1591-607.

104. Huang, X., et al., *MAX-1, a novel PH/MyTH4/FERM domain cytoplasmic protein implicated in netrin-mediated axon repulsion.* Neuron, 2002. **34**(4): p. 563-76.

105. Gerstein, M.B., et al., *Integrative analysis of the Caenorhabditis elegans genome by the modENCODE project.* Science, 2010. **330**(6012): p. 1775-87.

106. Huarcaya Najarro, E. and B.D. Ackley, *C. elegans fmi-1/flamingo and Wnt pathway components interact genetically to control the anteroposterior neurite growth of the VD GABAergic neurons.* Dev Biol, 2013. **377**(1): p. 224-35.

107. Zheng, C., M. Diaz-Cuadros, and M. Chalfie, *Hox Genes Promote Neuronal Subtype Diversification through Posterior Induction in Caenorhabditis elegans.* Neuron, 2015. **88**(3): p. 514-27.

108. Leto, K., C. Rolando, and F. Rossi, *The genesis of cerebellar GABAergic neurons: fate potential and specification mechanisms.* Front Neuroanat, 2012. **6**: p. 6.

109. Klausberger, T., et al., *Complementary roles of cholecystokinin- and parvalbumin-expressing GABAergic neurons in hippocampal network oscillations.* J Neurosci, 2005. **25**(42): p. 9782-93.

110. Bachy, I. and S. Retaux, *GABAergic specification in the basal forebrain is controlled by the LIM-hd factor Lhx7.* Dev Biol, 2006. **291**(2): p. 218-26.

111. Fragkouli, A., et al., *LIM homeodomain transcription factor-dependent specification of bipotential MGE progenitors into cholinergic and GABAergic striatal interneurons.* Development, 2009. **136**(22): p. 3841-51.

112. Hobert, O., K. Tessmar, and G. Ruvkun, *The Caenorhabditis elegans lim-6 LIM homeobox gene regulates neurite outgrowth and function of particular GABAergic neurons.* Development, 1999. **126**(7): p. 1547-62.

113. Zhou, H.M. and W.W. Walthall, *UNC-55, an orphan nuclear hormone receptor, orchestrates synaptic specificity among two classes of motor neurons in Caenorhabditis elegans.* J Neurosci, 1998. **18**(24): p. 10438-44.

114. Schwieterman, A.A., et al., *The Caenorhabditis elegans Ephrin EFN-4 Functions Non-cell Autonomously with Heparan Sulfate Proteoglycans to Promote Axon Outgrowth and Branching.* Genetics, 2016. **202**(2): p. 639-60.

115. Rhiner, C., et al., *Syndecan regulates cell migration and axon guidance in C. elegans.* Development, 2005. **132**(20): p. 4621-33.

116. Hartin, S.N., *Reduce, Reuse, Recycle: The tale of two Wnts and the lone C. elegans Syndecan, SDN-1*, in *Molecular Biosciences*. 2015, University of Kansas. p. 1-135.

117. Hartin, S.N.K., M; Ackley, B. D., *Syndecan functions to regulate Wnt-dependent axon guidance in C. elegans*, U.o.K. Department of Molecular Biosciences, Editor. 2017: bioRxiv. p. 52.

118. Walter, S. and J. Buchner, *Molecular chaperones--cellular machines for protein folding.* Angew Chem Int Ed Engl, 2002. **41**(7): p. 1098-113.

119. Franklin, T.B., et al., *The role of heat shock proteins Hsp70 and Hsp27 in cellular protection of the central nervous system.* Int J Hyperthermia, 2005. **21**(5): p. 379-92.

120. Ferguson, E.L. and H.R. Horvitz, *Identification and characterization of 22 genes that affect the vulval cell lineages of the nematode Caenorhabditis elegans.* Genetics, 1985. **110**(1): p. 17-72.

121. Golden, J.W. and D.L. Riddle, *A pheromone-induced developmental switch in Caenorhabditis elegans: Temperature-sensitive mutants reveal a wild-type temperature-dependent process.* Proc Natl Acad Sci U S A, 1984. **81**(3): p. 819-23.

122. Pascoe, H.G., Y. Wang, and X. Zhang, *Structural mechanisms of plexin signaling.* Prog Biophys Mol Biol, 2015. **118**(3): p. 161-8.

123. Ikegami, R., et al., *Integration of semaphorin-2A/MAB-20, ephrin-4, and UNC-129 TGF-beta signaling pathways regulates sorting of distinct sensory rays in C. elegans.* Dev Cell, 2004. **6**(3): p. 383-95.

124. Roy, P.J., et al., *mab-20 encodes Semaphorin-2a and is required to prevent ectopic cell contacts during epidermal morphogenesis in Caenorhabditis elegans.* Development, 2000. **127**(4): p. 755-67.

125. Wang, X., et al., *The C. elegans L1CAM homologue LAD-2 functions as a coreceptor in MAB-20/Sema2 mediated axon guidance.* J Cell Biol, 2008. **180**(1): p. 233-46.

126. Zarkower, D., *Somatic sex determination.* WormBook, 2006: p. 1-12.

127. Emmons, S.W., *Male development.* WormBook, 2005: p. 1-22.

128. Liang, J., et al., *The Caenorhabditis elegans schnurri homolog sma-9 mediates stage- and cell type-specific responses to DBL-1 BMP-related signaling.* Development, 2003. **130**(26): p. 6453-64.

129. Flibotte, S., et al., *Whole-genome profiling of mutagenesis in Caenorhabditis elegans.* Genetics, 2010. **185**(2): p. 431-41.

130. Thompson, O., et al., *The million mutation project: a new approach to genetics in Caenorhabditis elegans.* Genome Res, 2013. **23**(10): p. 1749-62.

131. Shen, Z., et al., *Conditional knockouts generated by engineered CRISPR-Cas9 endonuclease reveal the roles of coronin in C. elegans neural development.* Dev Cell, 2014. **30**(5): p. 625-36.

132. Strayer, A., et al., *Expression of the small heat-shock protein Hsp16-2 in Caenorhabditis elegans is suppressed by Ginkgo biloba extract EGb 761.* FASEB J, 2003. **17**(15): p. 2305-7.

133. Jackson, B.M., et al., *Use of an activated beta-catenin to identify Wnt pathway target genes in caenorhabditis elegans, including a subset of collagen genes expressed in late larval development.* G3 (Bethesda), 2014. **4**(4): p. 733-47.

134. Derynck, R. and Y.E. Zhang, *Smad-dependent and Smad-independent pathways in TGF-beta family signalling.* Nature, 2003. **425**(6958): p. 577-84.

135. Foehr, M.L. and J. Liu, *Dorsoventral patterning of the C. elegans postembryonic mesoderm requires both LIN-12/Notch and TGFbeta signaling.* Dev Biol, 2008. **313**(1): p. 256-66.

136. Haque, R. and A. Nazir, *SMAD Transcription Factor, Sma-9, Attunes TGF-beta Signaling Cascade Towards Modulating Amyloid Beta Aggregation and Associated Outcome in Transgenic C. elegans.* Mol Neurobiol, 2016. **53**(1): p. 109-119.

137. Yoshimura, S., et al., *mls-2 and vab-3 Control glia development, hlh-17/Olig expression and glia-dependent neurite extension in C. elegans.* Development, 2008. **135**(13): p. 2263-75.

138. Kim, K., R. Kim, and P. Sengupta, *The HMX/NKX homeodomain protein MLS-2 specifies the identity of the AWC sensory neuron type via regulation of the ceh-36 Otx gene in C. elegans.* Development, 2010. **137**(6): p. 963-74.

139. Lamoureux, P., et al., *Growth and elongation within and along the axon.* Dev Neurobiol, 2010. **70**(3): p. 135-49.

140. O'Toole, M., P. Lamoureux, and K.E. Miller, *A physical model of axonal elongation: force, viscosity, and adhesions govern the mode of outgrowth.* Biophys J, 2008. **94**(7): p. 2610-20.

141. Smith, D.H., *Stretch growth of integrated axon tracts: extremes and exploitations.* Prog Neurobiol, 2009. **89**(3): p. 231-9.

142. Suter, D.M. and K.E. Miller, *The emerging role of forces in axonal elongation.* Prog Neurobiol, 2011. **94**(2): p. 91-101.

143. Jorgensen, E.M., *GABA*, in *WormBook*, T.C.e.R. Community, Editor., WormBook.

144. Salinas, P.C., *Modulation of the microtubule cytoskeleton: a role for a divergent canonical Wnt pathway.* Trends Cell Biol, 2007. **17**(7): p. 333-42.

145. Krylova, O., M.J. Messenger, and P.C. Salinas, *Dishevelled-1 regulates microtubule stability: a new function mediated by glycogen synthase kinase-3beta.* J Cell Biol, 2000. **151**(1): p. 83-94.

146. Ciani, L., et al., *A divergent canonical WNT-signaling pathway regulates microtubule dynamics: dishevelled signals locally to stabilize microtubules.* J Cell Biol, 2004. **164**(2): p. 243-53.

147. Purro, S.A., et al., *Wnt regulates axon behavior through changes in microtubule growth directionality: a new role for adenomatous polyposis coli.* J Neurosci, 2008. **28**(34): p. 8644-54.

148. Wong, H.C., et al., *Structural basis of the recognition of the dishevelled DEP domain in the Wnt signaling pathway.* Nat Struct Biol, 2000. **7**(12): p. 1178-84.

149. Boutros, M., et al., *Dishevelled activates JNK and discriminates between JNK pathways in planar polarity and wingless signaling.* Cell, 1998. **94**(1): p. 109-18.

150. Yanagawa, S., et al., *The dishevelled protein is modified by wingless signaling in Drosophila.* Genes Dev, 1995. **9**(9): p. 1087-97.

151. Fagotto, F., et al., *Domains of axin involved in protein-protein interactions, Wnt pathway inhibition, and intracellular localization.* J Cell Biol, 1999. **145**(4): p. 741-56.

152. Schwarz-Romond, T., et al., *The DIX domain of Dishevelled confers Wnt signaling by dynamic polymerization.* Nat Struct Mol Biol, 2007. **14**(6): p. 484-92.

153. Zeng, X., et al., *Initiation of Wnt signaling: control of Wnt coreceptor Lrp6 phosphorylation/activation via frizzled, dishevelled and axin functions.* Development, 2008. **135**(2): p. 367-75.

154. Song, S., et al., *A Wnt-Frz/Ror-Dsh pathway regulates neurite outgrowth in Caenorhabditis elegans.* PLoS Genet, 2010. **6**(8).

155. Hartin, S.N., et al., *A Synthetic Lethal Screen Identifies a Role for Lin-44/Wnt in C. elegans Embryogenesis.* PLoS One, 2015. **10**(5): p. e0121397.

156. Benedetto, A., et al., *Extracellular dopamine potentiates mn-induced oxidative stress, lifespan reduction, and dopaminergic neurodegeneration in a BLI-3-dependent manner in Caenorhabditis elegans.* PLoS Genet, 2010. **6**(8).

157. Hoeven, R., et al., *Ce-Duox1/BLI-3 generated reactive oxygen species trigger protective SKN-1 activity via p38 MAPK signaling during infection in C. elegans.* PLoS Pathog, 2011. **7**(12): p. e1002453.

158. Sharma, V., et al., *Insight into the family of Na+/Ca2+ exchangers of Caenorhabditis elegans.* Genetics, 2013. **195**(2): p. 611-9.

159. Zheng, C., M. Diaz-Cuadros, and M. Chalfie, *Dishevelled attenuates the repelling activity of Wnt signaling during neurite outgrowth in Caenorhabditis elegans.* Proc Natl Acad Sci U S A, 2015. **112**(43): p. 13243-8.

160. Green, J.L., T. Inoue, and P.W. Sternberg, *Opposing Wnt pathways orient cell polarity during organogenesis.* Cell, 2008. **134**(4): p. 646-56.

161. Park, E.C. and C. Rongo, *RPM-1 and DLK-1 regulate pioneer axon outgrowth by controlling Wnt signaling.* Development, 2018. **145**(18).

162. Bonner, J., et al., *Proliferation and patterning are mediated independently in the dorsal spinal cord downstream of canonical Wnt signaling.* Dev Biol, 2008. **313**(1): p. 398-407.

163. Wang, I.E. and T.R. Clandinin, *The Influence of Wiring Economy on Nervous System Evolution.* Curr Biol, 2016. **26**(20): p. R1101-R1108.